UiT
THE ARCTIC UNIVERSITY OF NORWAY

Faculty of Science and Technology

Department of Geosciences

Salt movements in three provinces in the southwestern Barents Sea: development, timing, and implications of regional structural differences

Truls Thorsen

GEO-3900 Master thesis in Geology
May 2019

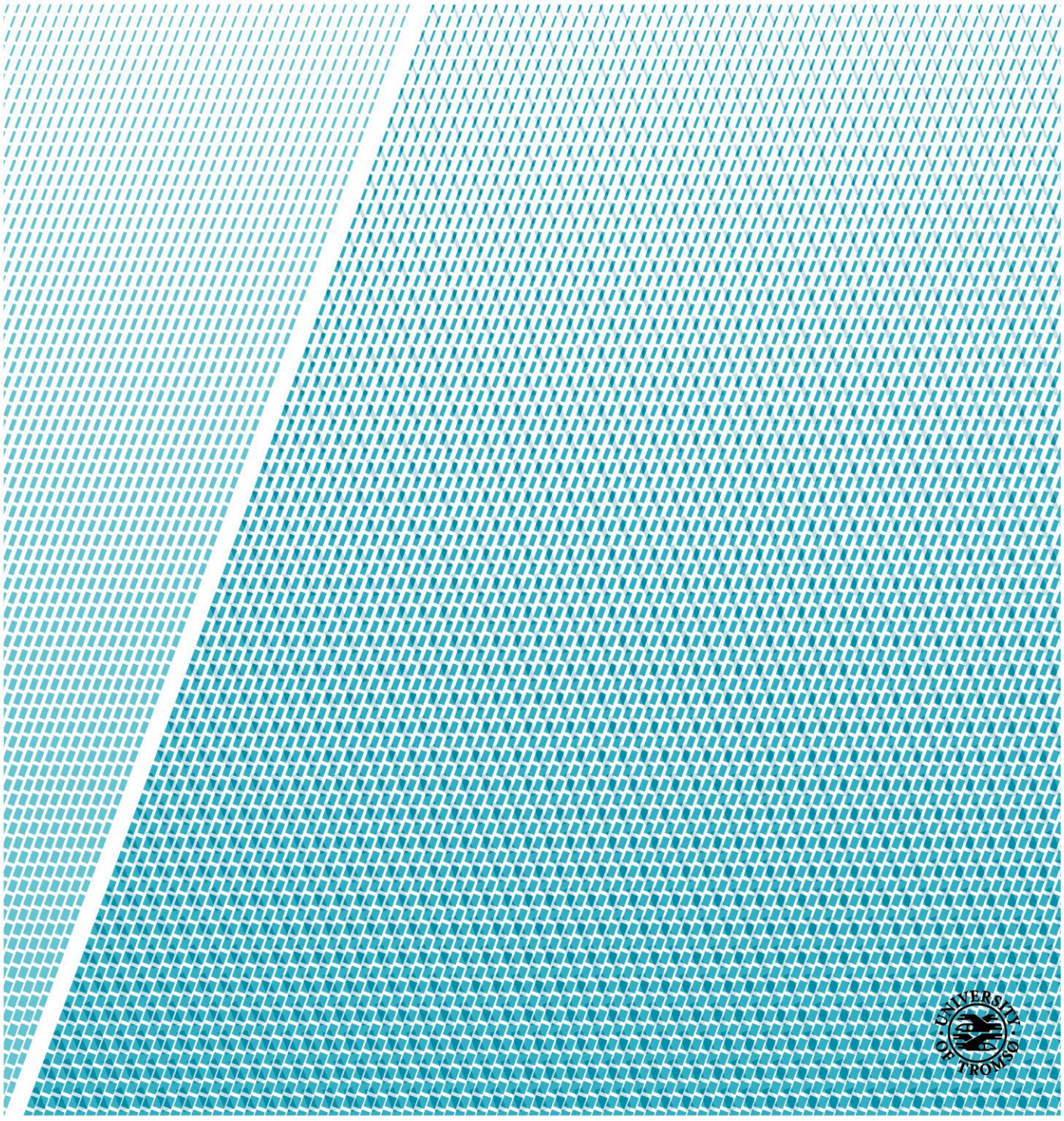

Abstract

This study has investigated salt movements in the Nordkapp Basin, on the Loppa High (Svalis Dome) and on the Bjarmeland Platform (Samson- and Norvarg domes). The aim is to discuss how differences in salt growth potentially relates to the structural evolution of - and differences between - these three provinces.

Evaluation of seismic 2D- and 3D data together with well correlation, allowed a regional stratigraphic framework to be established for the Permian-Quaternary succession. Four stratigraphic units were defined: Lower Triassic, Lower to Middle Triassic, Middle Triassic-Jurassic and Cretaceous-recent. Thickness variations and reflection configurations within these units, together with salt morphology, documented the timing of salt growth.

In the Nordkapp Basin, several phases of salt growth occurred throughout the Triassic, a period usually referred to as tectonically quiet in the southwestern Barents Sea. Extensional forces locally lead to subsidence and faulting/steepening of the basin margins. A regional extensional event lead to renewed salt growth during the Cretaceous, before Cenozoic regional compression squeezed the diapirs, resulting in a final growth phase. At the Svalis Dome, a salt pillow grew during the Early to Middle Triassic-Jurassic. Later uplift and erosion of the dome resulted in renewed growth and diapirism. Little or no salt movements are observed on the Samson- and Norvarg domes during the Mesozoic, but Cenozoic compression appears to have mobilized the salt.

The main differences in salt growth between the three provinces seem to relate to the different structural settings; in the Nordkapp Basin, diapirs grew already in the Triassic possibly due to extensional forces in and adjacent to the basin. On the Svalis Dome, the salt growth seems to relate to a large degree of uplift of the Loppa High. At the Bjarmeland Platform, a late initial growth stage reflects a tectonically stable environment until Cenozoic regional compression mobilized the salt.

Preface

This 60 ECT thesis has been written as the final stage of a 2-year master's degree in petroleum geology at UiT- the Arctic University of Norway. Stig-Morten Knutsen (UiT/NPD), Sondre Johansen (NPD) and Tom Arne Rydningen (UiT) have supervised the work. Seismic data was provided by Equinor Energy AS and TGS-NOPEC, and made available through NPD. The views expressed in this paper are the views of the author and do not necessarily reflect the views of Equinor Energy AS or TGS-Nopec.

Acknowledgments

Fem år med skole flyr forbi, så sitter man her med en master i geologi. Det siste året har vært lærerikt, frustrerende, morsomt og spennende. Så føles det litt vemodig at dette kapitlet nå er ved ende.

Jeg ønsker å rette en stor takk til min hovedveileder Stig-Morten Knutsen, og biveiledere Tom Arne Rydningen og Sondre Johansen. Dere har vært utrolig støttende, lett tilgjengelige og motiverende. En masteroppgave er en øvelse i selvstendig arbeid, men gode mentorer klarer å finne de rette knappene å trykke på for at det skal bli bra til slutt.

Videre er det på sin plass å takke familie og venner for støtten gjennom disse fem årene. Først og fremst tusen takk til Mamma; for støttende ord, gode middager, klesvask og økonomiske «lån». Takk til Marius, «Sjonkel» og Caroline; for fine turer, flotte middager og småfuktige kvelder. Takk til hele gjengen på geologibygget; for lange lunchpauser og morsomme sosiale sammenkomster. Tusen takk til Ina, for at du har støttet meg hver dag gjennom denne siste prosessen, og senket stressnivåene mine betraktelig!

Til slutt; takk til Equinor Energy AS og TGS-NOPEC for tilgangen til seismiske data. Og til Oljedirektoratet, for at dere tilrettelegger for deling av informasjon og data om norsk sokkel.

«So long, and thanks for all the fish»

-Douglas Adams

Contents

1 Introduction

1.1 Purpose of study and study area

This thesis has as its main objective to investigate salt movements in the southwestern Barents Sea. Salt structures are important in exploration geology as they can have a great effect on deformation styles, and form hydrocarbon traps. The study area includes the Nordkapp Basin, in addition to the Svalis-, Norvarg- and Samson domes, which are salt domes located on the northeastern margin of the Loppa High and on the southern part of the Bjarmeland Platform (Figure 1.1). Permian to Quaternary strata will be investigated, with a special focus on the Triassic stratigraphy. Interpretation of 3D- and 2D-seismic data, along with stratigraphic correlation through well data, will help to achieve the following:

- Establishing a stratigraphic framework for the study area.
- Mapping of salt in the study area.
- Analyzing the timing of salt structure growth, based on morphology and thickness variations in the bounding stratigraphy.
- Establishing if different timings of salt growth across the study area coincide with previous findings, and with the tectonic/structural evolution of the area previously described in the literature.

Generating time-thickness maps of sequences in the bounding stratigraphy can provide an insight into timing of diapiric growth. Coupled with the vast amounts of information about the tectonic history of the area from previous studies, and supplementary observations made in the seismic data, a better understanding of the driving forces behind the salt movements should be achieved.

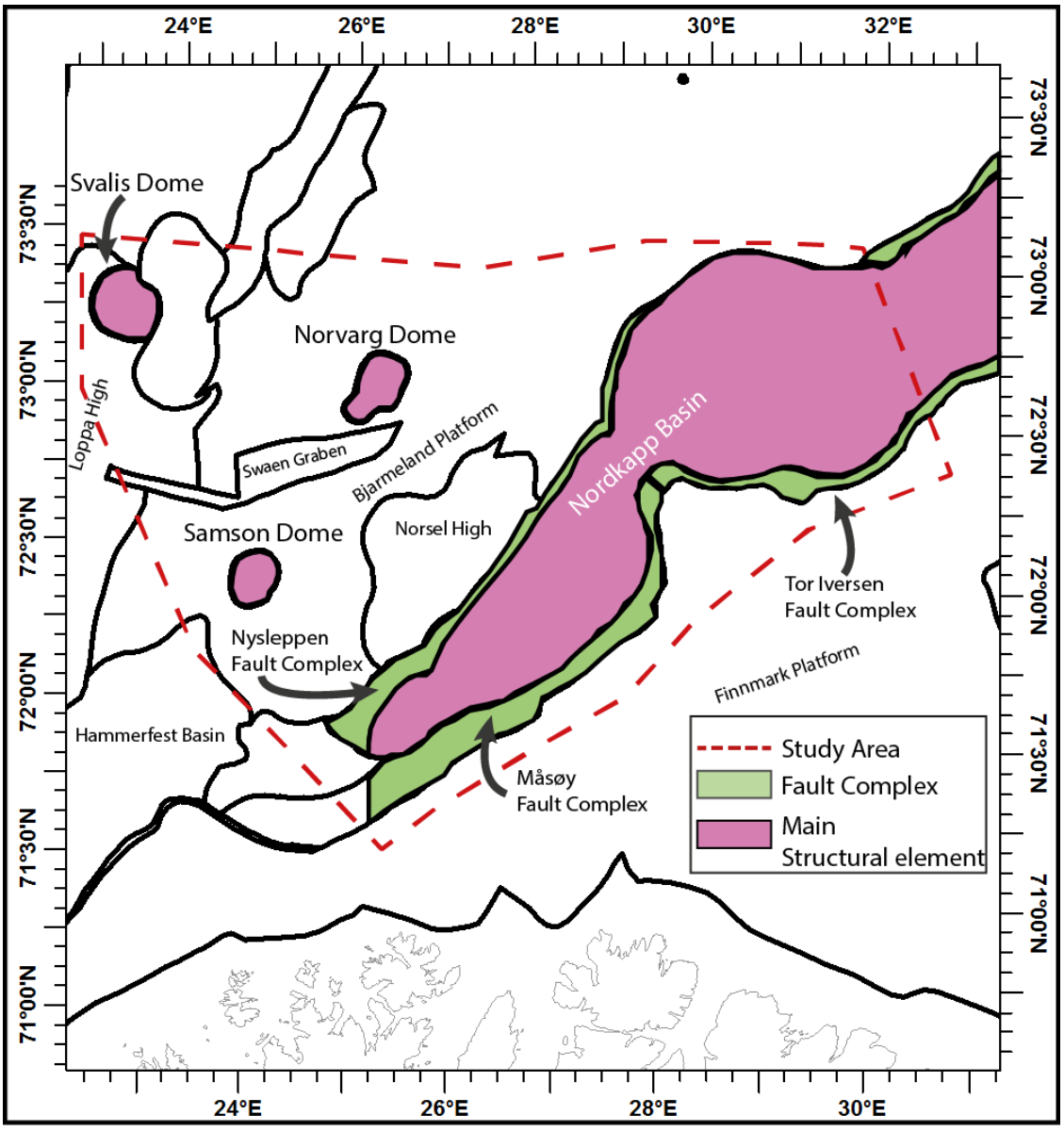

Figure 1.1: Map of the study area with the most important structural elements. The red dashed line indicates the rough outline of the study area. Structural elements and borders compiled from NPD.

1.2 Salt theory

Ideas on formation of salt domes date back as far as the mid-late 1800's, with the first ideas that salt structures in Rumania could have a diapiric origin proposed by František Posepny in 1871. Salt domes later received an increasing amount of interest after the discovery of abundant petroleum resources at the Spindletop dome in 1901. From 1916 and onwards theories regarding salt-flow principles started becoming widespread (Halbouty, 1967). The

following sections will focus on the generation and physical properties of rock salt, *halite,* and typical features related to *salt tectonics.*

1.2.1 Deposition of salt

Halite is an evaporite mineral formed from chemical precipitation in areas where rates of evaporation surpass the rate of input from atmospheric precipitation. Evaporites are typically formed in sequences where the most common mineral groups, next to halite itself, are the sulfates (anhydrite and gypsum) and the bittern salts (e.g. sylvite) (Jackson and Hudec, 2017). Early experiments showed that the evaporation of a column of seawater would initially lead to anhydrite precipitation, followed by halite, and finally the bitterns (Halbouty, 1967). In nature however, evaporite deposition is a complex process with many variables (e.g. basin architecture, brine concentration & temperature, hydrologic changes), so that actual evaporite deposits often times have very different compositions (Halbouty, 1967). Regarding massive salt diapirs and their related salt basins, the amount of salt deposition required for these features to be generated is so tremendous that we have no analogs from present day evaporite basins, and they could only have formed in conditions far different from what is present today (Halbouty, 1967; Jackson and Hudec, 2017). In general, greenhouse or even hothouse conditions are favored, as are large basins isolated from oceanic mixing (e.g. rift basins or foreland basins). From this it is evident that the assemblage or breakup of a supercontinent, which favors the climatic conditions and basin development mentioned above, is an ideal time for the deposition of saline giants (Jackson and Hudec, 2017).

1.2.2 Halokinesis and salt tectonics

The concept of *Halokinesis* can be explained as the autonomous plastic flow of salt, driven by density differences between that of the salt and the compacted surrounding sediments after burial. The density of pure rock salt is approximately 2040 kg/m^3 , and because of its relatively incompressible nature, its density can be surpassed by that of compacted sedimentary rocks from depths around 650 m in some cases (Jackson and Hudec, 2017). This leads to a gravitational non-equilibrium which in turn causes a buoyancy-driven upward flow of the comparatively less dense salt, with a variety of salt structures (e.g. *pillows*, *walls*, *stocks* etc.) as

possible outcomes (Halbouty, 1967). Trusheim (1960) described a model with three stages of diapiric growth, where depositional patterns in the adjacent areas were linked to the different stages of Rayleigh-Taylor instabilities and associated (buoyancy driven) growth stages. Later works, however, have shown that in the light of rock mechanics and under the assumption that a partly compacted overburden will not act as a Newtonian fluid, early or late regional tectonics and differential loading are usually important mechanisms to initiate diapiric growth in a salt body displaying low initial relief (Jackson and Talbot, 1986; Vendeville, 2002). Nevertheless, buoyancy becomes increasingly important as a salt dome grows, its relief increases and density of the overburden increases (Jackson and Talbot, 1986). While the term halokinesis implies salt deformation driven solely by buoyancy, *salt tectonics* does not exclude the contribution from regional extension or shortening (Jackson and Hudec, 2017).

1.2.3 Diapiric growth

An important feature of many salt dome basins is the *peripheral sink,* also named *salt withdrawal mini-basin* or *rim syncline* (Trusheim, 1960; Peel, 2014). In this thesis, the terms rim syncline and minibasin will be used. The idealized growth sequence of salt domes proposed by Trusheim (1960) is briefly explained in the following to highlight the formation of rim synclines (Figure 1.2). The first part of Trusheim's sequence is a pillow stage where salt predominantly flows laterally into the growing structure. This stage is followed by a diapiric stage, where the salt flow primarily has a vertical path. Finally there is a post-diapiric stage, where the diapir still slightly rises, even after the connection to the source layer has been cut off (Trusheim, 1960). Vendeville (2002) attributed this stage to one of two processes: either the diapir rises passively solely based on the fact that salt is more or less incompressible, while adjacent sediments are not, and therefore the sediments will sink past the salt. Alternatively, thin-skinned shortening leads to active diapiric rise through squeezing of the diapir (i.e. the

diapir does not need continued supply from a source layer, the narrowing of the diapir enables the vertical rise).

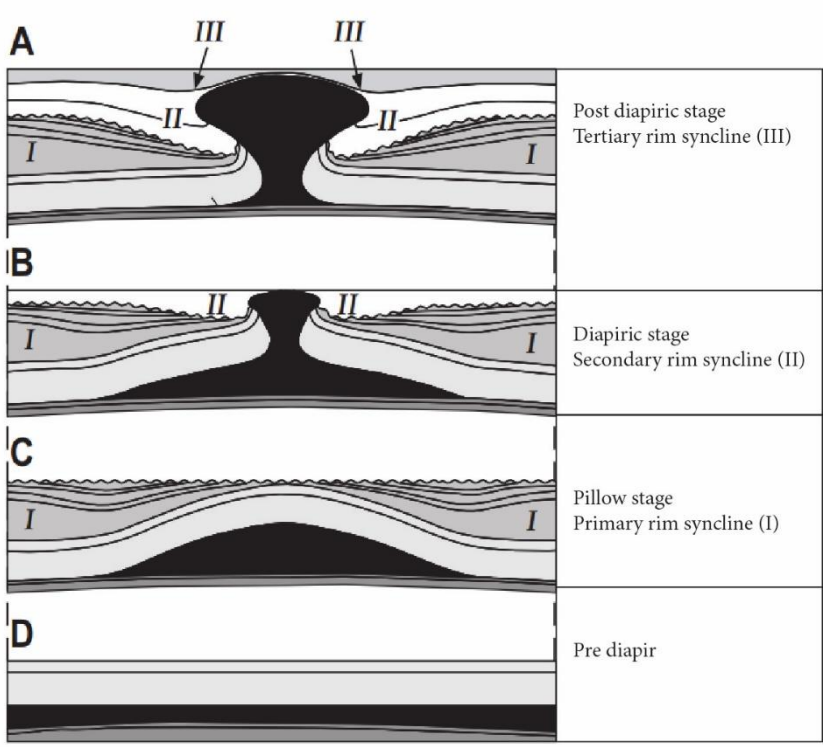

Figure 1.2: The formation of rim synclines originally proposed by Trusheim (1960) during diapiric salt movement. Salt in black. Modified from Vendeville (2002).

During the initial stage in Trusheim's model, the pillow stage, horizontal flow of salt from the mother salt bed towards the center of the growing structure results in subsidence of overlying sediments in the periphery of the dome. The resulting depression on the surface will be filled with sediments, and from this, a decrease in sediment thickness can be expected in the deposits from this stage (Figure 1.2 C). Trusheim (1960) named this the primary peripheral sink.

In the diapiric stage in Trusheim's sequence, salt from the pillow breaches the overburden and flows upwards through the strata until it reaches the surface, or, until the resistance of the overlying layers overcomes the driving forces. The diapiric growth is followed by a gradual destruction of the pillow and subsidence of adjacent overlying sediments (Trusheim, 1960). During this stage, the diapir will rise passively by *isostatic down building*, and sediments deposited during this stage are expected to increase in thickness towards the diapir. This

corresponds to the secondary peripheral sink (Trusheim, 1960; Halbouty, 1967) (Figure 1.2 B).

The process of isostatic down building was first proposed by Barton in 1933. During this process the growing salt structure remains at a more or less constant depth, while the surrounding sediments sink down past the salt, and the subsidence leads to continued horizontal salt flow from the mother salt bed into the base of the salt (Halbouty, 1967). During down building, the relationship between sedimentation rate and rise rate of the salt will control the shape of the salt structure. If the sedimentation rate exceeds the rise rate of the salt, the structure will be narrowing upwards. If the rise rate of the salt exceeds the sedimentation rate, the structure will be widening upwards (Fossen, 2016). At some point in the diapir evolution, the salt layer feeding the structure might exhaust. At this stage, the supra- and subsalt layers will become attached, with only a small amount of remnant salt separating them. This is often times referred to as a *salt weld* (Fossen, 2016)

1.2.4 Salt structure classification and nomenclature

The term salt structure in the context of salt tectonics involves all deformed salt bodies that are large enough to be visible on seismic scale imaging, but smaller than entire salt basins (Jackson and Hudec, 2017). Classification of salt structures mostly follows the description of their shape. They vary from elongated in map view (e.g. salt walls, salt anticlines, salt rollers and salt overthrusts) to more equidimensional (e.g. salt pillows, salt stocks and their associated stems and bulbs) (Figure 1.3). In some cases larger structures can be highly complex and form massifs and sheets, or be connected through canopies (Jackson and Hudec, 2017). A typical trait of diapirs is that the top swells out laterally to form a bulb, and the part of the bulb that is wider than the stem is referred to as the *overhang*. The topmost surface of the diapir is called the *crest* (Jackson and Talbot, 1986). At time of deposition, salt will be more or less stratiform and subhorizontal, although with minor variations in thickness if the basin floor on which it was deposited was irregular or differential subsidence took place (Jackson and Talbot, 1986). These irregularities together with lateral and vertical facies

changes into other evaporites and clastics can focus later salt movements, and thereby affect the shape of salt structures (Jackson and Talbot, 1986).

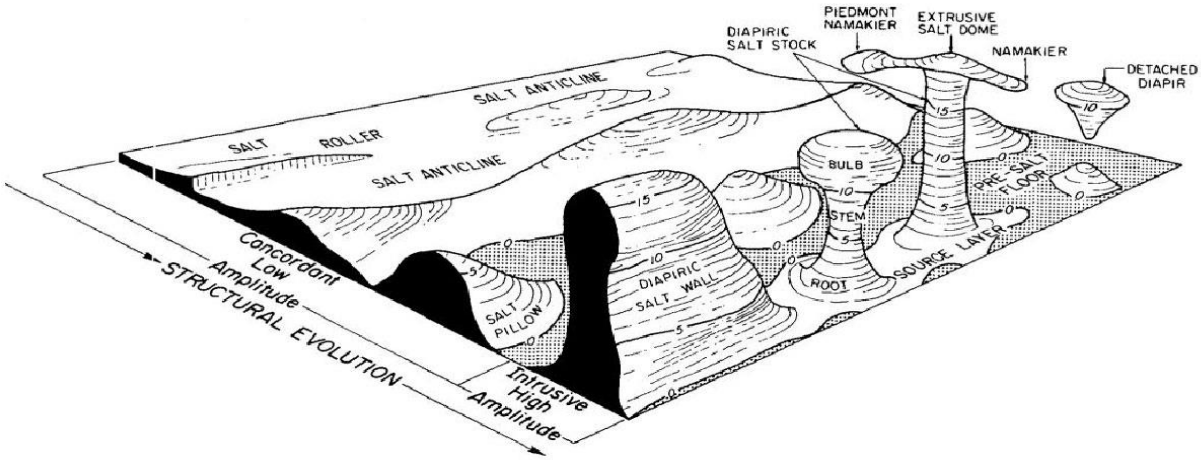

Figure 1.3: Common terms for different salt structures. Modified from Jackson & Talbot (1986)

In Figure 1.3, it can be seen that structures initiate with low amplitudes concordant with the overburden, and later evolve into higher amplitude structures that breach the overlying strata. Arguments have been made that such a connection is not always the case, i.e. that a present day dormant salt pillow does not represent an early stage diapir, and that it never was likely to evolve further. In the same manner, some diapirs do not evolve from pillows, but pierce their overburden without a prior pillow stage (Vendeville, 2002). Nonetheless, it seems evident that the shape of salt structures together with depositional patterns in the rim synclines can provide useful information about the salt structure genesis (Jackson and Hudec, 2017).

2 Geological background

The Barents Sea shelf covers the area from the Arctic Ocean in the north to the Norwegian and Russian coastal areas in the south, and from the Norwegian-Greenland Sea in the west to Novaya Zemlya in the east. This is an area of approximately 1.3 million km^2, with a complex and geographically varied geological history leading up to the present day configuration (Dorè, 1995; Worsley, 2008). A sub-division of the shelf into two major provinces is possible: an eastern and a western province separated by a massive north- south trending monoclinal structure in the middle. The geology of the two provinces differ in the way that tectonic events have influenced them, and the focus of this thesis is on the southern part of the western province; which with its basins, platforms and highs, reflect a complex tectonic history with several rifting phases since post-Caledonian times (Dorè, 1995; Smelror et al., 2009).

2.1 Tectonic framework

2.1.1 Paleozoic

The earliest tectonic event that has affected the basement of the western Barents Sea is the Caledonian orogeny, which culminated in the Devonian approximately 400 million years ago (Ma). This was an event where the closing of the Iapetus Ocean lead to consolidation of the Laurentian and Baltic plates into a new continent named Laurasia. A north-south structural grain along the western Barents margin, and a northeast-southwest grain in the southwestern Barents Sea reflect this event (Gabrielsen et al., 1990; Dorè, 1995; Smelror et al., 2009). The Uralian orogeny, the final stage of the consolidation of the Pangea supercontinent, culminated approximately 240 Ma during the latest Permian- Early Triassic, but the Uralian structural grain can only be found in the major basins of the eastern Barents Sea (Dorè, 1995).

Following the Caledonian orogeny, the late Paleozoic was a period characterized by crustal extension in the western Barents Sea area, a setting caused by the collapse of the recently formed Caledonides (Gernigon et al., 2014). The southwestern Barents sea was at this time located at the northern margin of the newly formed continent Pangea, at equatorial latitudes (Worsley, 2008). A rifting episode during the Carboniferous resulted in formation of extensional rift basins and grabens striking predominantly north-south and northeast-

southwest (i.e. Tromsø-, Bjørnøya-, Nordkapp-, Fingerdjupet-, Maud- and Ottar basins) (Figure 2.1).

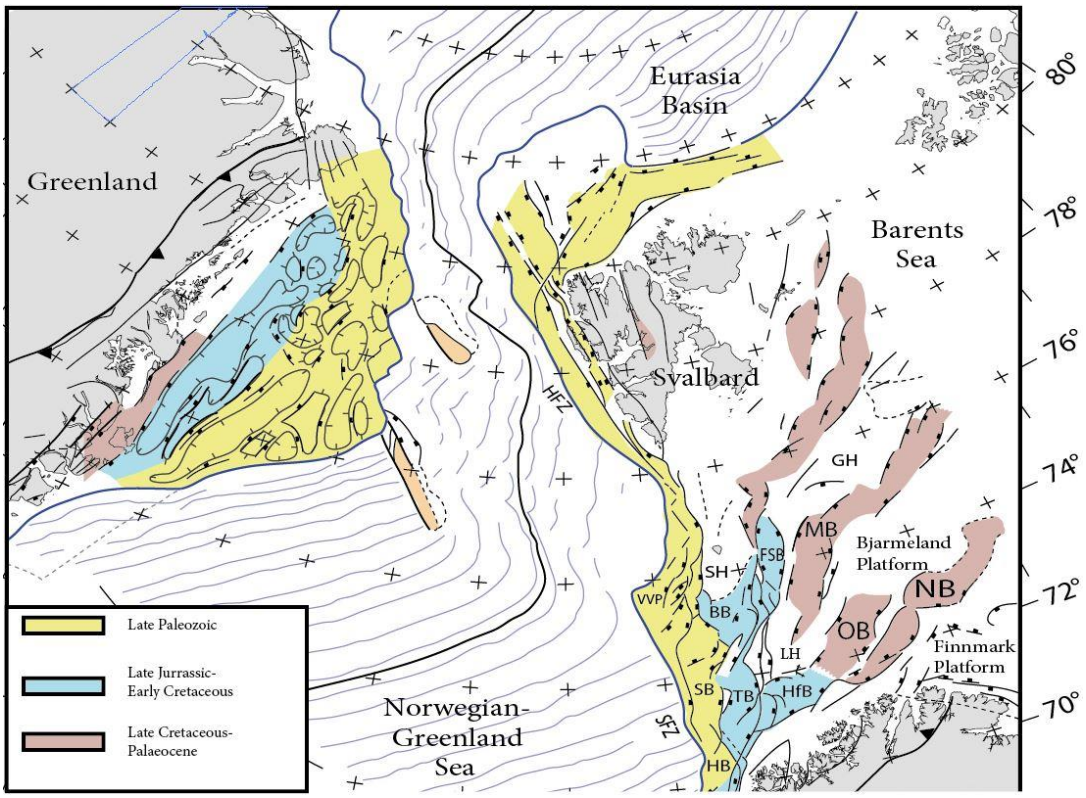

Figure 2.1: Overview of basins and selected structural elements in the western Barents Sea. BB=Bjørnøya Basin, FSB= Fingerdjupet Subbasin, GH=Gardarbanken High, HB=Harstad Basin, HfB=Hammerfest Basin, HFZ=Hornsund Fault Zone, LH=Loppa High, MB=Maud Basin, NB=Nordkapp Basin, OB=Ottar Basin, SB=Sørvestnaget Basin, SFZ=Senja Fracture Zone, SH=Stappen High, TB=Tromsø Basin, VVP=Vestbakken Volcanic Province. Modified from Faleide et al. (2015)

Structures related to this rifting phase can be recognized locally on seismic data below carbonate platform deposits from Upper Carboniferous-Lower Permian strata (Smelror et al., 2009; Faleide et al., 2015).

During Permian-Early Triassic times, renewed faulting took place along the western part of the rift zone in the North Atlantic region, which is evident by normal faulting along Loppa High and erosion due to uplift of the high itself (Faleide et al., 2015).

2.1.2 Mesozoic

A series of continued rifting episodes, regarded as the precursors to the Cenozoic opening of the North Atlantic, characterized the Mesozoic. A subsequent tectonically quiet period in the Barents Sea followed the previously mentioned Permian-Early Triassic major rifting episode. A number of discrete minor tectonic events (e.g. a series of uplifts of the Bjørnøya area,

evident here by an angular unconformity between the Permian and Triassic strata) can be recognized in the Middle-Late Triassic deposits (Smelror et al., 2009; Vigran et al., 2014). However, it was post-rift thermal subsidence that otherwise characterized the period, until renewed tectonic activity in the Atlantic and Arctic regions occurred near the end of the Late Triassic. This event resulted in renewed faulting on the Barents Shelf, while the Canadian and Alaskan parts of the Arctic experienced uplift and erosion (Smelror et al., 2009).

From Middle Jurassic to Early Cretaceous the southwestern Barents Sea was affected by renewed rifting in the Atlantic region, and a continuous northwards propagation of the rift eventually established a marine connection across the Barents Shelf, connecting the Atlantic and Arctic realms through a marine seaway (Smelror et al., 2009; Gernigon et al., 2014). Strike-slip adjustments along pre-existing lineaments also developed the Bjørnøya-, Tromsø- Harstad- and Hammerfest basins as rift basins (Worsley, 2008; Brekke and Olaussen, 2013).

A major volcanic event characterizes the Cretaceous development of the southwestern Barents Sea. From the Early Cretaceous, major uplift occurred in the northern areas of the shelf, along with volcanic activity in the northeastern parts of Svalbard. A possible correlation with magmatic intrusion in the southern Barents Sea suggests that a tectono-magmatic event related to break up and spreading in the Arctic Ocean took place (Dorè, 1991; Smelror et al., 2009). Major rifting in the Amundsen Basin further north also took place in the Late Cretaceous (Dorè, 1995; Smelror et al., 2009).

2.1.3 Cenozoic

In the early Cenozoic, the Arctic and Atlantic spreading centers related to the Late Cretaceous rifting were linked through a relay zone formed along the Hornsund Fault Zone and the Senja Fracture Zone further south (Dorè, 1995; Smelror et al., 2009). The Spitsbergen Orogeny took place in Paleogene, with subsequent deposition of sediments derived from the fold-and thrust belt into a newly formed foreland basin (Central Basin) taking place in Eocene (Smelror et al., 2009). Seafloor spreading was occurring south of the Greenland-Senja Fracture Zone already in early Eocene, however it was not until after a reorganization of the spreading patterns that it propagated further north to reach the Hornsund Fault Zone during mid Eocene (Smelror et

al., 2009). early Oligocene marks the final separation of Greenland and Svalbard, and a transition from the previously transpressional and transtensional environment along the sheared margin, into the establishment of a passive margin (Golonka et al., 2003).

During Eocene, it is assumed that shallow marine seas with little deposition, or even uplifted hinterlands, persisted in a stable epicontinental megaregion. Deposition that may have taken place has nevertheless been removed by later Neogene uplift and erosion (Smelror et al., 2009). From Late Pliocene through Pleistocene, fluvial and glacifluvial erosion removed an average of 420 meters of sediments in the Barents Sea. The last 0.8 Ma the Barents Shelf has been through several cycles of shelf-edge glaciations, and the removal of as much as 2-3 km of sediments since Late Pleistocene is evident in the northernmost areas and on Svalbard. Further south (e.g. Nordkapp Basin and Loppa High) however, net erosion is assumed to generally be less than 2 km (Vorren et al., 1991; Smelror et al., 2009; Laberg et al., 2012).

2.2 Stratigraphy and depositional environments

The Barents Sea area has moved from the southern hemisphere arid zone to the equatorial tropic zone sometime in the Devonian, and onwards to the present day location between 71°N (present day Nordkapp) and 80°N (present day northern Spitsbergen) (Worsley, 2008; Smelror et al., 2009).

2.2.1 Paleozoic

Deposits from latest Devonian-middle Permian in the southwestern Barents Sea can be separated into three distinct lithostratigraphic groups (Figure 2.2), each representing a significant change in depositional environment because of tectonic, climatic and relative sea level changes. The late Permian deposition of siliceous shales of the Tempelfjorden Group supersede a transition from a non-marine humid environment in Late Devonian-early Carboniferous, into a warm water carbonate platform persisting into early Permian (Larssen et al., 2002), and a subsequent change to cold-water carbonates, lasting until mid-Permian (Worsley, 2008).

Billefjorden Group

The deposits of the Billefjorden group represent a period with deposition of predominantly fluvial and lacustrine clastic sediments. Lower Devonian (?) to lower Upper Carboniferous strata were deposited in extensional grabens (Nilsen et al., 1995; Faleide et al., 2015).

Some marine influence is evident locally on the southeastern part of the Finnmark Platform, linked to a probable marine seaway through the Nordkapp Basin (Bugge et al., 1995). From the Viséan onwards a more widespread depositional environment was established, with warm and humid hinterlands showing increasingly marine influences eastwards (Worsley, 2008).

Gipsdalen Group

The Gipsdalen Group primarily consists of platform carbonates deposited in a hot and dry environment, following uplift and reactivation of existing half grabens in the Serphukovian-Bashkirian transition. The Gondwanan glaciation had a large impact on the depositional environment in this period; frequent glaciations and deglaciations resulted in cyclical dolomites, evaporites and limestones (Faleide et al., 2015). During glacio-eustatic sea level lowstand, the platform areas were sub-aerially exposed, resulting in karstification and collapse-breccias (Worsley, 2008). The Nordkapp Basin was a fault-bounded basin at this time, and the large negative relief of this depression coupled with later thermal subsidence allowed the deposition of a 4-5 km thick halite sequence (Faleide et al., 2015)

Bjarmeland Group

The Bjarmeland Group marks a major flooding event that took place in mid-Sakmarian times. The cold-water carbonates of the group mark a transgression of the previously shallow warm-water carbonate platform, coinciding with the culmination of the Gondwana glaciation.

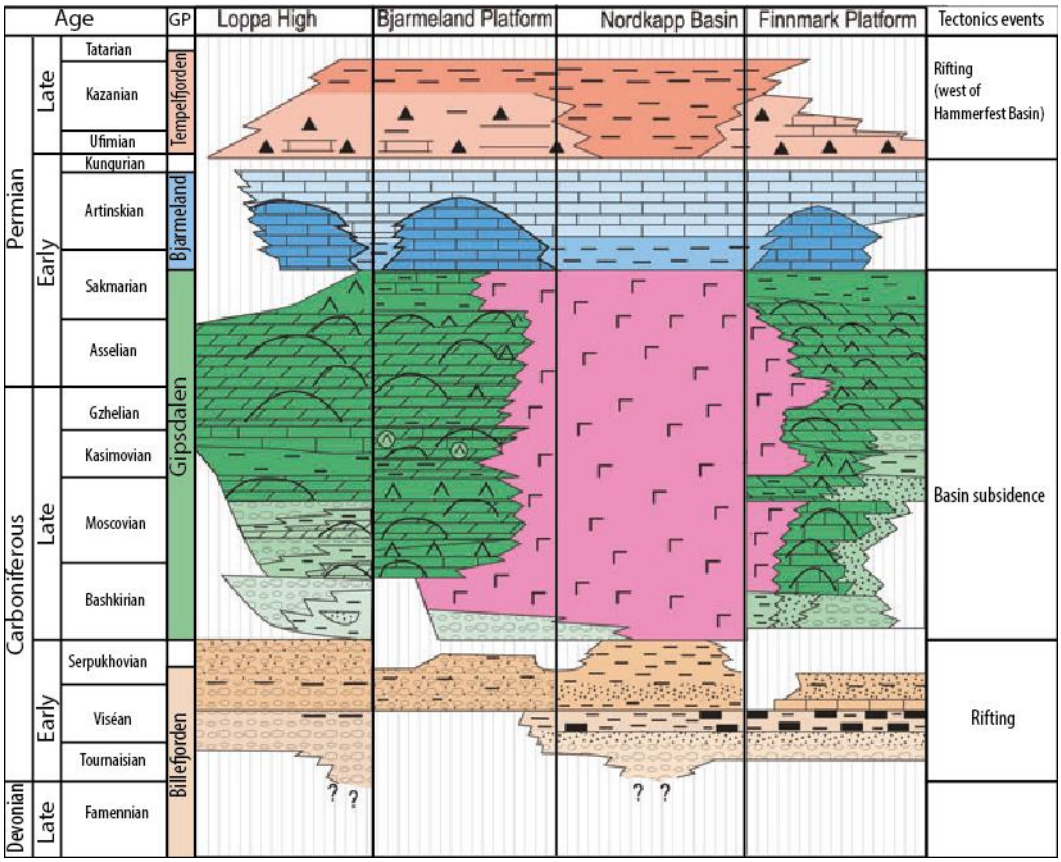

Figure 2.2: Lithostratigraphic groups of the late Paleozoic in southwestern Barents Sea with lithofacies for Bjarmeland Platform and Nordkapp Basin. Modified from Worsley (2008). Tectonic events from Gernigon et al. (2014)

The transition to cooler waters in the Boreal Ocean is probably also connected to the closing of a previously existing marine seaway to the Tethys Ocean during the Uralian orogeny. (Worsley, 2008).

Tempelfjorden Group

The Tempelfjorden Group of the latest Permian, perhaps most known for its spiculite shales, represents increasingly deep- and cold-water conditions. It overlies an erosional surface linked to sub-aerial exposure on platform areas, and represents a flooding event that also coincided with significant deepening of basins and basin-marginal areas (Worsley, 2008).

2.2.2 Mesozoic

Triassic

At the Permian-Triassic boundary, there is evidence of a significant hiatus and changing oceanic conditions (Vigran et al., 2014). The soft basal shales of the Sassendalen Group lack

the siliceous signature of the cemented spiculite cherts of the Tempelfjorden Group that it overlies. There have been some uncertainties regarding the age of the basal shales of the Sassendalen Group based on the palyno- and macrofauna; the former could suggest a Permian age, while the latter is indicative of a Mesozoic age (Worsley, 2008). These matters have now been resolved, and the basal shales are considered Triassic (Vigran et al., 2014). The deposits from Early Triassic show a general regressive trend, with high sedimentation- and subsidence rates. A repeated cycle of transgressions punctuates the regressive trend. Clinoforms across the Hammerfest Basin and onto Bjarmeland Platform suggest a paleo-coastline that was prograding in a northwesterly direction, with sediments sourced from the Baltic Shield, and eventually from the Urals (Glørstad-Clark et al., 2011; Lundschien et al., 2014; Klausen et al., 2015). The hydrocarbon-bearing Kobbe Formation (Figure 2.3) was deposited in this time interval (Worsley, 2008).

Sediments from the Storfjorden Subgroup (Figure 2.3) show a complex pattern across the Barents Shelf. On Spitsbergen, delta systems prograding from Greenland to the west had been active since Early Triassic, and continued into the Ladinian. Deposition of Late Triassic sandstones in the northern regions happened in a delta plain environment, with sediments sourced from the Urals (Glørstad-Clark et al., 2011).

These sandstones are typically immature with high content of volcanic fragments, possibly linked to a volcanic province northeast of the area, west of Franz Josef Land (Worsley, 2008; Smelror et al., 2009). Further south however, sands were derived from the more mature areas in the Baltic shield; coastal and channel sand bodies here (Snadd Formation) are generally better reservoir units, with higher primary porosity (Klausen et al., 2015).

The latest Triassic deposits came after a supra-regional transgression in the Norian; coastal and shallow-marine conditions dominated at a time where subsidence- and sedimentation rates were reduced to 5 % of those that had existed earlier in the Triassic (Worsley, 2008).

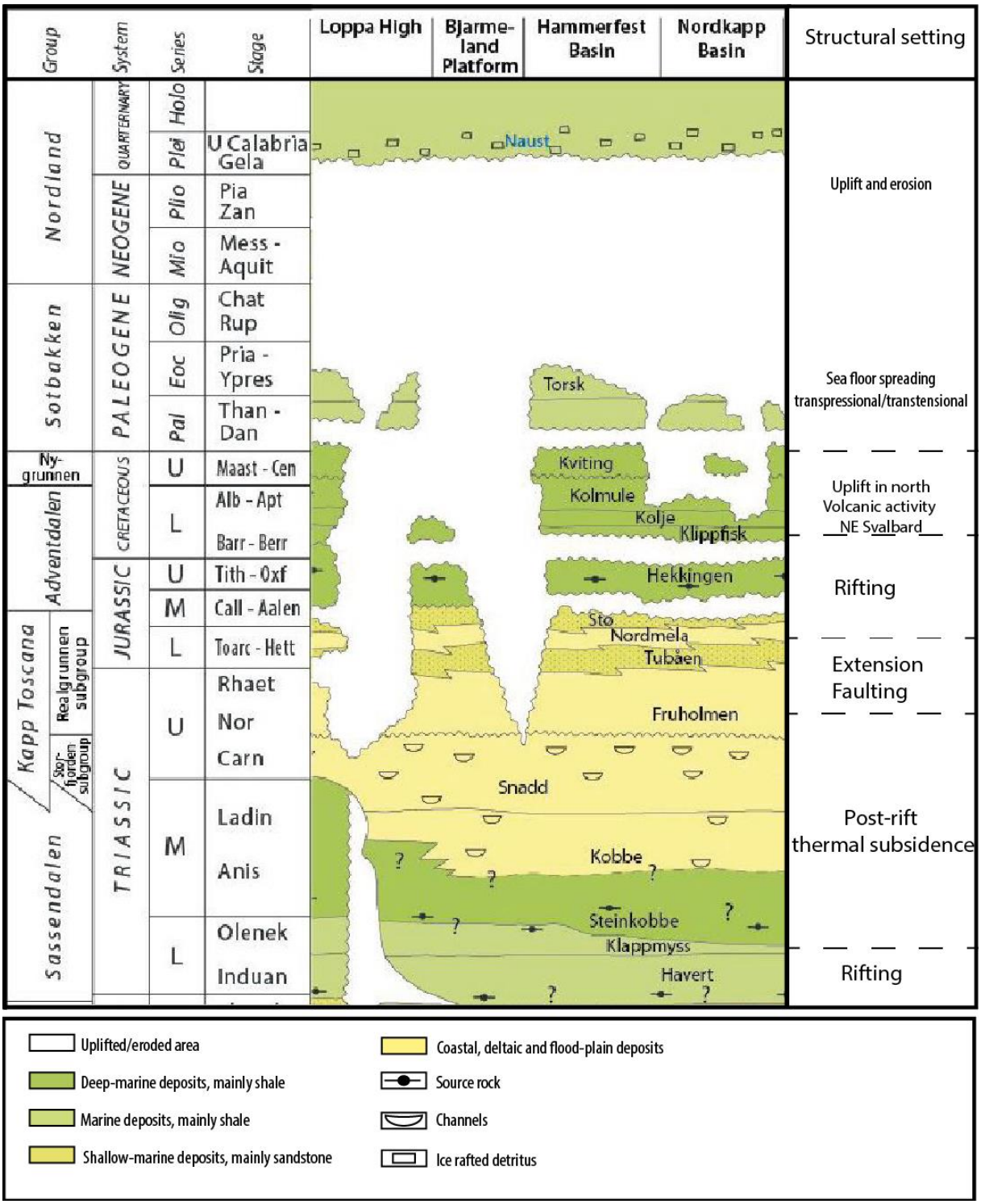

Figure 2.3: Lithostratigraphic chart showing the groups and formations from the Permian-Triassic boundary up until Holocene. Tectonic events from Gernigon et al. (2014), Smelror et al. (2009) and Worsley (2008) Modified from NPD (2014).

Jurassic

In the Hettangian, the Barents Shelf was uplifted and eroded, resulting in a largely missing sedimentary record in the region. The interval is represented by the sand dominated Tubåen Formation in smaller areas such as the Nordkapp-, Tromsø- and Hammerfest Basins. The facies suggest a tidally influenced environment dominated by estuarine and lagoonal conditions.(Smelror et al., 2009).

Renewed transgression in early Toarcian led to a change from the floodplain environments described above into a prograding coastal setting. The Stø Formation (Figure 2.3) consists of typical sand-dominated shoreface facies, with minor shale content, and is found in the Nordkapp Basin and on the Bjarmeland Platform among other areas. The sandstones of the Lower-Middle Jurassic interval is one of the main reservoirs in the southwestern Barents Sea (Faleide et al., 2015). In other areas across the Barents Shelf the interval is poorly represented, and condensed sections with phosphate-conglomerates are common in many places (Worsley, 2008; Smelror et al., 2009).

Renewed transgression in Mid-Jurassic resulted in a deeper marine setting, and coupled with anoxic conditions, resulted in the deposition of the Upper Jurassic black shales of Hekkingen Formation (Adventdalen Group), with high organic carbon content. Submergence of previous platforms and highs resulted in an evened out structural relief, however; Jurassic tectonism is still evident by thickness variations of hundreds of meters between basins and platforms (Worsley, 2008).

Cretaceous

Renewed regression followed the transgression that reached its maximum in Late Jurassic, and at the same time, the opening of the Amerasian Basin caused uplift of the northernmost areas. Anoxic conditions ceased as most areas saw renewed circulation, and the basins received fine-grained fan deposits sourced from nearby platform areas. The limestone/dolomite interbedded shales of Knurr-, Kolje- and Kolmule formations were deposited in the Hammerfest Basin and on southwestern shelf areas (Smelror et al., 2009). On the elevated platform areas however, sequences are much more condensed and carbonate-dominated

(Worsley, 2008). In the Late Cretaceous most areas were uplifted, and the deposition of the time-equivalent Nygrunnen Group was generally restricted to western marginal basins (Maher, 2001)

2.2.3 Cenozoic

The Sotbakken Group (Figure 2.3) represents the Paleogene record in the southwestern Barents Sea. The deposits, largely restricted to the western marginal basins, predominantly consist of grey- to olive colored claystone (Worsley, 2008; Smelror et al., 2009).

The Nordland Group (Figure 2.3) consists of Neogene and Quaternary sediments derived from repeated cycles of Plio-Pleistocene isostatic uplift and glacial erosion, and rest unconformably on top of Paleogene and Mesozoic units. It appears as a wedge that spills over the shelf edge, with the largest accumulations along the western shelf margin and in trough-mouth fans (i.e. Bjørnøya and Storfjorden Fans) (Worsley, 2008; Smelror et al., 2009).

2.3 Main structural elements

The Nordkapp Basin, Svalis Dome, Samson Dome and Norvarg Dome are the structural elements mainly focused on herein (Figure 1.1.). Some differences are evident directly by observing seismic data: while the Nordkapp Basin and Svalis Dome show salt movements that reach the Upper Regional Unconformity (*URU*) and seafloor, the Samson- and Norvarg domes are defined at Triassic/Jurassic level, with salt accumulations only in their cores. Furthermore, the Samson- and Norvarg domes are located on a platform area, whereas the Svalis Dome is a structural high with a related rim syncline in the Maud Basin, and the entire Nordkapp Basin is a structural depression.

2.3.1 Nordkapp Basin

The Nordkapp Basin is a more than 300 km long salt-controlled basin with an assumed age of Late Devonian- early Carboniferous. The basin is bounded by the Nysleppen- and Polstjerna fault complexes to the northwest, and by the Måsøy- and Tor Iversen fault complexes in the southeast. Further northwest and southeast lies the Bjarmeland- and Finnmark platforms respectively. The pre-salt history of the basin is lacking in detail, but the evaporites have an inferred age of late Carboniferous (Gabrielsen et al., 1990). At this time, the basin was probably a large-scale salina in a stable platform area, where evaporites were deposited at times of lowstand. However, evaporite deposition also occurred outside the basin margins (Gabrielsen et al., 1990; Nilsen et al., 1995). A two-part subdivision of the basin is common; a northeast-trending narrow southwestern subbasin and a wider east-trending northeastern subbasin, separated by an inter-basinal ridge (Koyi et al., 1993; Nilsen et al., 1995). These will be referred to as the northern and southern subbasins herein. Thickness of the evaporite layer has been reported to be up to 2 and 4-5 km in the southern and northern subbasin respectively (Nilsen et al., 1995; Faleide et al., 2015).

Central parts of the basin is dominated by several salt diapirs (Koyi et al., 1992, 1993; Nilsen et al., 1995), while the basin margins are associated with salt pillows and deep faults (Gabrielsen et al., 1992). Salt movements have been attributed to three main stages, each possibly also interrupted by minor lulls; initiation and continued growth throughout the Triassic, a

Cretaceous reactivation phase and a final reactivation phase in middle Cenozoic (Nilsen et al., 1995). Evidence of early-stage pillow formation is lacking according to Gabrielsen et al (1990). Contrarily, Koyi et al. (1993) argue that some of the diapirs show evidence of an early pillow stage.

2.3.2 Samson Dome

The Samson Dome is located on the southern part of Bjarmeland Platform, slightly west of the southwestern Nordkapp Basin. The core of Carboniferous evaporites has a circular-elliptical shape in map view, and overlying Cretaceous strata show the same doming. No primary rim syncline has previously been described in the literature. The URU truncates the crest of the dome, leaving only a thin Lower Cretaceous unit. (Gabrielsen et al., 1990). Both Cretaceous and pre-Cretaceous salt movements have been described in previous works, attributed to the opening of the North Atlantic Ocean, and the Middle to Late Triassic shelf progradation respectively (Gabrielsen et al., 1990; Mattos et al., 2016). The salt is assumed to be of Carboniferous age, deposited in the Paleozoic Ottar Basin with thicknesses up to 2.4 km (Breivik et al., 1995)

2.3.3 Norvarg Dome

Situated near the northeastern termination of the Swaen Graben on the southern Bjarmeland Platform, the Norvarg dome appears as a circular-elliptical positive feature. As with the Samson dome, a Carboniferous age is estimated for the evaporites in its core. There is also no primary rim syncline related to the structure. A thinning of overlying Triassic and Jurassic strata have been described, suggesting that salt movements may have taken place in this period. Here too, the URU truncates the crest of the dome leaving a thin unit of Lower Cretaceous strata at the crest. (Gabrielsen et al., 1990). The salt at the core of the Norvarg Dome was deposited in the Ottar Basin, and assumed to be of Carboniferous age (Breivik et al., 1995).

2.3.4 Svalis Dome

The Svalis Dome is a sub circular salt dome situated at the northeastern margin of Loppa High, in immediate vicinity to the Maud Basin, and has a diameter of approximately 35 km. The Svalis Dome can be classified as a salt pillow, with a possible minor diapir at its crest. The salt here is probably of late Carboniferous age. Several growth phases are recognized from Early Triassic to Cenozoic. Due to its location, salt movements may be related to repeated uplift of Loppa High (Gabrielsen et al., 1990).

3 Data and Methods

Seismic 2D- and 3D data, made available through the Norwegian Petroleum Directorate (NPD), is the foundation of this study. In addition, implementation of well logs that are publicly available through NPD provide the means for chronostratigraphic tie-in with the seismic horizons.

3.1 Seismic data

Interpretation of the seismic- and well data was performed in Schlumberger's *Petrel 2016* software package. Nomenclature regarding seismic wave attributes, such as phase and polarity, follow the SEG standard convention (Badley, 1985). By this definition, a reflection from a unit boundary with positive acoustic impedance will generate a wavelet peak as seen in Figure 3.1, assuming the data is normal polarity. The impedance contrast is given by the following equation:

$$z = \rho V$$

where (ρ)=density of the sediment, and (V)= the velocity that the wave travels through the sediment.

For a reverse polarity dataset, the same unit boundary would result in a trough, representing negative values. To determine phase and polarity of the surveys, the seafloor was used as reference, as it will always display positive acoustic impedance.

If the data is minimum-phase, the energy will be frontloaded, with minimum amplitude located immediately before time-zero, while if processed to zero-phase it will be symmetrical with the peak or trough centered at the unit boundary (time-zero), as seen in Figure 3.1 (Brown, 2011). A zero-phase signal can be beneficial in seismic interpretation, due to the ease

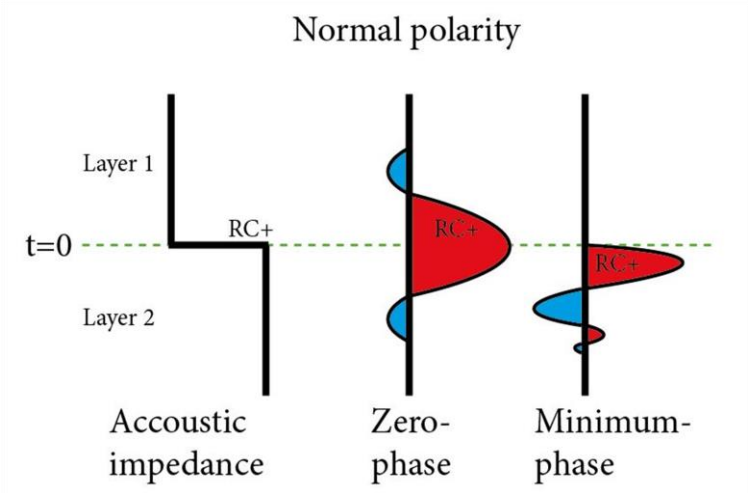

Figure 3.1: Zero-phase and normal-phase signal at a boundary with increasing acoustic impedance assuming normal polarity following the SEG standard. RC= reflection coefficient (Modified from Brown, 1999)

of picking between peak and trough for any seismic horizon. The fact that energy arrives before time-zero in the case of a zero-phase signal is a theoretical problem not considered in the regional interpretation performed for this thesis. Tables 3.1 and 3.2 show the polarity and phase of the available 2D- and 3D surveys, along with general information attained from NPD. None of the seismic surveys were depth-converted, so all profiles and maps are based on two-way travel time (TWT).

Table 3.1: General information about the 2D-surveys used. Gathered from NPD factpages.

Dataset	Phase	Polarity	Shot by	Shot for	Acquisition Year	Number of lines in study area
NBR06	Zero	Normal	Fugro/TGS	Fugro/TGS	2006	10
NBR07_RE09	Zero	Normal	Fugro/TGS	Fugro/TGS	2007	12
NBR08	Zero	Normal	Fugro/TGS	Fugro/TGS	2008	30
NBR09	Zero	Normal	Fugro/TGS	Fugro/TGS	2009	20
NBR10	Zero	Normal	Fugro/TGS	Fugro/TGS	2010	15
NBR11	Zero	Normal	Fugro/TGS	Fugro/TGS	2011	6
NBR12	Zero	Normal	Fugro/TGS	Fugro/TGS	2012	27
NBR14	Minimum?	Normal	Fugro/TGS	Fugro/TGS	2014	14

Table 3.2: General information regarding the available 3D-surveys. Gathered from NPD factpages.

Dataset	Phase	Polarity	Shot by	Shot for	Year	Diapirs Covered
ST0309	Zero	Normal	PGS	Statoil	2003	5
ST0624	Zero	Normal	WesternGeco	Statoil	2006	1
ST0811	Minimum	Normal	PGS	Statoil	2008	3
ST0828	Zero	Normal	Fugro	StatoilHydro	2008	0
ST10011	Minimum	Normal	Fugro	Statoil	2010	9
ST9403R01	Zero	Normal	Geco	Statoil	1994	4

3.1.1 2D data

The 2D-seismic surveys used in this thesis are all part of the dataset *Norwegian Barents Renaissance* (NBR) collected by TGS-NOPEC Geophysical Company ASA in collaboration with Fugro N.V. between 2006 and 2014 (Table 3.1). The dataset (Figure 3.2) covers the southwestern Barents Sea, interpretation of the data however is confined to the areas immediately between, in, and surrounding Nordkapp Basin and the Svalis-, Norvarg-, and Samson domes. Data coverage is limited in the northeastern part of Nordkapp Basin, where line spacing is upwards of 10 km. In the remaining areas, line spacing is in many instances less than 5 km. The number of lines from each survey present within the study area is given in Table 3.1. The benefit of using this dataset is that it was collected by the same company over a large area, and data collection parameters are thus expected to be consistent.

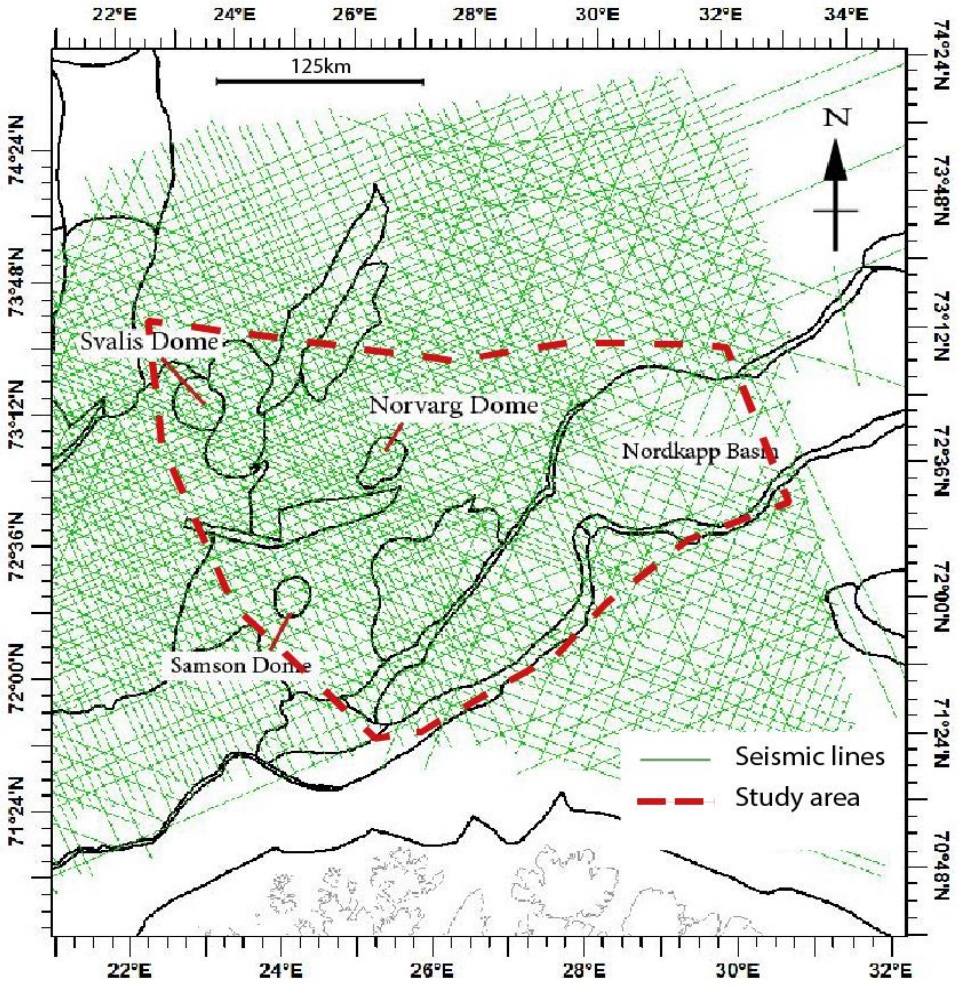

Figure 3.2: 2D-seimsic coverage from the NBR dataset (green lines) in the Nordkapp Basin and around the studied domes. Structural elements compiled from NPD.

3.1.2 3D data

Six 3D-seismic surveys were available in this thesis (Figure 3.3), all collected on behalf of Statoil ASA (also StaoilHydro ASA, now Equinor ASA) in the period 1994-2010. (Table 3.2). 3D-seismic data has some advantages over 2D-seismic data; the line spacing is closer, and when migrated it offers a better horizontal resolution. Processed 3D data offers a horizontally continuous image of the subsurface, while with 2D data, interpolation between lines several km apart is necessary. This means that 3D data offer a more detailed depiction of interpreted horizons in the salt-distorted areas surrounding and between the salt structures of Nordkapp Basin. The 3D seismic data increased the certainty of interpreted horizons within the basin. ST0828 covers no salt structures, but was essential when correlating horizons in the southern Nordkapp Basin across the Nysleppen Fault Complex to well 7226/11-1.

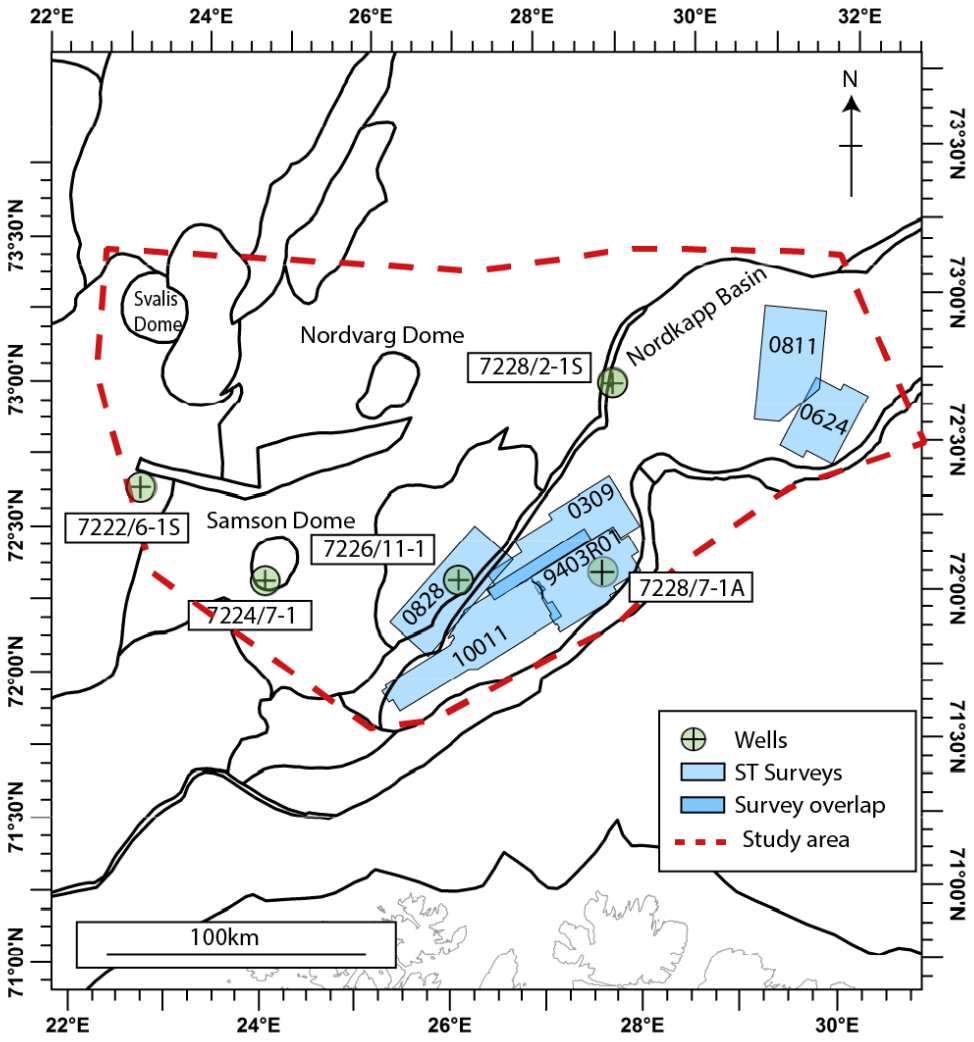

Figure 3.3: Location of the 3D seismic surveys and wells that were available for the study. Structural elements and seismic survey polygons compiled from NPD.

3.2 Seismic resolution

3.2.1 Vertical resolution

Vertical resolution is a measurement of the smallest vertical size an object or a layer can have to be distinguishable in seismic data. It is found using the following equation:

$$v_r = \frac{\lambda}{4}$$

Where the wavelength (λ) can be found if velocity (v) and frequency (f) is known:

$$\lambda = \frac{v}{f}$$

Dominating frequencies were found using spectral analysis on cropped volumes around key horizons in the datasets, and velocities gathered from the sonic log of well 7226/11-1. The calculated vertical resolutions for datasets NBR06, NBR12 and ST0828 are shown in Tables 3.3, 3.4 and 3.5 respectively. The NBR06 and NBR12 numbers were chosen because they represent the oldest and newest 2D data that are processed to zero phase, and show that there has been a minor improvement in resolution over the years. The ST0828 is representable of the increased horizontal resolution offered from a migrated 3D seismic dataset.

3.2.2 Horizontal resolution

The horizontal resolution is the distance needed horizontally to differentiate between two subsurface features in seismic data. The horizontal resolution is defined by the radius of the first Fresnel zone, which is given by the following equation:

$$r_f = \frac{v}{2}\sqrt{\frac{t}{f}}$$

Where (v) = velocity, (f) =frequency and (t) =two-way travel time in seconds.

When migrating seismic data the Fresnel zone is reduced to a sphere of which radius equals the vertical resolution, so then horizontal resolution can be calculated using the same equation:

$$H_r = \frac{\lambda}{4}$$

Tables 3.3, 3.4 and 3.5 show the calculated horizontal resolution for the previously mentioned datasets, and in the case of the ST0828 dataset, this includes both pre-migration and migrated horizontal resolution between Base Cretaceous Unconformity (BCU) and Near-top Permian (NT-Permian).

Table 3.3: Calculated vertical (Vr) and horizontal (Hr) resolution for the NBR06 dataset.

Horizon	Velocity (m/s)	Frequency (Hz)	Wavelength (m)	Vr (m)	Hr (m)
BCU	2628	37.43	70.21	17.55	223
Kobbe	3175	24.84	127.82	31.96	390
Havert	4354	24.67	176.49	44.12	633
NT-Permian	5255	13.58	386.97	96.74	1130

Table 3.4: Calculated vertical (Vr) and horizontal (Hr) resolution of the NBR12 dataset.

Horizon	Velocity (m/s)	Frequency (Hz)	Wavelength (m)	Vr (m)	Hr (m)
BCU	2628	38.10	68.98	17.25	221
Kobbe	3175	24.84	127.82	31.96	390
Havert	4354	19.74	220.57	55.14	708
NT-Permian	5255	15.32	343.02	85.76	1061

Table 3.5: Calculated vertical (Vr) and horizontal (Hr) resolution of the ST0828 dataset. U=unmigrated, M= migrated.

Horizon	Velocity (m/s)	Frequency (Hz)	Wavelength	Vr (m)	Hr (m) U/M
BCU	2628	38.02	69.12	17.28	221 / 17
Kobbe	3175	28.71	110.59	27.65	363 / 28
Havert	4354	19.26	226.06	56.52	717 / 57
NT-Permian	5255	14.93	351,98	88.00	1075 / 88

Figure 3.4 shows examples of the different resolutions offered from 2D- and 3D seismic data. The increased horizontal resolution offers a better depiction of layers towards the salt, and the salt body appears to have a smaller lateral extent in the 3D seismic image (ST9403R01).

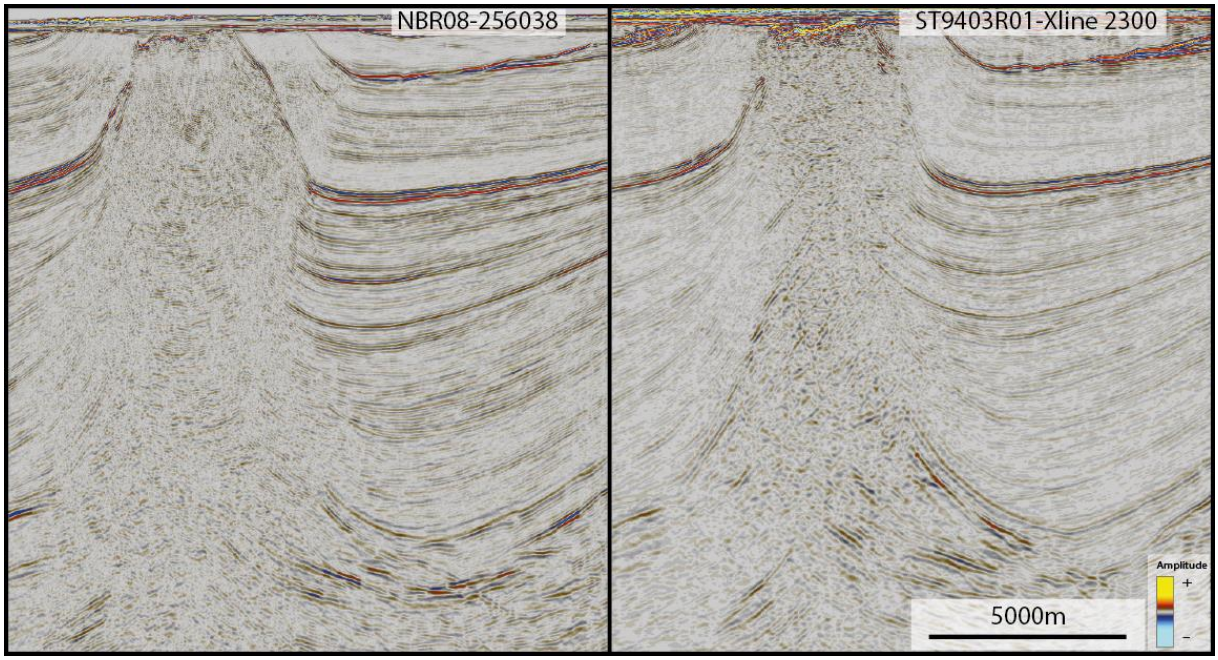

Figure 3.4: The two seismic sections show the effect of different resolution in the datasets. The 3D data (right frame) has higher horizontal resolution, resulting in a narrower zone of chaotic reflections. Note that the orientation is slightly different, but show the same salt body.

3.3 Well Data

Five wells were applied for seismic tie and age constrain in this study; general information about these can be seen in Table 3.6. The wells were chosen based on location at or adjacent to the structures investigated and / or that the well had penetrated as old as possible units, to ensure that chronostratigraphic correlation of interpreted horizons would be possible throughout the study area. Figure 3.3 shows their location.

Table 3.6: General information about the five wells used in this study. Gathered from NPD factpages.

Well	Location	Drilled by	Year drilled	Oldest penetrated formation	Content
7222/6-1S	Bjarmeland Platform	StatoilHydro	2008	Havert Fm	Oil/Gas
7224/7-1	Samson Dome	Statoil	1988	Havert Fm	Shows
7226/11-1	Norsel High	Statoil	1988	Basement	Gas
7228/2-1S	Nordkapp Basin	Mobil	1989	Havert Fm	Shows
7228/7-1A	Nordkapp Basin	Statoil	2001	Klappmyss Fm	Oil/Gas

Figure 3.5 shows the interpreted horizons and how they were tied to well 7226/11-1. Information about the wavelet-phase pick can be seen in Table 3.7. Well 7226/11-1 is the only well applied that penetrated Permian strata, while the other wells used herein all penetrate Triassic strata. This means that more well ties across the study area offer a higher degree of certainty to the regional interpretation of the Triassic horizons than for the NT-Permian.

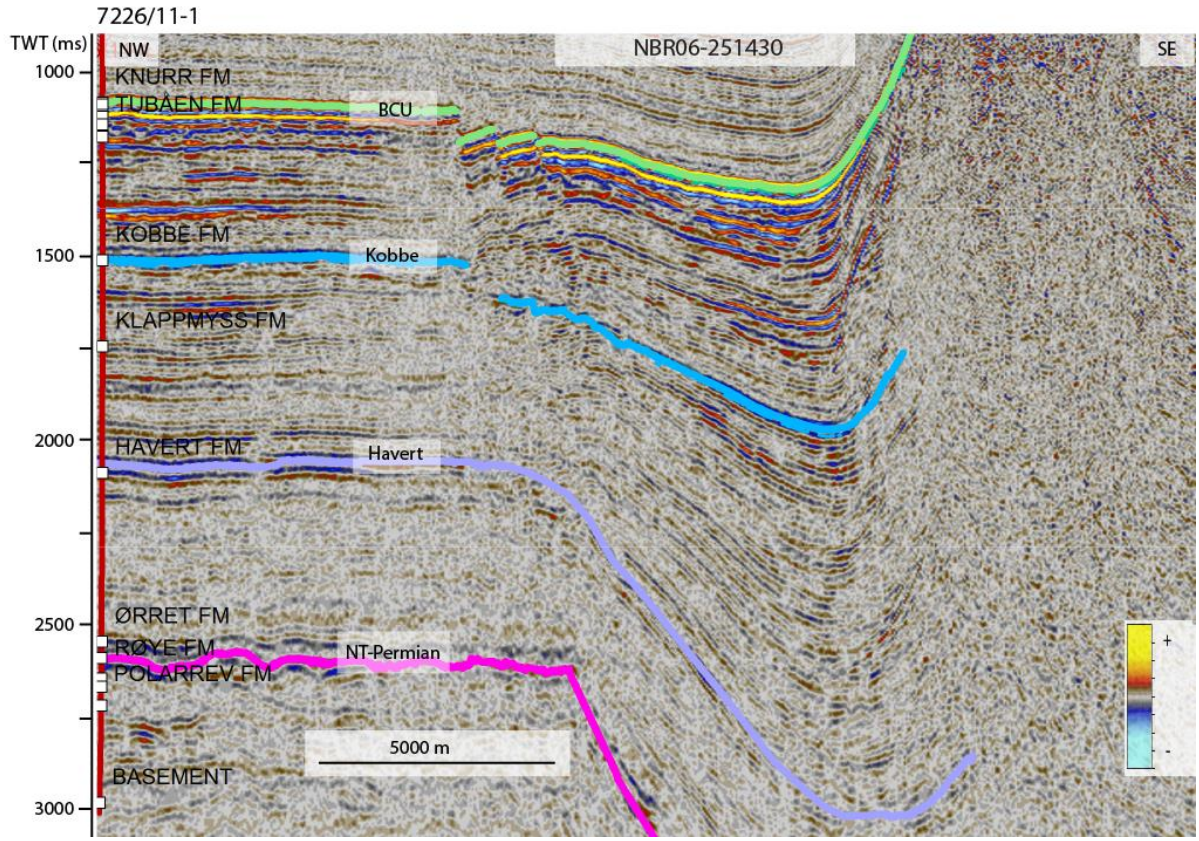

Figure 3.5: Welltops of well 7226/11-1 on seismic line NBR06-251430. The lowermost horizon is tied to Røye Formation in this case, but is named Near-Top (NT) Permian due to uncertainties in other areas. The uppermost horizon (BCU) represents the transition from the Cretaceous Knurr Formation to the Upper Jurassic shales of Hekkingen-, Stø- and Tubåen Formations. Top Kobbe and Top Havert horizons are tied to the Kobbe FM and Havert FM welltops respectively.

Table 3.7: Information regarding wavelet phase pick for interpretation and color codes of the interpreted horizons.

Horizon	Phase pick	Color code	Pick confidence
BCU	Trough	Green	High
Kobbe Fm	Peak	Blue	Medium-High
Havert Fm	Peak	Purple	Low-Medium
NT-Permian	Peak	Pink	Medium

3.4 Interpretation in a salt tectonic setting

3.4.1 Time vs depth

While interpreting in a salt influenced setting, some factors need to be taken into account:

- With its velocity of 4,500 m/s pure salt has a considerable higher transit time of seismic waves than siliciclastic sediments, which results in a pull-up effect of any subsalt sediments (Jackson and Hudec, 2017). For this thesis however, subsalt interpretation will not be of much significance, so another related issue is more pressing;
- Lateral misplacement of reflections during migration can also happen if the model used does not have salt velocities built in (Jackson and Hudec, 2017). In the Nordkapp Basin with its abundant salt structures and rim synclines, this leads to some uncertainties regarding the image in areas in close vicinity to the salt, especially if there is a salt overhang present.

3.4.2 Amplitude

With the mentioned velocity of salt and it's density of 2040 kg/m^3 salt will usually appear as a strong positive reflection when surrounded by moderately compacted siliciclastic rocks so that strong amplitudes can be one of the criterions when identifying the salt. If there is a salt overhang, it can lead to a distorted seismic image below the overhang, which can be an issue when interpreting strata in close vicinity to the salt body. If surrounded by carbonates or highly cemented siliciclastic rocks however, the acoustic impedance contrast could be lowered or even reversed, resulting in negative amplitudes or no amplitude at all (Jackson and Hudec, 2017).

3.4.3 Internal reflections

Due to the generally homogenous nature of salt, a good criterion for recognition is the chaotic pattern of reflections that appear in the salt bodies. Except for some impurities, there is no reason to expect any layering internally, so juxtaposed to sedimentary rocks the salt bodies should stand out. Delimiting the salt flanks however, is not necessarily straightforward considering abovementioned problems regarding misplacement of reflectors. The generally

strong reflection coefficient appearing at the top of salt can also lead to a masking-effect in deeper parts.

3.4.4 Jump-correlation

Due to the complex pattern of salt structures and related rim synclines in the Nordkapp Basin, interpretation of the horizons could not always be based on well correlation. In these instances the jump-correlation method was used, where interpreted horizons are extrapolated across the salt structure (Grimstad, 2016) (Figure 3.6). The main criteria to achieve a convincing result was seismic signature; i.e. reflector configuration, amplitude trends and unit thickness, together with visual depth estimation. *Petrel's* "Seismic Ghost" tool allows the user to crop a part of the seismic, and put the cropped image as a partly transparent overlay over other parts, for visual comparison. The tool was used accordingly when jump correlating between diapirs. It is still worth mentioning that this method adds some uncertainty to the interpreted horizons.

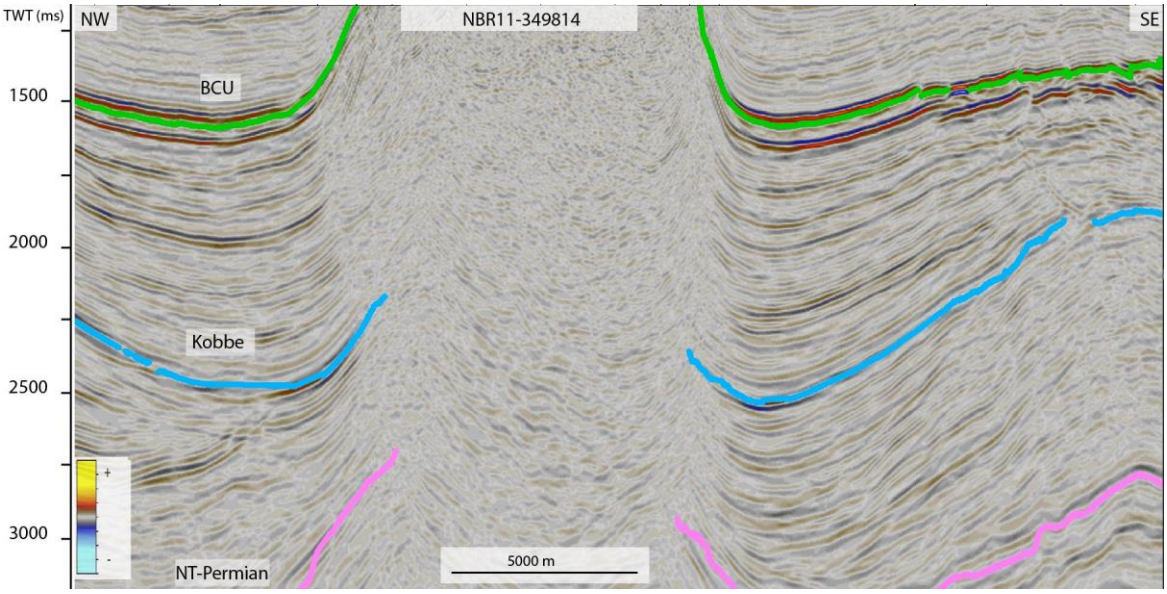

Figure 3.6: Extrapolation of BCU, Top Kobbe and NT Permian from the northwestern side of a diapir, where well 7226 nearby provided a well-tie. Note the similar seismic signature and depth on the southeastern side.

4 Results

4.1 Stratigraphic framework and regional profiles

This chapter presents documentation of the seismic interpretation performed for the study. An overview of the interpreted horizons (Figure 4.1) is presented below, displaying the corresponding seismic units that will be covered in this chapter. The boundary between the Lower and Lower to Middle Triassic is defined herein at the base of the Olenekian Klappmyss Formation (section 2.2.2).

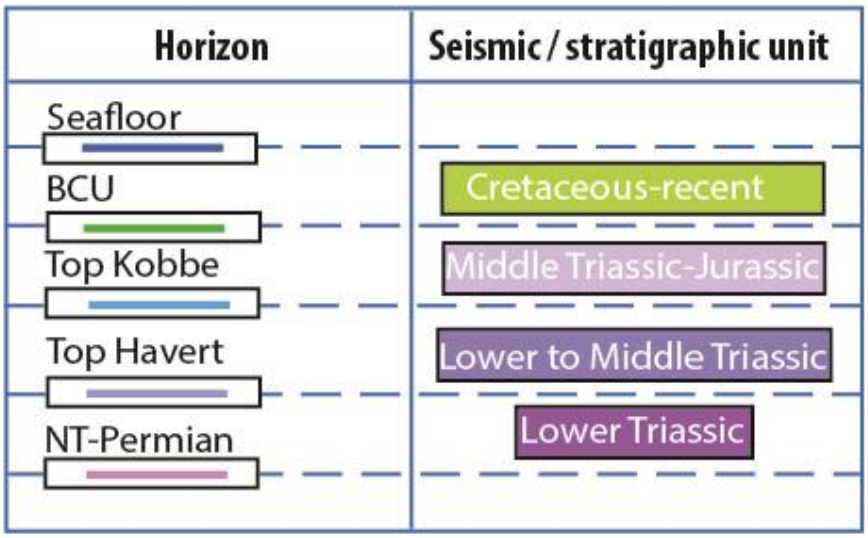

Figure 4.1: An overview of how the seismic units correspond to the regional horizons interpreted for the study.

Figure 4.2 shows a structural map of the study area, along with the seismic lines interpreted in Figures 4.3-4.7. These lines present the regional development of the seismic units and horizons across the major structural elements in the study area.

The following depths and thicknesses given for horizons and units are all in milliseconds (*ms*) two-way travel time (*TWT*).

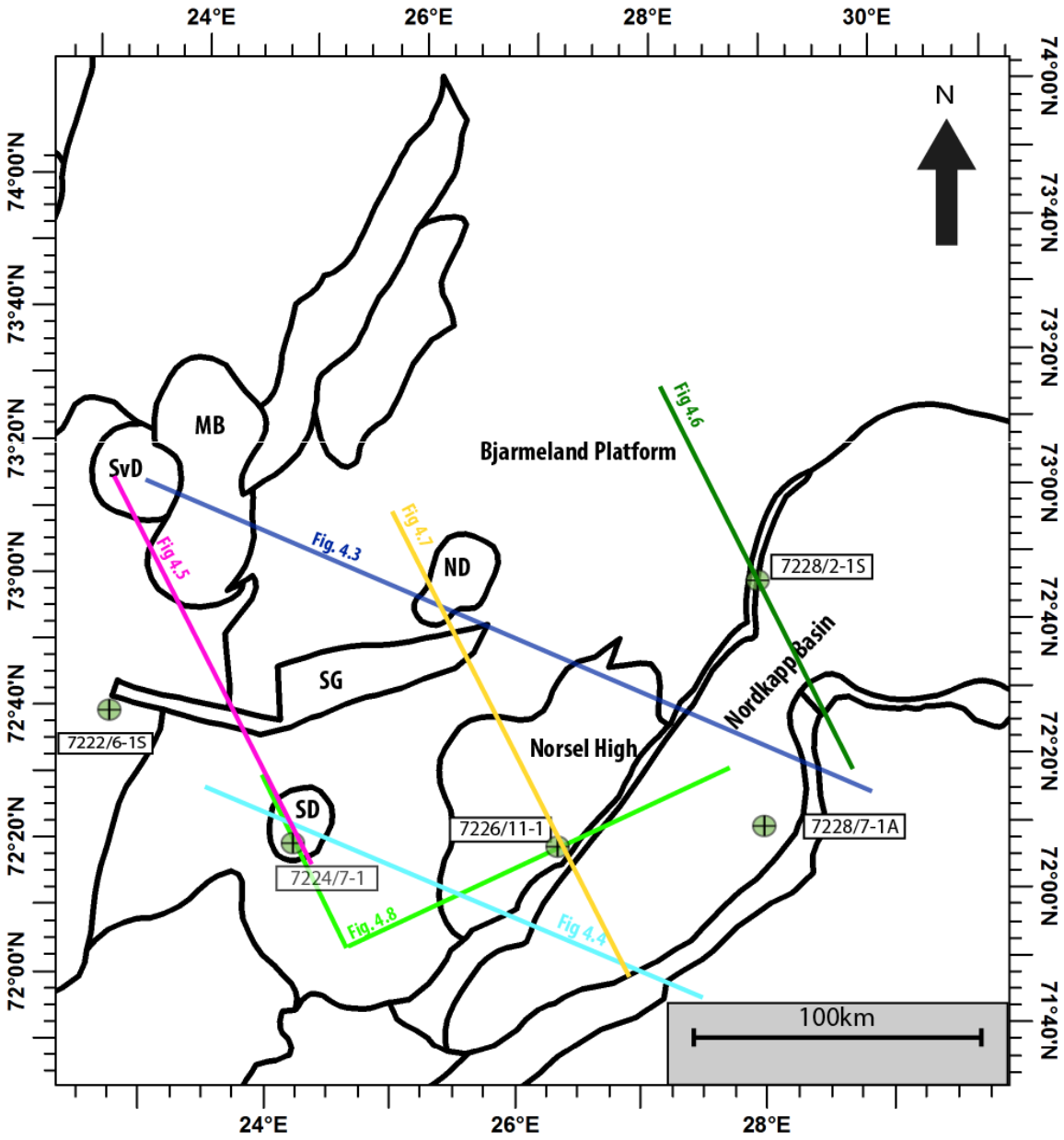

Figure 4.2: Map showing the location of regional seismic profiles presented in this chapter, in relation to the major structural elements of the area. MB=Maud Basin, ND=Norvarg Dome, SD=Samson Dome, SvD=Svalis Dome. Structural elements from NPD. Locations of key exploration wells 7222/6-1S, 7224/7-1, 7226/11-1, 7228/7-1A and 7228/2-1s, used for stratigraphic correlation, are shown in relation to the structural elements.

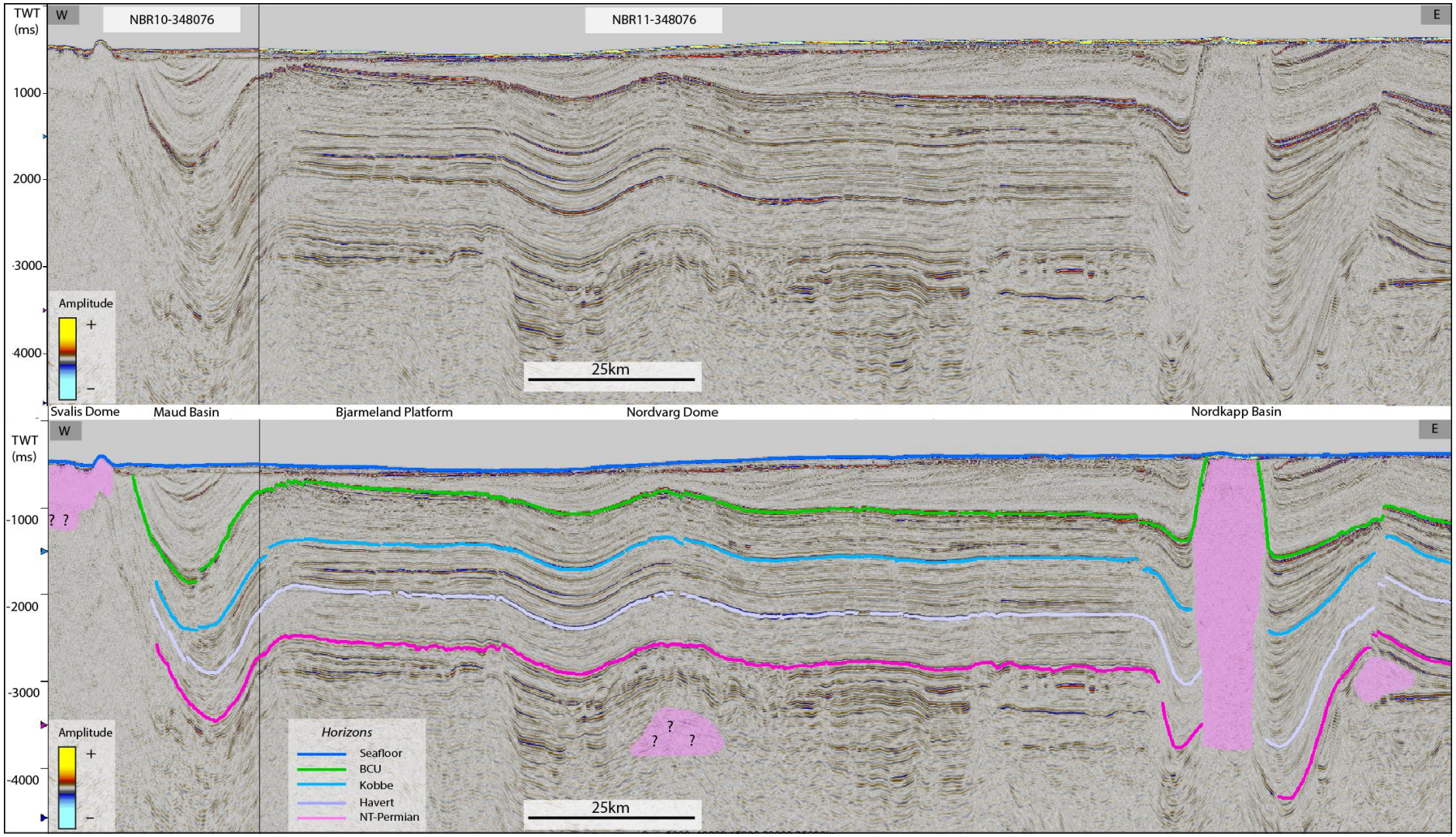

Figure 4.3: A) Seismic profile extending from the Svalis Dome (west) to the Nordkapp Basin (east). A depression appears directly west of the Norvarg Dome, affecting all the key horizons. B) Interpreted version of the same line showing all horizons. The profile is a composite line from surveys NBR10 and NBR11. Location of the composite line is shown in Figure 4.2.

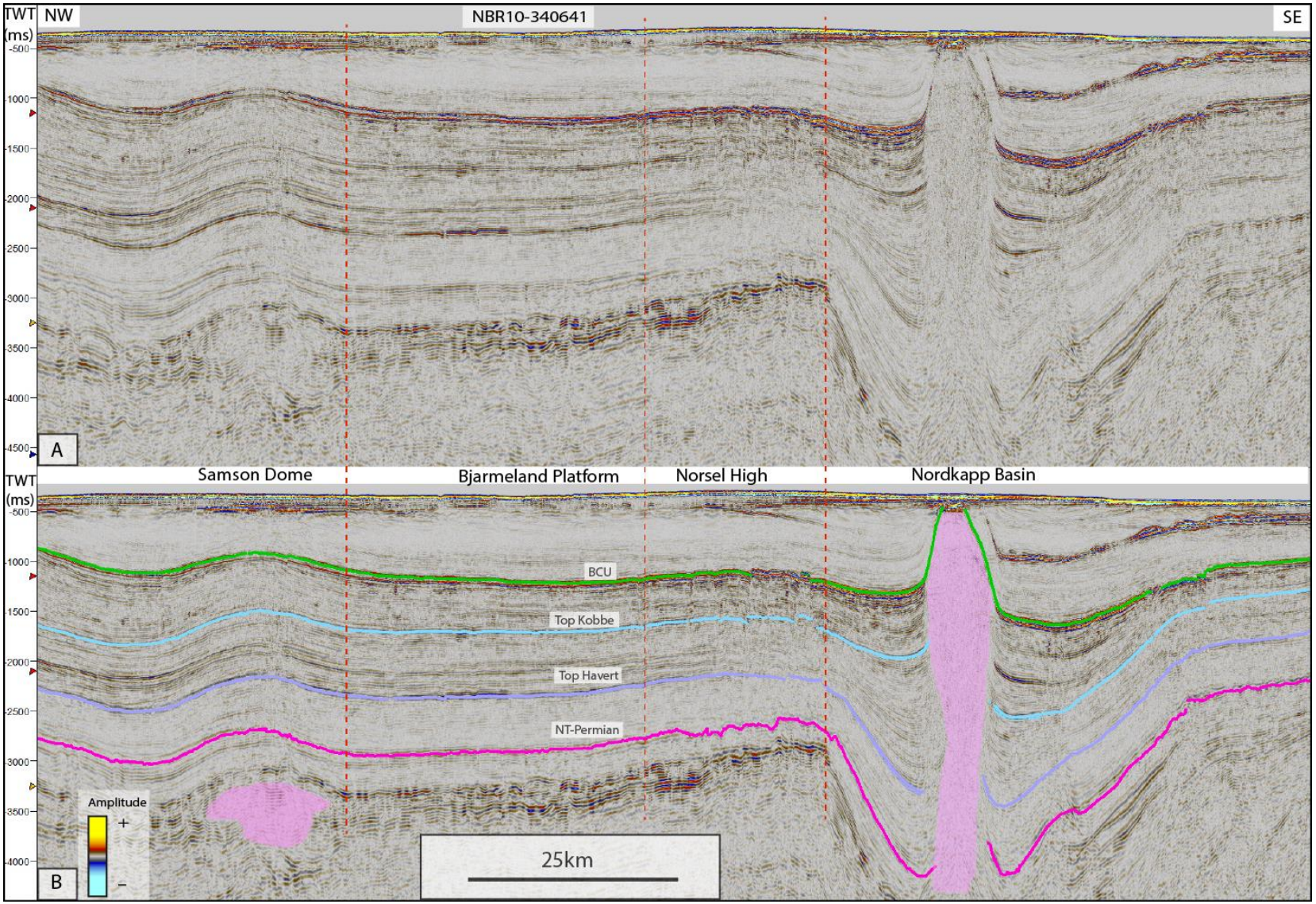

Figure 4.4: Regional line extending from the Samson Dome to the southern Nordkapp Basin. A salt diapir in the Nordkapp Basin is shown in pink. Figure 4.2 displays the location of the line.

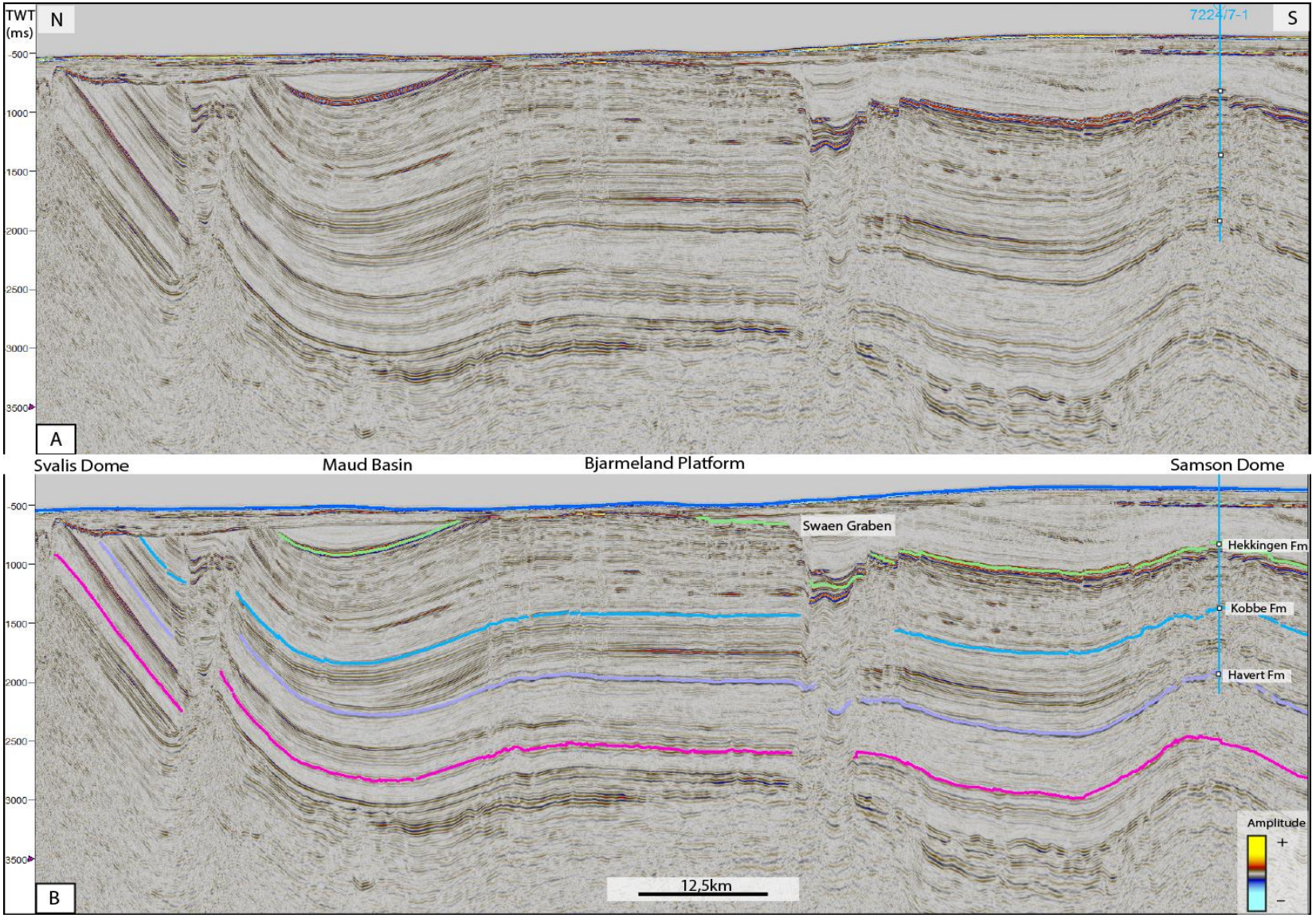

Figure 4.5: Regional line extending from the Svalis Dome to the Samson Dome. Well 7224/7-1 is seen towards the south (Samson Dome). The horizons are truncated by the URU towards the Svalis Dome. A) Uninterpreted. B) Interpreted. Figure 4.2 displays the location of the line.

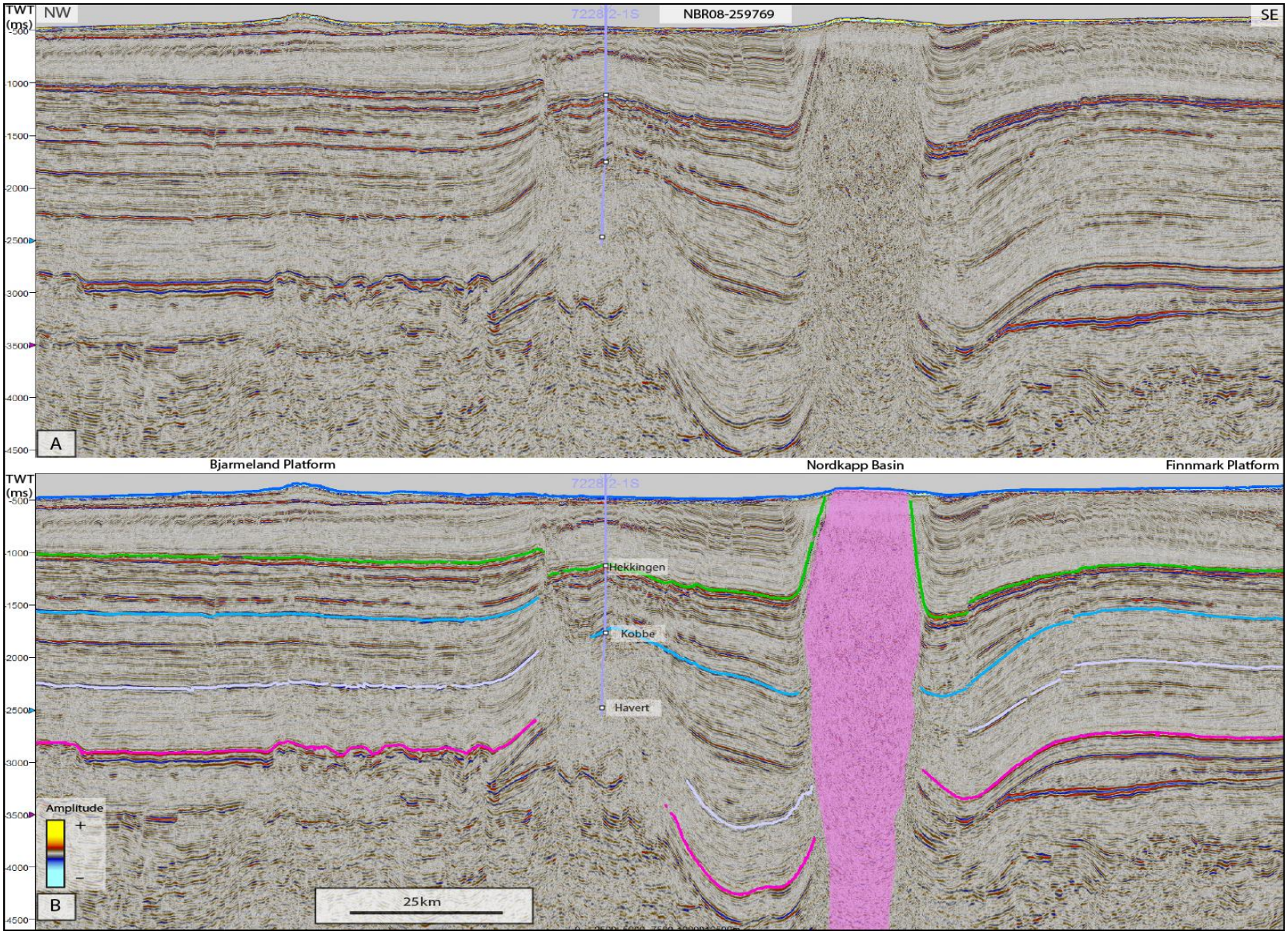

Figure 4.6: Regional line extending across the central Nordkapp Basin, with Bjarmeland Platform to the northwest, and Finnmark Platform to the southeast. Well 7228/2-1s can be seen in a faulted area at the northwestern basin margin. A) Uninterpreted. B) Interpreted. Location of line is shown in Figure 4.2.

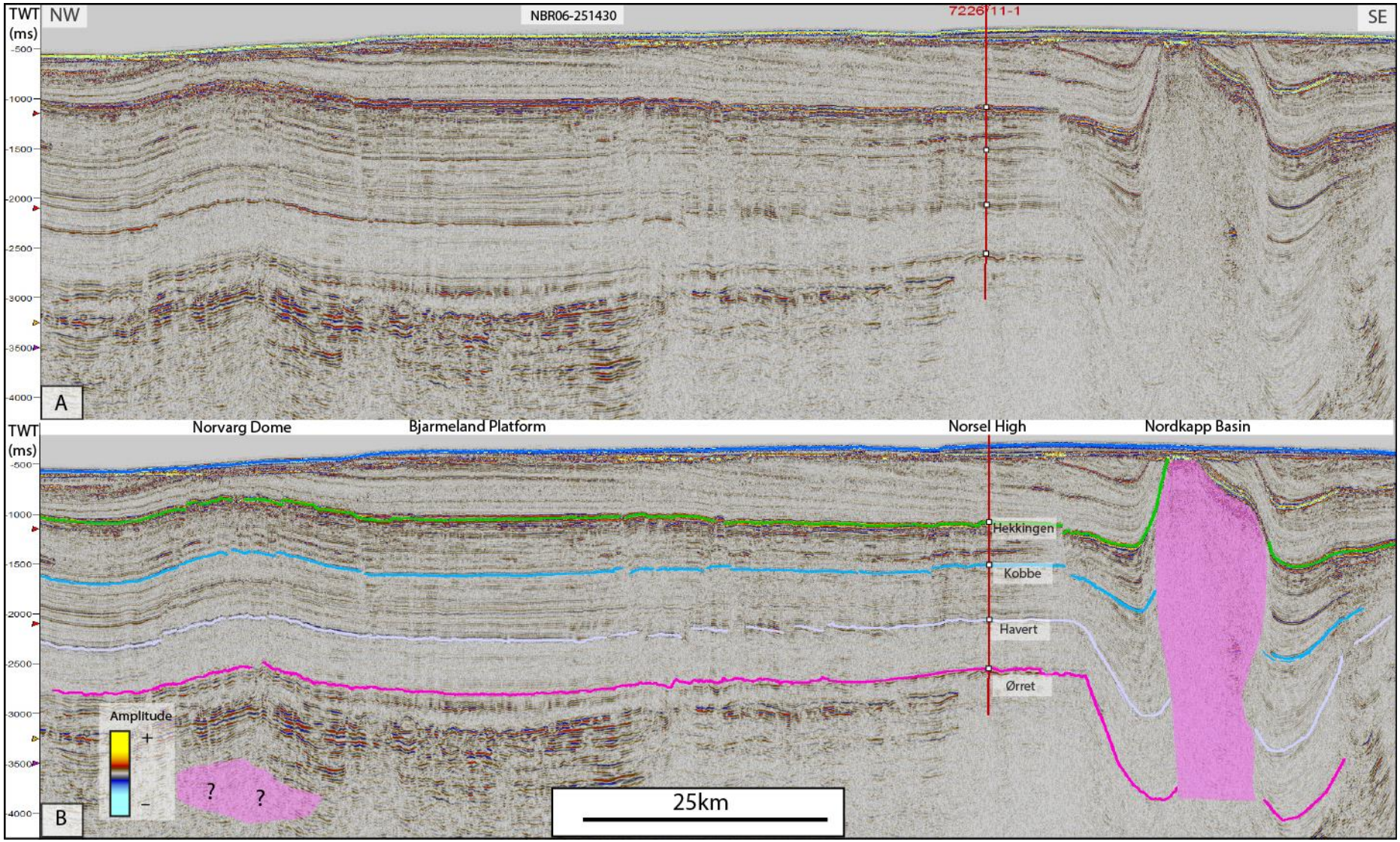

Figure 4.7: Regional seismic line extending from the Norvarg Dome to the Nordkapp Basin. Well 7226/11-1 penetrates NT-Permian (Ørret Formation) on the Norsel High. A) Uninterpreted, B) interpreted. Location of the line displayed in Figure 4.2.

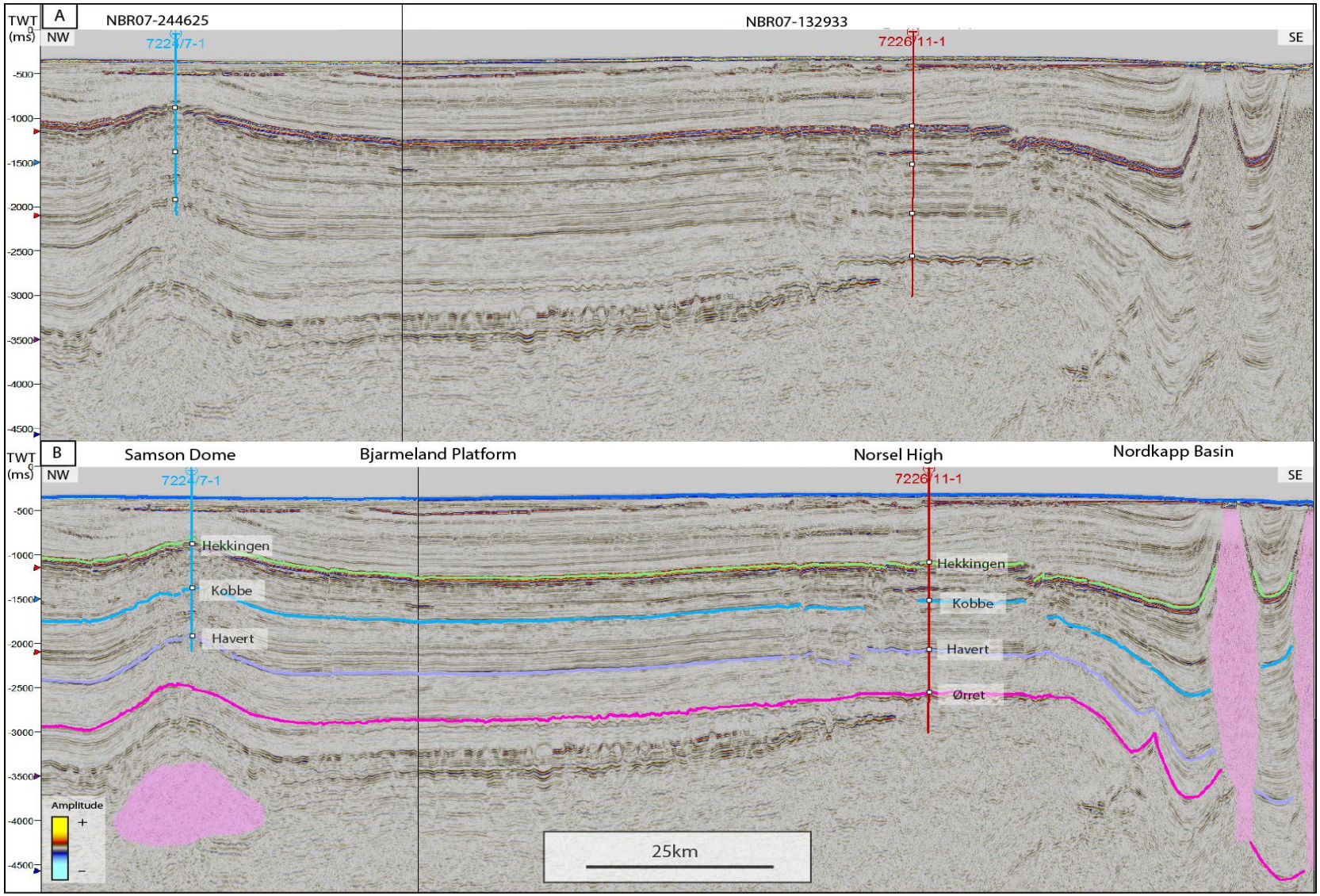

Figure 4.8: Regional profile extending from the Samson Dome to Nordkapp Basin through the Norsel High. The profile is made from a composite line, of which location is shown in Figure 4.2.

4.2 Seismic horizons

4.2.1 NT-Permian

The NT-Permian horizon (Figure 4.9) represents the transition between Permian carbonates and overlying Triassic siliciclastic sediments (see sub-chapters 1.2.1- 1.2.2 and 3.3). The horizon shows local differences in seismic signature across the study area, with amplitudes ranging from low to high. In the Nordkapp Basin, low amplitudes and a discontinuous reflection are characteristic. The horizon was generally picked on a peak, where the transition from overlying shales of the Sassendalen Group to spiculites of Tempelfjorden Group represents a positive reflection coefficient. It is worth noting however, that a negative reflection coefficient might represent the boundary in places where spiculites were not deposited.

The horizon generally follows the morphology of the larger structural elements present in the study area, i.e. the deepest areas are found in the Maud Basin (3500 ms) and Nordkapp Basin (deeper than 4000 ms) (Figure 4.3). The northern part of the Nordkapp Basin appears to have a higher relief to surrounding platform areas compared to its southern counterpart, 2000 ms and 1000-1500 ms respectively. Interpretation in the northern Nordkapp Basin is mostly restricted to the outermost parts due to the large salt presence in the center of the basin.

The horizon is shallowest around the Svalis- (1000 ms), and Norvarg- and Samson domes (2500 ms), where they arch up to generate a relief to the surrounding areas. The relief is greatest at the Svalis Dome (2500 ms), while at the Samson Dome a depression located to the southwest of the dome gives a relief of approximately 800 ms (Figure 4.4). At the Norvarg Dome, the difference in elevation from the dome to a depression situated directly west is 400 ms (Figure 4.3). A flat morphology characterizes the central parts of the study area, i.e. Bjarmeland Platform (excluding the Samson- and Norvarg domes), and the horizon is here situated between 2500 and 2800 ms.

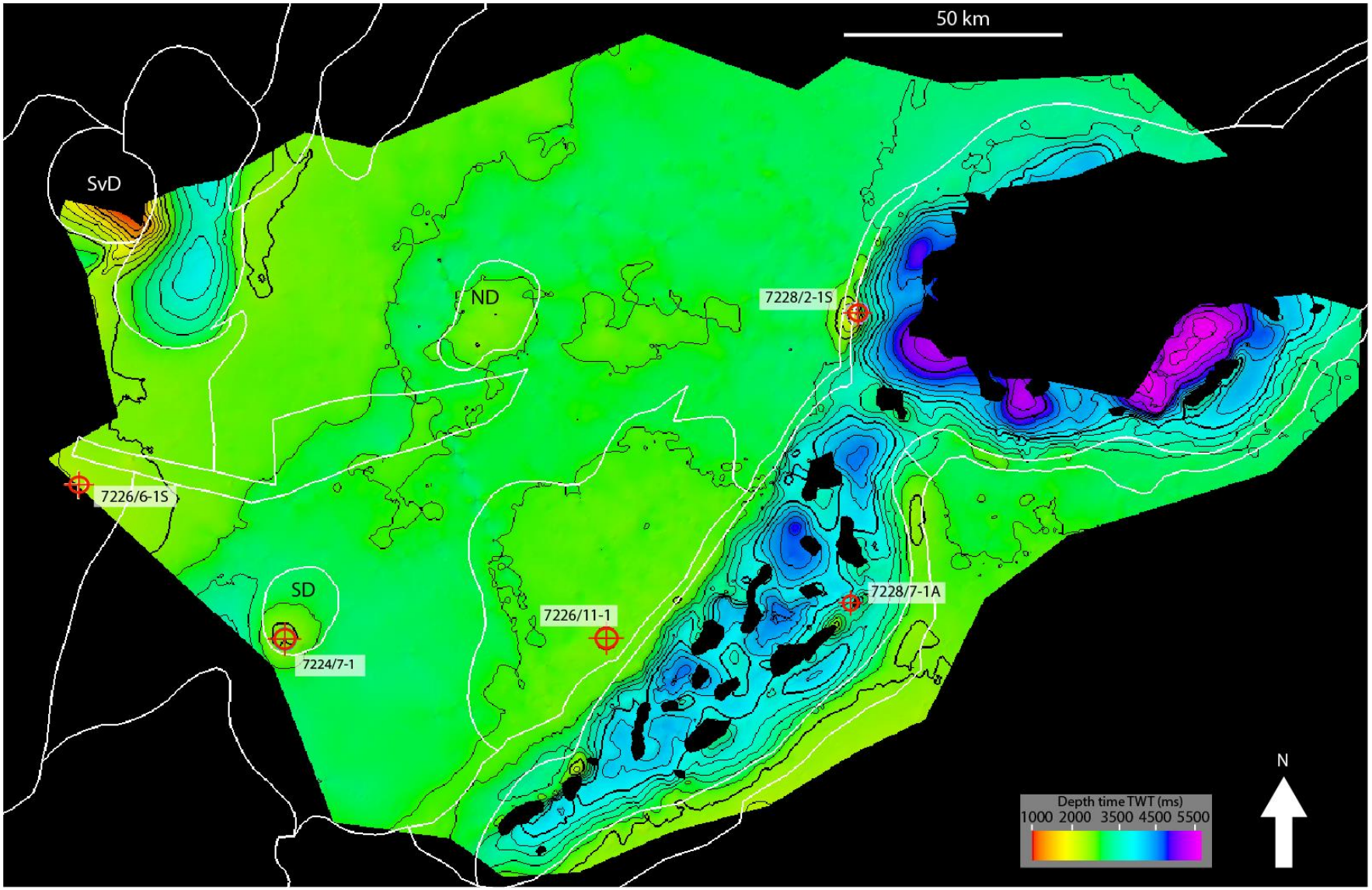

Figure 4.9: Isochron map of the NT-Permian horizon, depths displayed in TWT (ms). SvD=Svalis Dome, SD=Samson Dome, ND=Norvarg Dome. Contour lines are set to 250 ms intervals. Location of the wells used in the study shown as red symbols.

4.2.2 Top Havert

The Top Havert horizon (Figure 4.10) is a medium to – high amplitude positive reflection, representing the transition from the overlying Steinkobbe and (a very thin) Klappmyss formations (see section 2.2.2). The highest amplitudes are found on the Bjarmeland Platform (including the Norvarg- and Samson domes), while it is characterized by a lower reflection amplitude and continuity at the faulted Nordkapp Basin margin. Inside the basin amplitudes generally remain low.

Across large parts of the Bjarmeland Platform, the horizon is sub-parallel to the underlying NT-Permian horizon (Figure 4.5). This is true also in the Nordkapp Basin, where the relief to surrounding platform areas is similar to that of the NT-Permian horizon. The relief is lower in the southern subbasin (between 800 and 1200 ms in most places) than in the northern counterpart (more than 1500 ms in most places). Lacking interpretation in the central parts of the northern basin is due to a large presence of salt.

At the Norvarg- and Samson domes, the horizon is located at shallower depths (1950 ms) compared to the surrounding platform areas where it is situated around 2250 ms. The deepest parts, in the previously mentioned depressions that are present next to these two domes, are located at 2850 ms (Samson Dome) and 2400 ms (Norvarg Dome). This results in a relief similar to that of the NT-Permian horizon (Figures 4.7 & 4.8).

The horizon is sub-parallel to the NT-Permian also in the Maud Basin, with maximum depths of about 3000 ms. Towards the Svalis Dome to the northwest, it becomes shallower and sub crops towards the URU at around 650 ms.

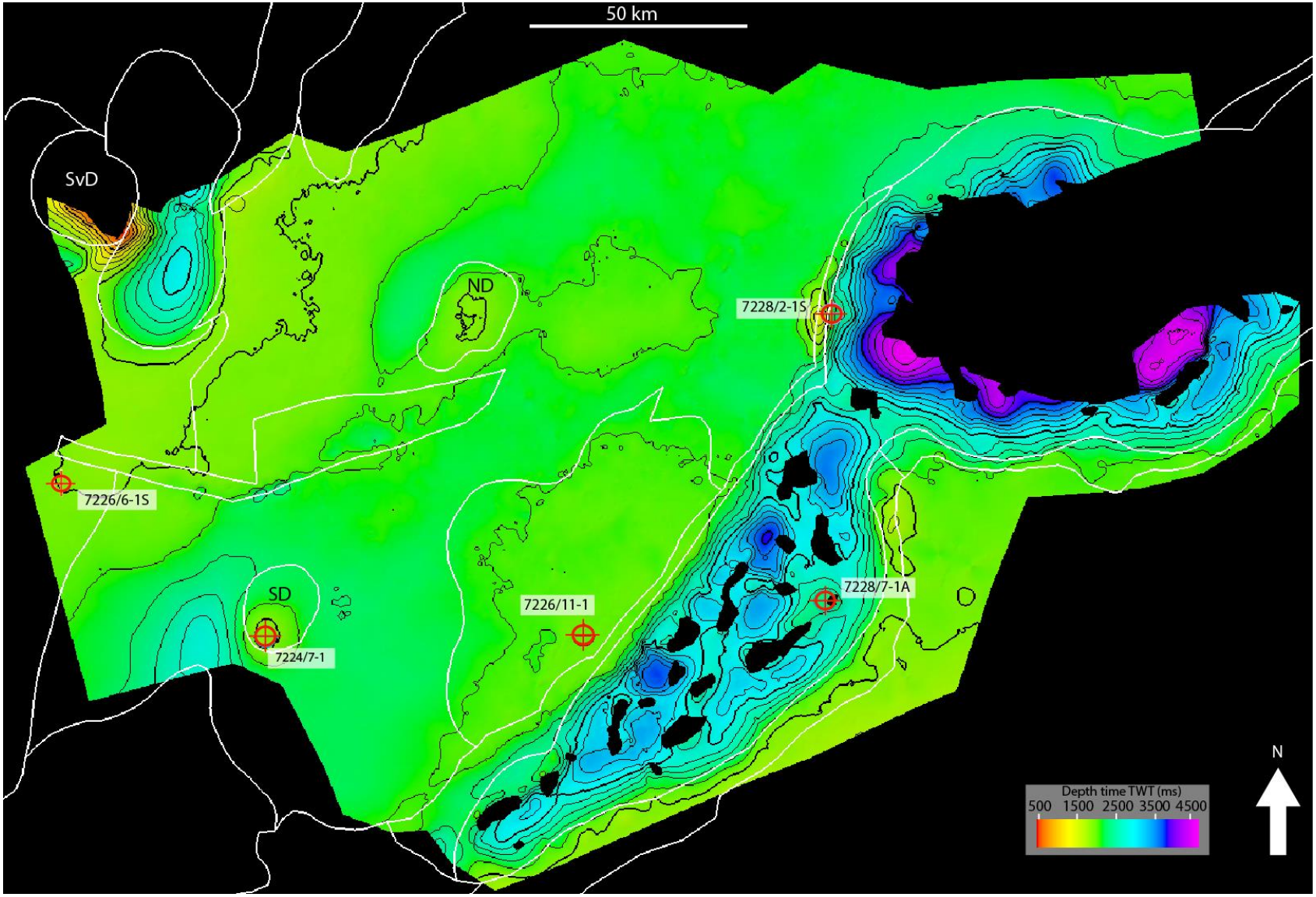

Figure 4.10 Isochron map of the Havert horizon, depths displayed in TWT (ms). SvD=Svalis Dome, SD=Samson Dome, ND=Norvarg Dome. Contour lines are set to 250 ms intervals. Location of exploration wells used for stratigraphic correlation marked by red symbols.

4.2.3 Top Kobbe

The Kobbe horizon (Figure 4.11) has amplitudes ranging from high to low across the study area. It has a positive reflection coefficient, and varies in degree of continuity from high to low. The horizon represents the transition from the overlying Snadd Formation (see section 2.2.2). In the Nordkapp Basin, the continuity and amplitudes are generally high. Across Bjarmeland Platform, amplitudes are generally medium-high with high continuity. However, at the Samson- and Norvarg Domes there is a significant decrease of both amplitude and continuity above the salt structures.

Overall, the morphology of the horizon is comparable to the NT-Permian and Havert horizons; the main differences are observed in the Nordkapp Basin. The horizon dips into the southern subbasin creating a relief locally of up to 1000 ms to the Norsel High, while in the northern subbasin the relief is generally less pronounced (500 ms) (Figures 4.6 and 4.11). This indicates that the horizon is generally situated relatively shallower in the northern subbasin than in the southern counterpart.

A relief similar to the NT-Permian and Havert horizons is present at the Norvarg- and Samson domes. At the Samson Dome, the deepest areas in the adjacent depression are around 2150 ms, creating a relief of 850 ms to the crest of the structure, which is situated at 1300 ms. From the deepest parts adjacent to Norvarg Dome (1700 ms), there is a 400 ms relief up to the crest, situated at 1300 ms.

At the Svalis Dome, the horizon sub-crops towards the URU at depths around 750 ms. The deepest parts in the adjacent Maud Basin are at approximately 2500 ms, creating a relief of about 1750 ms. Uplift of the area has led to erosional truncation by the URU, following the morphology of the dome (Figure 4.5). In other words, across large parts of the structure the horizon is not present.

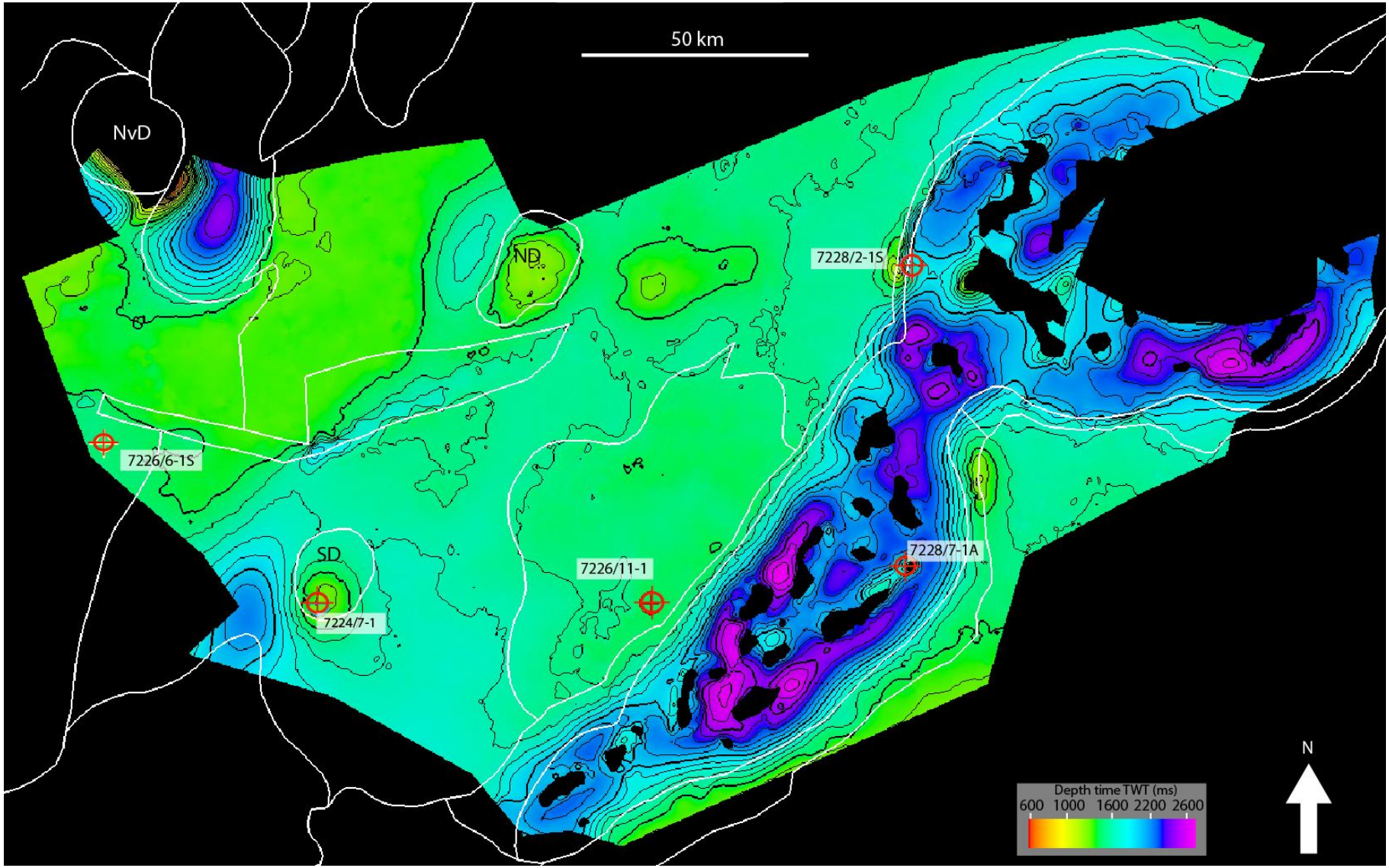

Figure 4.11: Isochron map of the Kobbe horizon, depths displayed in TWT (ms). SvD=Svalis Dome, SD=Samson Dome, ND=Norvarg Dome. Contour lines are set to 100 ms intervals. Location of exploration wells used for stratigraphic correlation marked by red symbols.

4.2.4 Base Cretaceous unconformity - BCU

The BCU horizon (Figure 4.12) was picked on a trough across the entire study area. It represents the erosional transition between the limestone interbedded shales of Lower Cretaceous, and underlying, organic rich Upper Jurassic shales (see section 2.2.2). High amplitudes and a generally continuous reflection characterize the interpreted horizon all across the study area.

At the Bjarmeland Platform, the horizon is generally flat, with depths averaging between 1000 and 1200 ms. The shallowest parts of the horizon are located at depths between 600 ms and 650 ms at Loppa High. Shallower parts are also observed at the Samson- and Norvarg domes, where depths around 750 and 800 ms respectively creates a positive relief, similar to that of the previously described horizons.

The deepest parts of the horizon are found in the Nordkapp- and Maud basins. The horizon approaches depths of 2200 ms in the deepest parts of Maud Basin, while adjacent to the salt structures of southwestern Nordkapp Basin it deepens to 1600 ms. No difference in relief between basin and adjacent platform areas are found between the two subbasins (approximately 400 ms in both instances).

Near the top of salt structures in the Nordkapp Basin and at the Svalis Dome, the URU truncates the horizon. In immediate vicinity of the diapirs in the Nordkapp Basin, the BCU represents the sidewall of the salt structures (Figures 4.3, 4.4, 4.6, and 4.7). Followingly, the isochron map in Figure 4.12 displays areas in the Nordkapp Basin where the BCU is not mapped; these areas represent the points where individual salt structures penetrate the URU, and hence where the URU truncates the BCU.

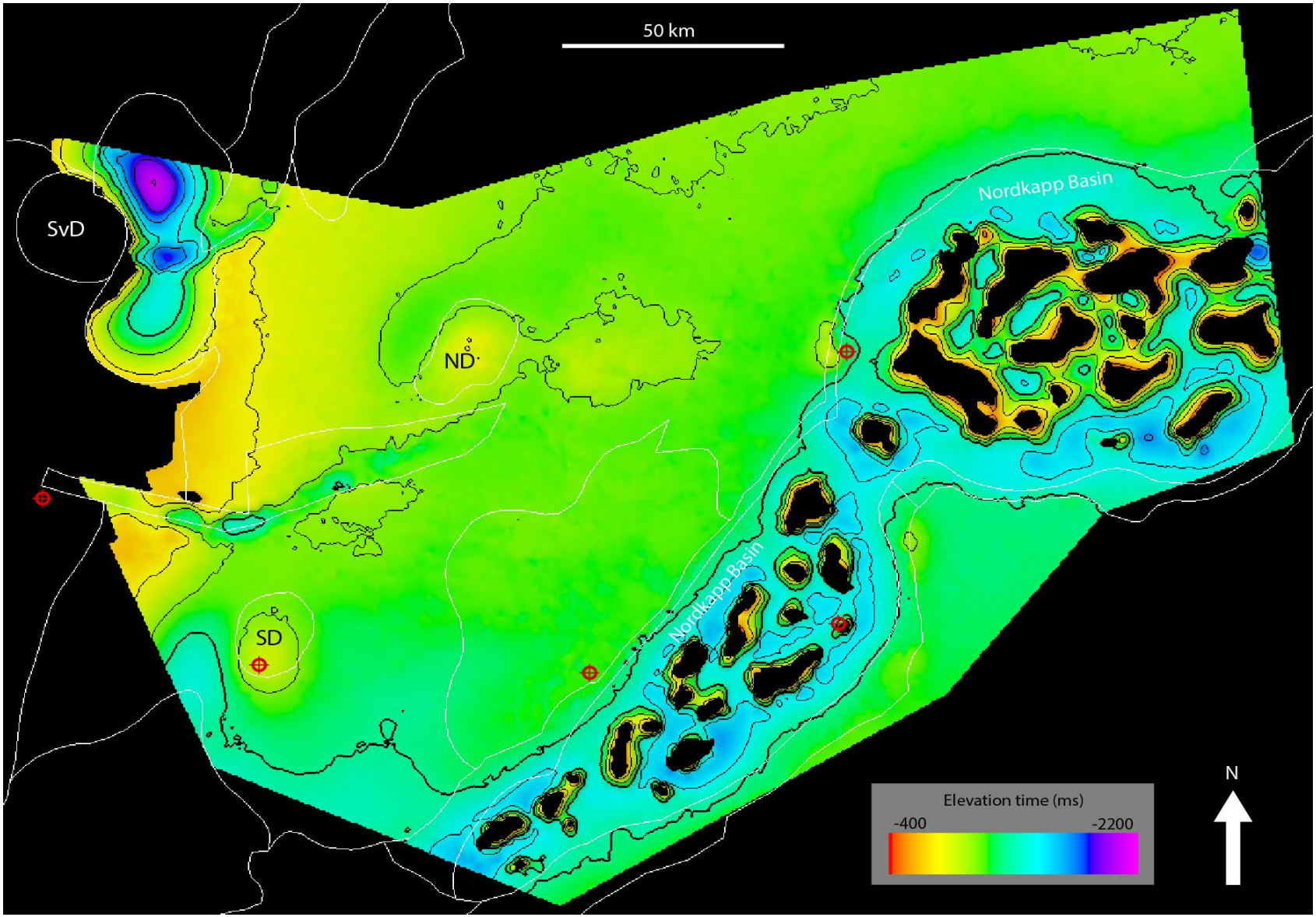

Figure 4.12: Isochron map of the BCU horizon, depths displayed in TWT (ms). SvD=Svalis Dome, SD=Samson Dome, ND=Norvarg Dome. Contour lines are set to 250 ms intervals.

4.3 Seismic units

4.3.1 Lower Triassic

The lower Triassic unit (Figure 4.13), defined between the NT-Permian horizon (lower limit) and Top Havert horizon (upper limit), is dominated by low to medium amplitude reflections. The unit appears uniform across large parts of the study area, with very limited thickness variations on Bjarmeland Platform (including the Samson- and Norvarg domes) and in the Maud Basin.

In the northern Nordkapp Basin, there is no clear trend in thickness variations. The thickness is generally uniform to slightly thinning in the outermost rim synclines of most diapirs (Figure 4.13). Increasing thicknesses also appear in certain areas between basin margin and the outermost diapirs. However, there is no evidence of rim synclinal growth in the seismic data that connects to this observation.

In the southern Nordkapp Basin, thicknesses are generally uniform to slightly thinning in the rim synclines. Maximum thicknesses (upwards of 850 ms) are found in the central parts of the basin, where it is approximately 200 ms thicker compared to the surrounding platform areas.

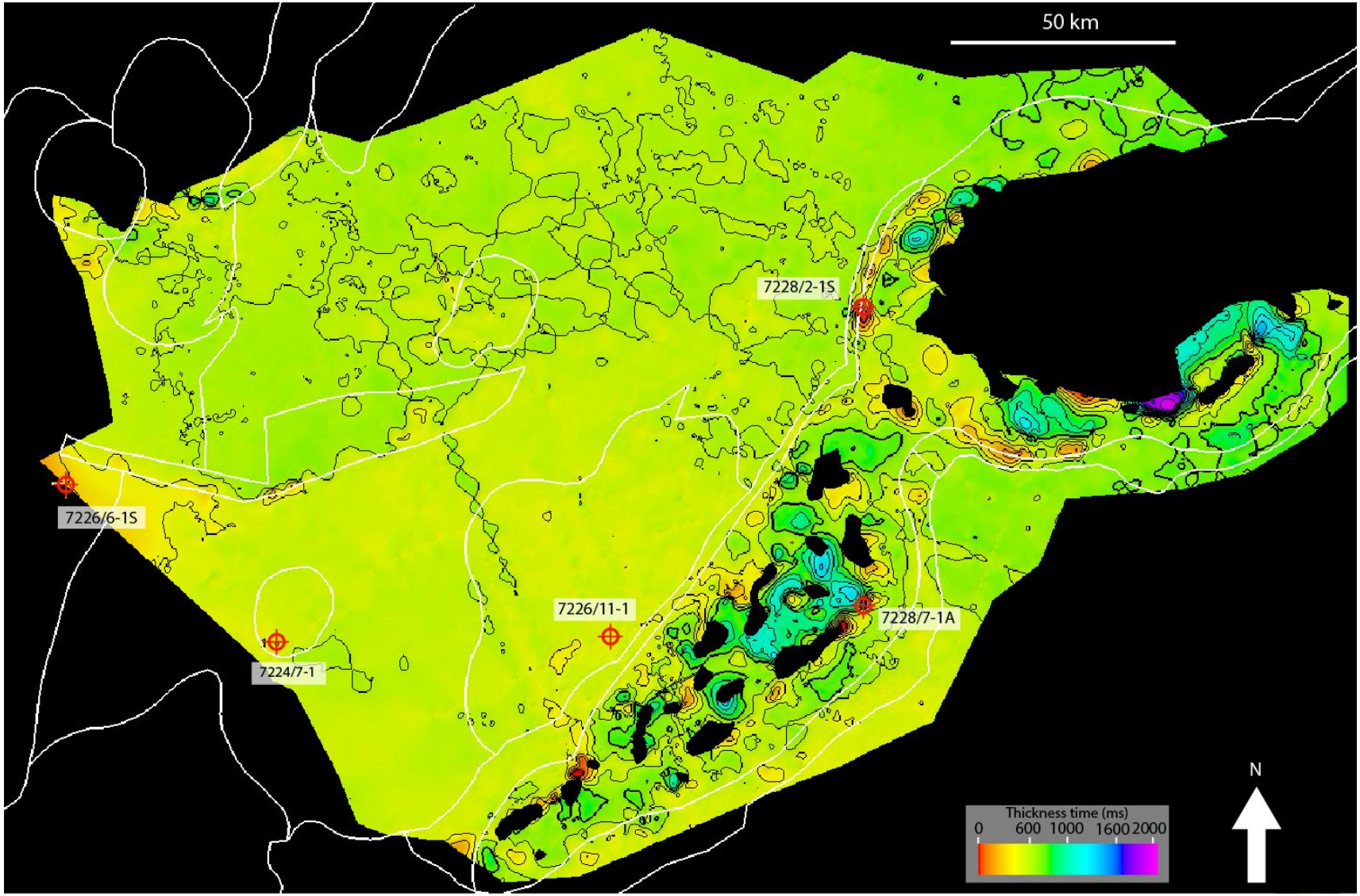

Figure 4.13: Time thickness map of the lower Triassic unit across the study area. Contour lines are set to 250 ms intervals. Structural elements from NPD. Location of key wells marked with red symbols

4.3.2 Lower to Middle Triassic

The Lower to Middle Triassic unit, herein defined between the Top Havert horizon and Top Kobbe horizon, is characterized by medium-high sub-parallel internal reflections across the study area. Figure 4.14 presents a time thickness map, displaying variations between the different structural elements.

The most significant thickness change is located in the rim synclines of the northern Nordkapp Basin. Maximum thickness approaches 3000 ms in the rim synclines between basin margin and the outermost salt structures, an increase of up to 1500 ms from the 500-700 ms thicknesses observed on the adjacent platform areas.

A less prominent change occurs in the southern Nordkapp Basin, where thicknesses are up to 1500 ms in the deepest parts of the basin. The actual growth in the rim synclines located between basin margin and the outermost diapirs however, is generally no more than 500 ms. Uniform thicknesses are also observed towards several of the outermost diapirs. In other words, there is less growth in the rim synclines in the southern subbasin than in the northern subbasin.

In the Maud Basin, the unit is thickest to the southeast (700 ms), and it thins significantly towards the Svalis Dome to the northwest, where thicknesses decrease down to about 300 ms directly below the URU truncation (Figure 4.3).

A minor change in thickness occurs in a small area at the southwestern border of the Samson Dome. The unit has a thickness of approximately 570 ms at the crest, some 50 ms thinner than the surrounding areas (640 ms). There are no thickness variations at the Norvarg Dome.

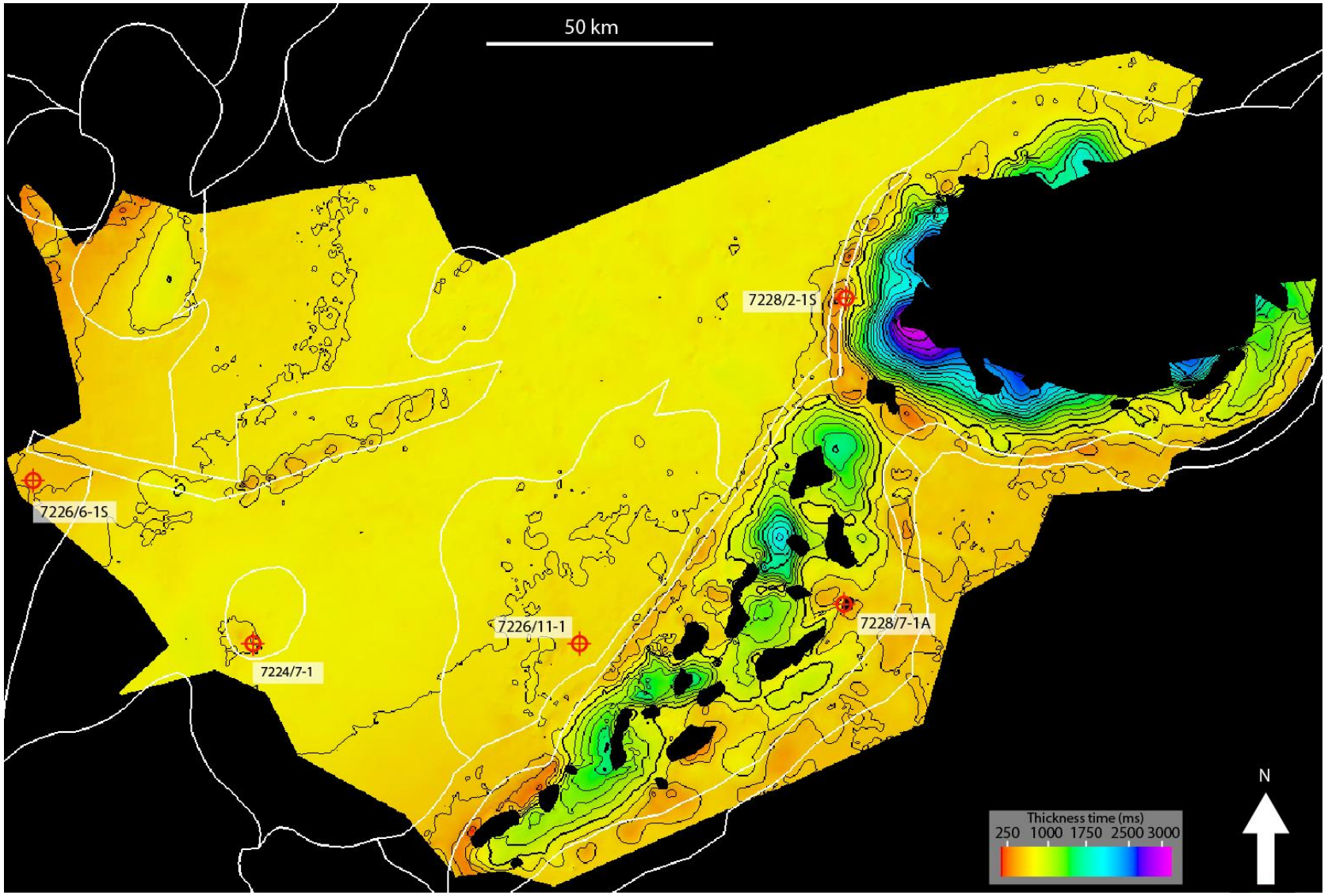

Figure 4.14: Time-thickness map of the Lower to Middle Triassic unit across the study area. Contour lines are set to 150 ms intervals. Structural elements from NPD. Location of key well shown with red symbols.

4.3.3 Middle Triassic- Jurassic

The Middle Triassic- Jurassic unit, delimited by the Top Kobbe horizon below and BCU above, shows an overall increasing thickness trend towards the northwest, i.e. the thinnest accumulations are found on Finnmark Platform (350 ms). The unit gradually increases westwards on Bjarmeland Platform from around 400 ms, up to around 800 ms towards Loppa High, where it is truncated by the URU (Figure 4.15).

In the southern Nordkapp Basin, which overall shows greater thicknesses (between 700 and 1000 ms) than the surrounding platforms, a clear increase in thickness (200 to 300 ms) occurs in the rim synclines of many diapirs, particularly in the central parts of the basin (e.g. Figure 4.8).

This trend is less prominent in the northern Nordkapp Basin. The thickness is greater in the basin (typically upwards of 750 ms) than on the surrounding platforms, but is relatively uniform in many of the outermost rim synclines (Figure 4.15, also section 4.4.1).

No significant thickness variations are present at the Samson- and Norvarg domes. The unit is slightly thinner over the crest compared to the area west of the Norvarg Dome, and thicker to the north and west of the Samson Dome. For the Samson Dome in particular, the change seems concordant to the regional trend described for the entire study area, and might not be attributed to the evolution of the salt structure. At the Norvarg Dome, the increasing thickness is found in a synclinal depression adjacent to the dome. However, there is no change in thickness to the south or east of the dome.

In the Maud Basin, the thickest areas are found in the central parts (1000ms), while a sharp decrease in thickness is observed towards the Svalis Dome in the northwest, where the unit sub-crops towards the URU with a thickness of approximately 500 ms.

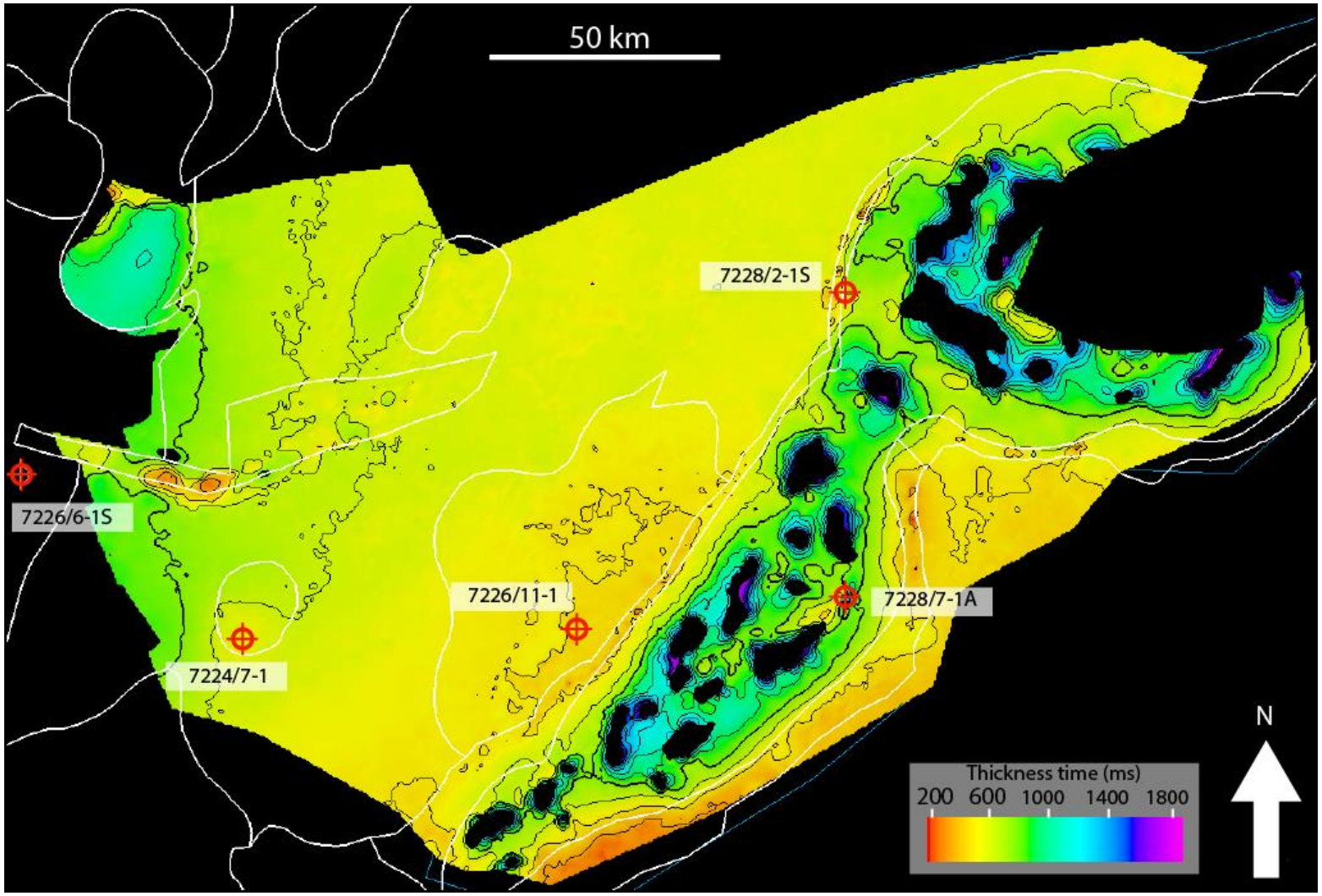

Figure 4.15: Time-thickness map of the Middle Triassic - Jurassic unit across the study area. Contour lines are set to 150 ms intervals. Structural elements from NPD. Location of key well shown with red symbols.

4.3.4 Cretaceous- recent

The Cretaceous-recent unit (Figure 4.16*)* is delimited by the BCU (bottom) and seafloor (top). An angular unconformity, i.e. the URU, is present in the upper part of the unit, separating Cretaceous strata from the younger Quaternary strata. There is an overall northwest-southeast increase in thickness, approaching 1000 ms at the southeastern Bjarmeland Platform. However, the Nordkapp- and Maud basins stand out with substantially greater thicknesses (1400 and 1600 ms respectively).

Thicknesses decrease to between 0 and 50 ms towards the diapirs in the Nordkapp Basin. The BCU sub-crops towards the URU at the diapirs, hence only the most recent seafloor sediments (deposited post-URU) remain there. The northern subbasin differs from its southern counterpart in the sense that the unit is generally thinner than 1000 ms in the deepest rim synclines. Meanwhile, thicknesses of 1000 to 1300 ms are common in the southern basin.

The thinnest areas on Bjarmeland Platform are towards the northwest (about 100 ms). At Loppa High and the Svalis Dome, the URU has eroded the entire Cretaceous unit, so only recent sediments remain above the older units. A wide range of thicknesses are found in the areas immediately surrounding the Samson- and Norvarg domes, from 750 to 1150 ms near the former and 400 to 600 ms near the latter. Due to doming of the BCU (lower boundary of the unit), a thinning is observed over the crests of the domes, with thicknesses of 550 and 250 ms respectively.

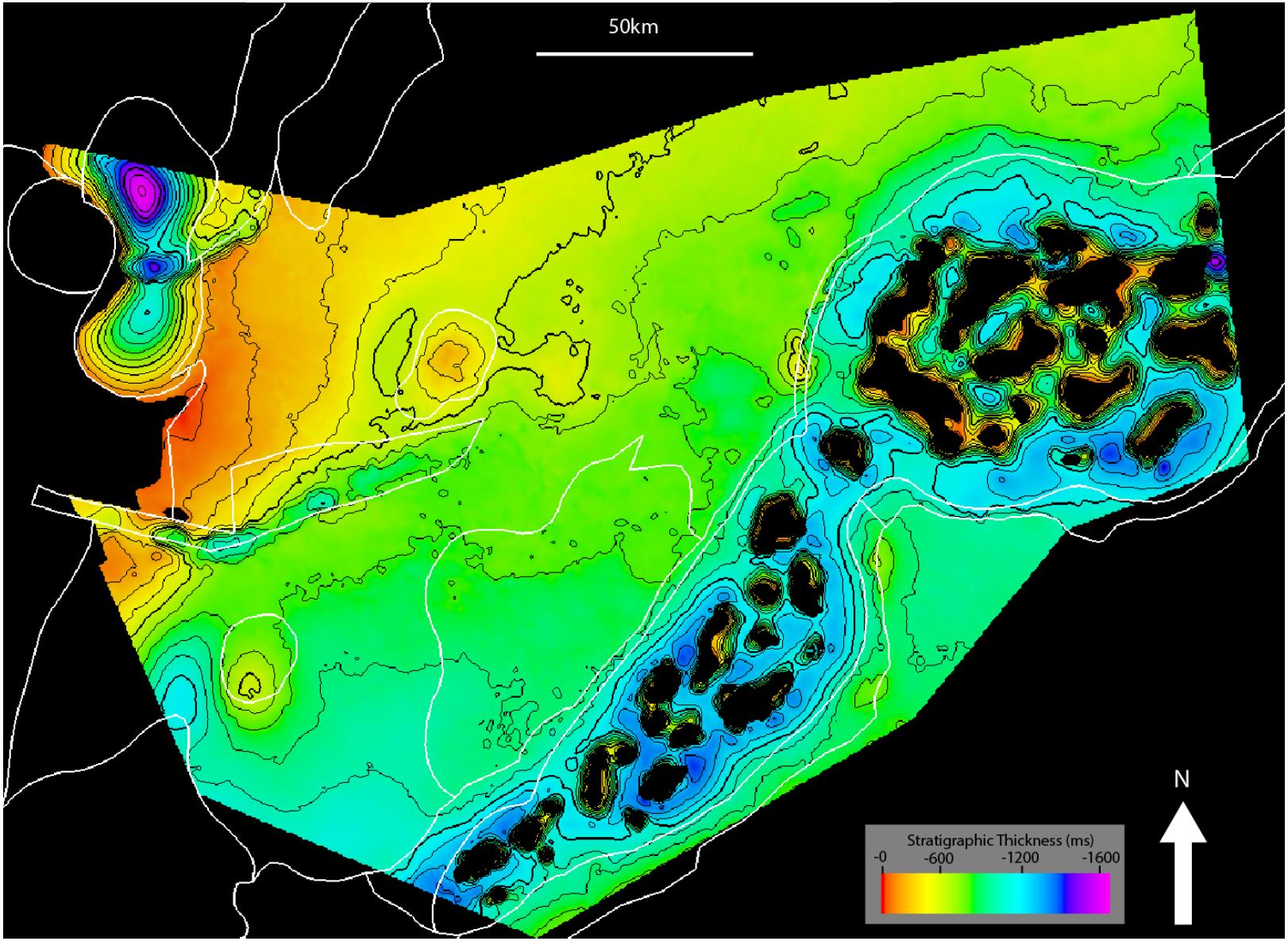

Figure 4.16: Time-thickness map of the Cretaceous- recent unit across the study area. Contour lines are set to 100 ms intervals. Structural elements from NPD.

4.4 Salt structures

Figure 4.17 is a salt structure map based on the previously described BCU-salt sub-crop polygons in the Nordkapp Basin. Arbitrary numbers assigned to the diapirs are in ascending order throughout the basin from southwest to northeast. The two following sections present seismic profiles representing the variations seen in salt morphology and bounding stratigraphy from the two subbasins of Nordkapp Basin, and Figure 4.16 displays their location on the salt structure map. The Svalis-, Samson- and Norvarg domes follow, together with a summary, in the final sections.

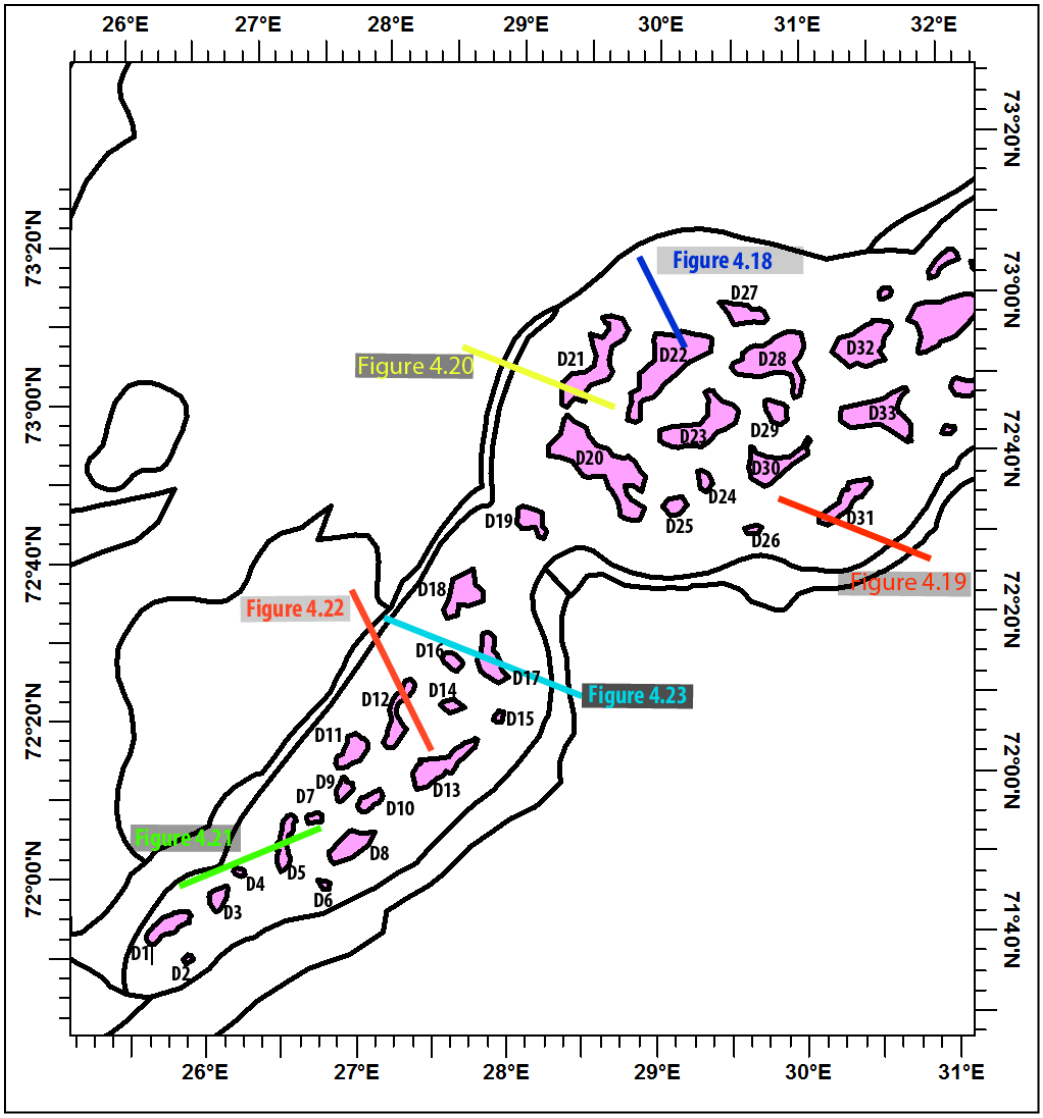

Figure 4.17: Map of the salt structures influencing the BCU level. The figure also shows location of the seismic profiles presented in the following sections. Structural elements from NPD.

4.4.1 Northern Nordkapp Basin

Salt structure D22:

The D22 salt structure (Figure 4.18) is an elongated diapir located on the northern side of the central part of the northern subbasin. Strata in the adjacent rim syncline are representative of the previously described thickness trends of the northern basin. The crest of the diapir sub-crops towards a generally flat URU at depths of approximately 500 ms. The diapir appears to be bulb-shaped, and bulges out at the Upper Triassic level (between Top Kobbe and BCU horizons).

Thickness changes are particularly evident in the upper half of the Lower to Middle Triassic unit, where the reflections diverge greatly, resulting in a substantial thickness increase of around 700 ms towards the diapir (illustrated by the black stippled lines in Figure 4.18). In the lower half of the unit however, thickness appears to be uniform.

A discrete increase in thickness is also present in the overlying Middle Triassic- Jurassic unit, of about 200 ms. The uppermost part of this unit however, appears to rest conformably on top of sidewall/crest of the structure, sub-cropping towards the URU.

For the lowermost unit, there is a decrease in thickness from the distal parts of the rim syncline of about 100 ms. Resolution for the NT-Permian horizon is rather low however, leading to uncertainties whether this trend continues further towards the salt.

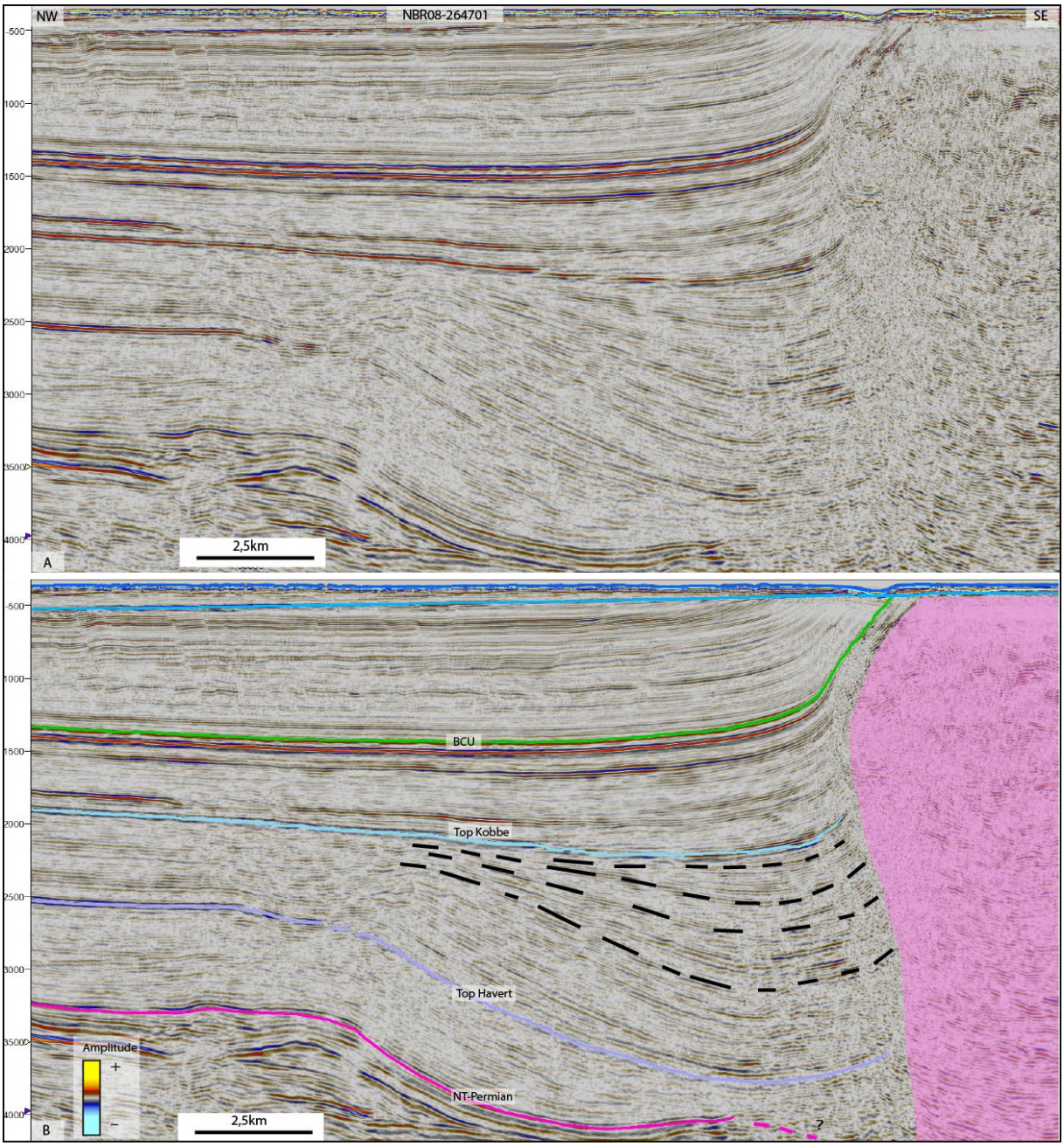

Figure 4.18: Diapir D22 in the northern Nordkapp Basin, the upper part of the Lower to Middle Triassic unit shows divergent reflections (black lines) and significant growth towards the salt (transparent pink). A) Uninterpreted, B) Interpreted.

Salt structure D31:

The D31 diapir (Figure 4.19) is located near the southeastern margin of the northern subbasin. In cross section, the diapir is bulb-shaped, albeit with a narrow asymmetric crest truncated by the URU to the southeast. The diapir is at its widest adjacent to Middle to Upper Triassic strata.

Thinning of Lower Triassic strata is evident towards the salt body, where a deep fault offsets the Top Havert and NT-Permian horizons by more than 1500 ms down to the northwest. A discrete thinning of some 200 ms. is also observed in the Lower to Middle Triassic unit on the footwall side of the fault, whereas on the northwestern side of the salt structure the unit is approximately 1400 ms thicker.

In the Middle Triassic-Upper Jurassic unit, there is a 200-300 ms increase in thickness from the southeastern basin margin towards the diapir. Contrarily, the thickness appears to be uniform in the northwestern rim syncline. The upper part of the unit appears to drape over the salt structure, with the BCU horizon following the morphology of the top of salt.

Cretaceous strata, seemingly undisturbed by faulting, are folded over the crest and truncated by the URU.

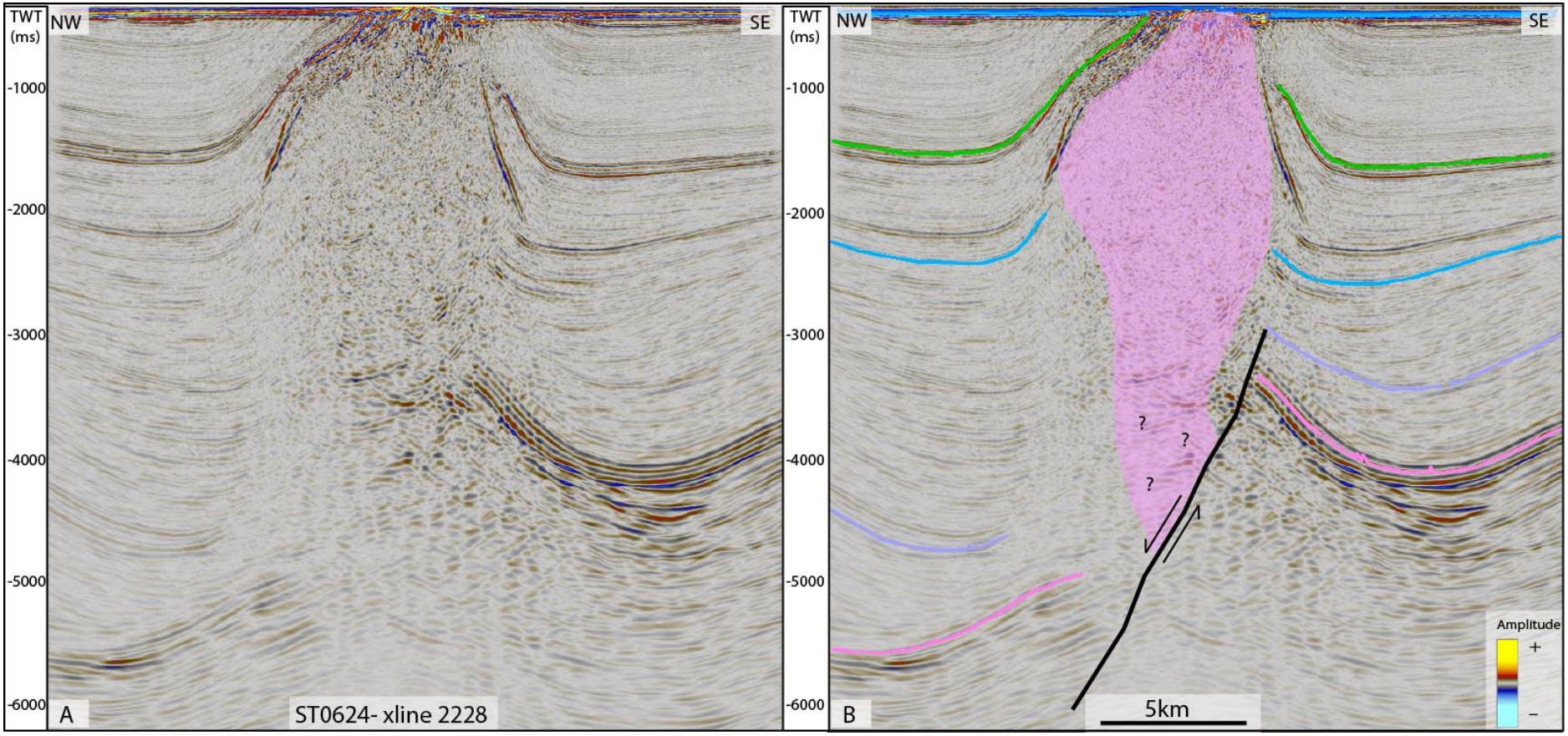

Figure 4.19: Diapir D31 in the northern sub- basin. A salt structure (pink) occurs over a deep fault. The fault offsets Lower Triassic strata, which thin towards the structure. Lower to Middle Triassic strata are significantly thicker in the NW rim syncline.

Salt structure D21:

The D21 diapir (Figure 4.20) is located near the Nysleppen Fault Complex along the northwestern margin of the northern subbasin. It is an elongated structure, approximately 23 km long, and in the presented cross-section approximately 12 km at its widest. It has an asymmetric crest which is truncated by the URU in the northwest, while it is located deeper at around 1000 ms further southeast. A salt pillow is present in relation to the deepest fault at the basin margin.

The largest thickness increase is located in the Lower to Middle Triassic unit, which increases with up to 1500 ms from the adjacent platform area to the deepest part of the rim syncline. Divergence is clearly visible in the middle part of the unit, while parallel reflections characterize the uppermost 130 ms section. The lowermost part of the unit has low amplitudes, making it challenging to detect reflection patterns.

The Middle Triassic-Jurassic unit has a uniform thickness of approximately 800 ms in the rim syncline, an abrupt change from the approximately 500 ms recorded on the adjacent platform area where the unit also exhibits uniform thickness. The upper part of the unit drapes onto the structure, and is preserved on top of the salt in the southeast.

Several faults are present between the URU and BCU, and a deep normal fault that can be traced into the Permian offsets the BCU by almost 300 ms. The offset of the fault increases with depth, to approximately 750 ms at the NT-Permian level.

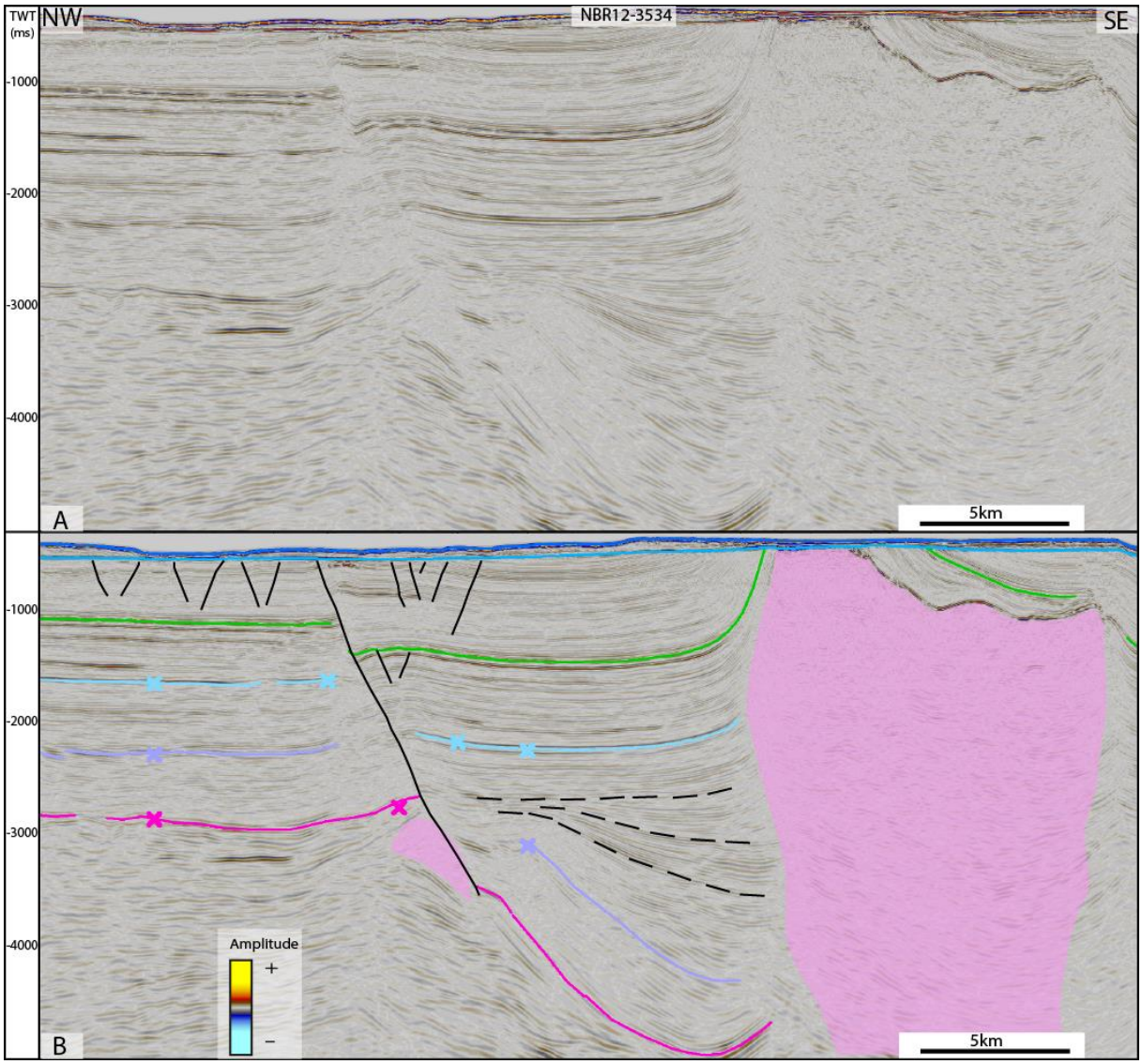

Figure 4.20: Diapir D21 in the northern subbasin. The Lower to Middle Triassic strata thicken towards the salt (pink). A major fault extends from the URU down to a salt pillow below the NT-Permian.

4.4.2 Southern Nordkapp Basin

Salt structure D5:

Figure 4.21 shows salt structure D5, an elongated salt structure in the southwestern part of the southern subbasin. At the crest of the salt structure, which sub-crops towards the URU, there is a convex contact between URU and salt. The diapir bulges out, with maximum lateral extent near the Top Kobbe horizon (around 2000 ms), before it becomes narrower towards the URU. At the crest of the structure, the URU becomes deeper, and truncates the salt.

On the northwestern side of the structure, the rim syncline is located between the salt and a nearby fault complex, separating it from the Bjarmeland Platform. A salt pillow is located below the faults, over which the Lower- and Lower to Middle Triassic units seem to decrease in thickness by approximately 200 ms each on the footwall side. In the rim syncline towards the diapir, the Lower Triassic unit appears with uniform thickness towards the diapir (about 750 ms).

Thickness variations in the rim syncline are found in the Lower to Middle Triassic unit, where diverging reflections appear in the lower half of the unit, resulting in a 700 ms thickness increase towards the diapir.

The thickness increase ceases in the uppermost half of the unit, except for a minor increase of about 200 ms towards the diapir. In the Middle Triassic- Jurassic unit, thickness remains uniform (600 to 650 ms) all over the rim syncline, including the area located above the salt pillow. Hence, the structure represents one of a few exempts to the subbasins previously described Middle Triassic- Jurassic thickness trend.

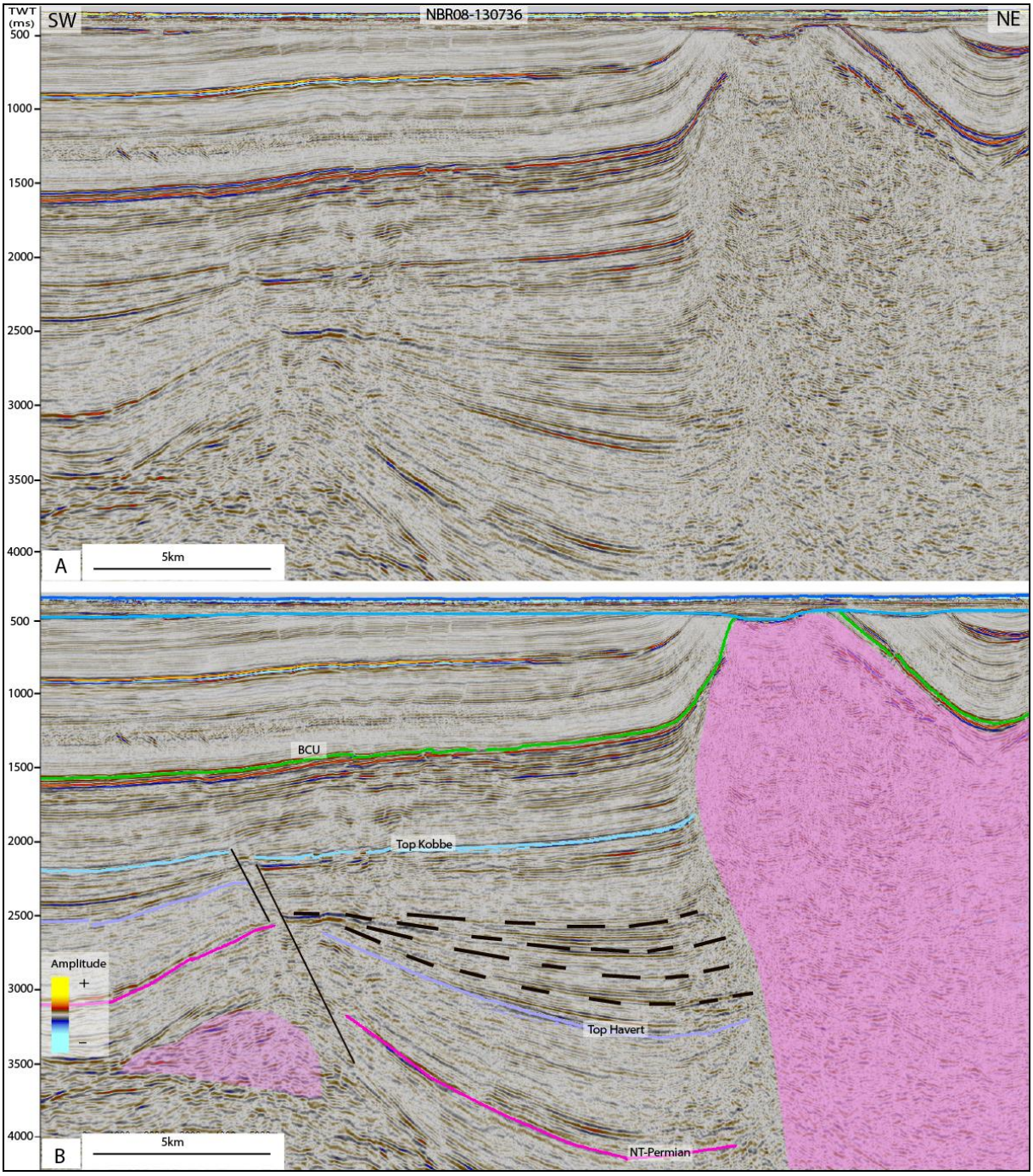

Figure 4.21: Salt structure D5 in the southern subbasin of Nordkapp Basin. A salt pillow is located below the faulted area. In the rim syncline, growth is mainly in the lower part of the Lower to Middle Triassic unit, where reflectors diverge (black lines). The interpreted salt is in transparent pink. A) Uninterpreted, B) Interpreted.

Salt structure D12:

The D12 structure (Figure 4.22) is another elongated salt structure, located in central parts of the southern subbasin, further northeast of the D5 structure. The structure appears asymmetric, with a narrow crest sub-cropping towards the URU at the northwestern boundary of the structure.

Both the Lower Triassic and Lower to Middle Triassic units appear with uniform thicknesses (approximately 400 and 700 ms respectively) in the rim syncline adjacent to the salt structure. Divergent reflections and a thickness increase of more than 300 ms appear in the Middle Triassic-Jurassic sequence, where a set of faults are also observed to cut across the unit further southwest, near the basin margin. This Middle Triassic-Jurassic thickness increase is in accordance to the units previously described thickness trend.

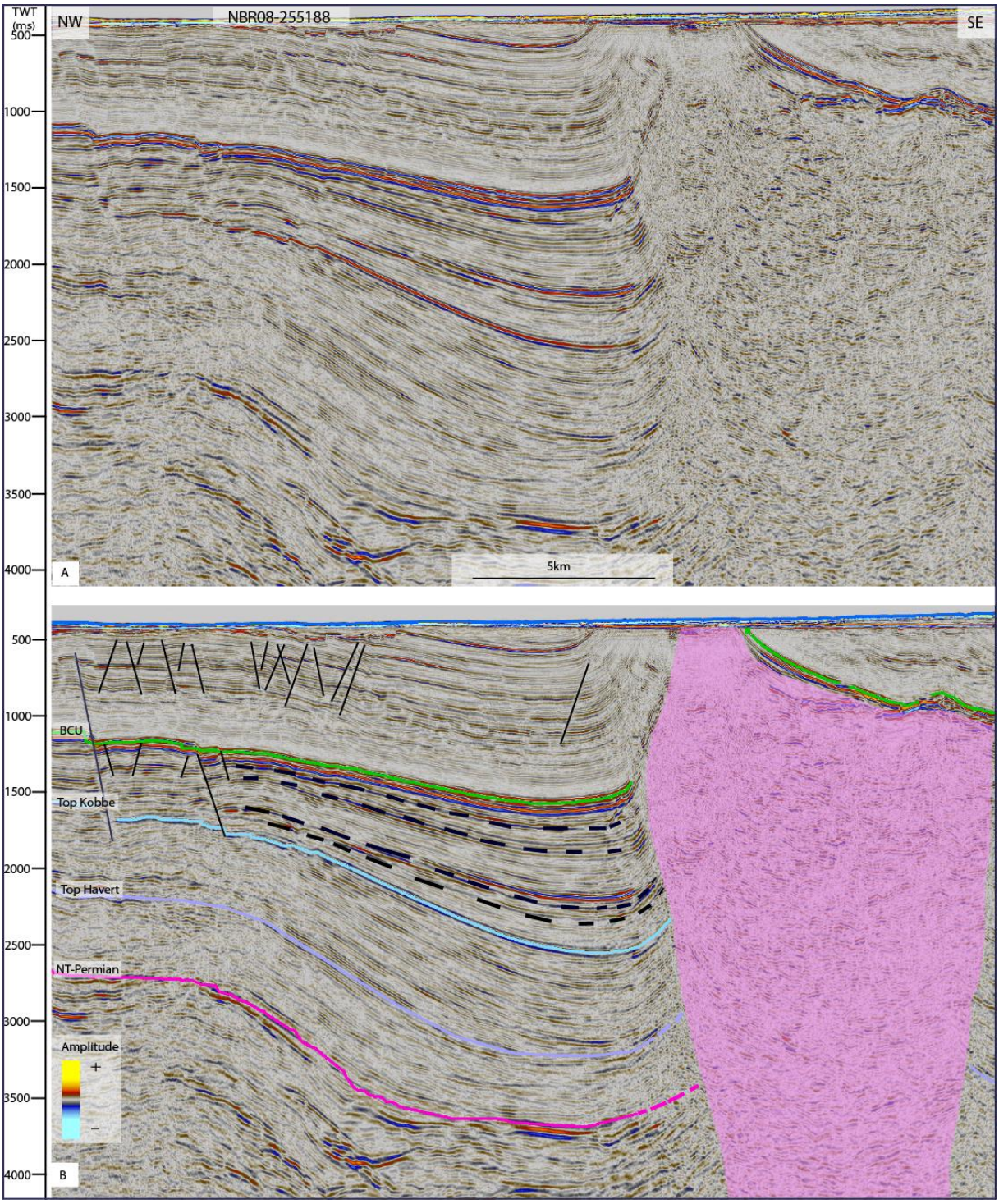

Figure 4.22: Salt structure D12 in the southern subbasin of Nordkapp Basin. The most pronounced reflector divergence (black lines) is located in the Middle Triassic-Jurassic sequence. Salt in transparent pink. A) Uninterpreted. B) Interpreted.

Salt Structure D17a and b:

D17a and D17b are two neighboring diapirs in the northeastern part of the southern Nordkapp Basin. Differences in thickness variations in adjacent strata, and the different depths to top of salt, makes these two structures excellent examples of the large variations observed between diapirs in the entire Nordkapp Basin.

D17a (Figure 4.23) is an elliptical-elongated salt structure when defined at BCU level, is located near the northeastern margin of the southern basin. The diapir has it crest near the seafloor, possibly penetrating the URU. Directly north-west of it, diapir (D17b) emerges, with its crest situated directly below the BCU at about 1000 ms, meaning it does not penetrate the URU. The seismic section (Figure 4.23), which spans from the northwestern margin to the southeastern margin, displays a distinct asymmetry at the NT-Permian level. A substantially thicker sediment package is present between NT-Permian and BCU on the deeper, northwestern side.

At the northwestern basin margin, adjacent to D17b, a set of faults cut across the uppermost Triassic unit, and further up towards the URU. The Lower Triassic unit shows a minor thickness increase towards the diapir, while a thickness increase of more than 700 ms occurs in the Lower to Middle Triassic unit. Here, reflections show a divergent pattern throughout most of the unit, bar the uppermost part. Strata of the Middle Triassic- Jurassic unit here appear to exhibit a very limited thickness increase (up to 100 ms); much less pronounced than in the Lower to Middle Triassic unit.

At the southeastern basin margin, a set of faults cut across the Triassic units and further up towards the URU. The faults here trace further down in the stratigraphy than at the northwestern margin, with displacement internally in the Lower Triassic unit as well. The rim syncline of D17a exhibits a more pronounced thickness increase (400 ms) in the Middle Triassic- Jurassic unit than that of D17b. Furthermore, a discrete growth of some 100 ms in the Lower to Middle Triassic unit is restricted to the upper half of the unit.

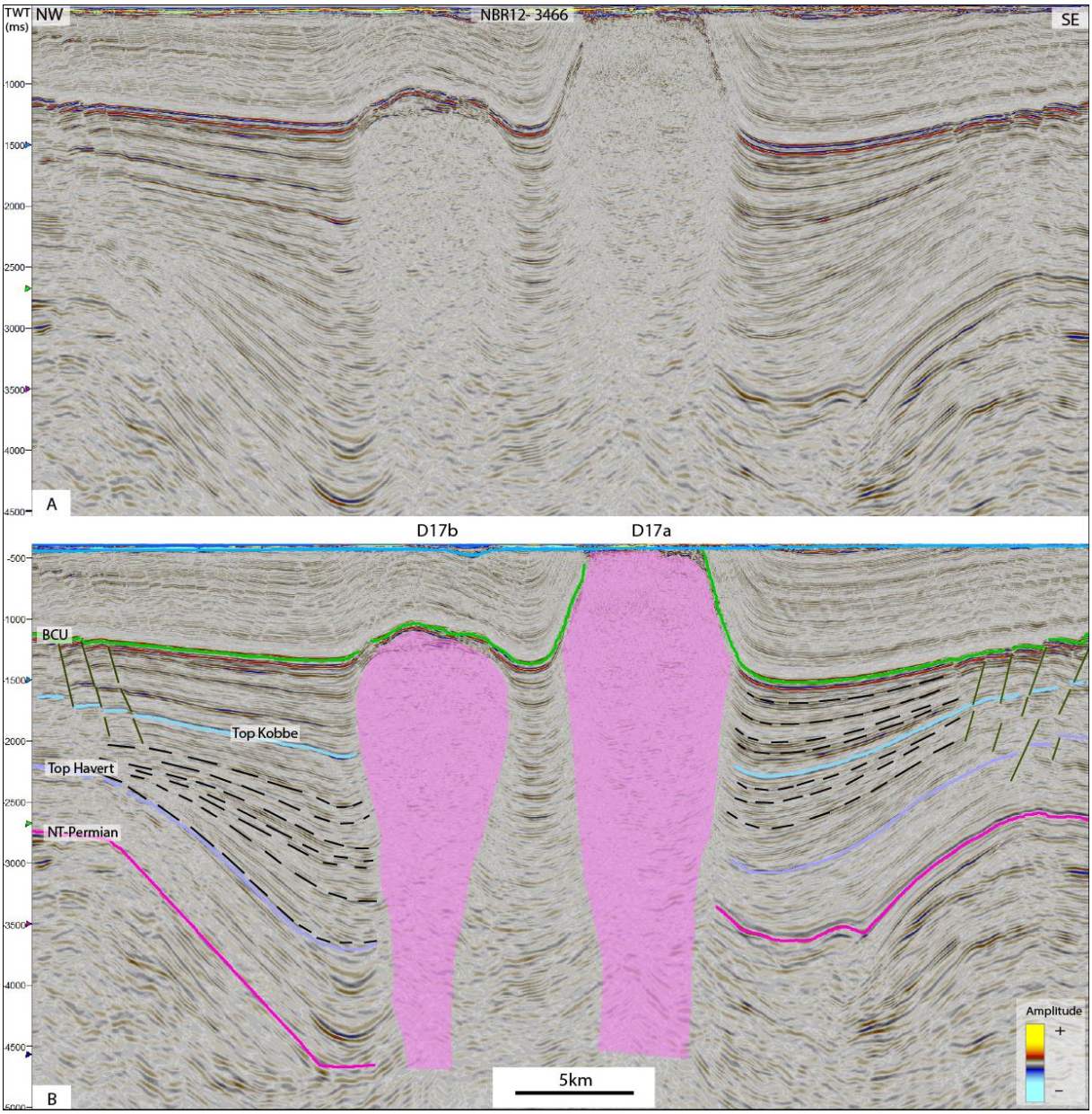

Figure 4.23: Salt structure D17 in the southern sub-basin of Nordkapp Basin. A small thickness increase if observed in the Lower Triassic adjacent to D17b. Divergence of reflectors (black lines) is most prominent in the lower part of the Middle Triassic sequence next to the same structure. Adjacent to D17a thickness increase if found in the upper Lower to Middle Triassic- and Middle Triassic-Jurassic units. Salt in transparent pink. A) Uninterpreted section. B) Interpreted section.

4.4.3 Norvarg Dome

At the Norvarg Dome (Figure 4.24), the mapped horizons from NT-Permian to BCU show doming with a sub-parallel internal pattern of all units. The crest of the salt dome is interpreted at around 200 ms below the NT-Permian. The delineation of the salt in the Norvarg Dome is uncertain due to poor seismic resolution. Over the dome, Lower- and Lower to Middle Triassic strata appear uniform in thickness (500 and 650 ms respectively).

On the southwestern side of the dome, thickness of the Middle Triassic-Jurassic sequence decreases towards the dome, from 600 to 500 ms at the crest. The thickest area corresponds to an already described structural depression to the west of the dome (Figures 4.10, 4.11 & 4.14). A distorted seismic image, due to faults and zones of high transparency, makes it challenging to document convergence of reflections internally in the Middle Triassic-Jurassic unit.

Over the BCU, there is a thin package of sediments truncated by the URU. This unit is around 150 ms thick over the crest, and 450 ms thick away from the structure. The URU itself contrasts the underlying horizons with its flat appearance. The strata between BCU and URU appear domed with sub-parallel reflections that pinch out to the southwest. These strata do not appear to onlap the dome.

Faults are present throughout the stratigraphy, with the extent of the largest ones stretching from directly below the URU and down to Top Havert horizon at the least. The highest concentration of faults occur in the Middle Triassic-Jurassic unit.

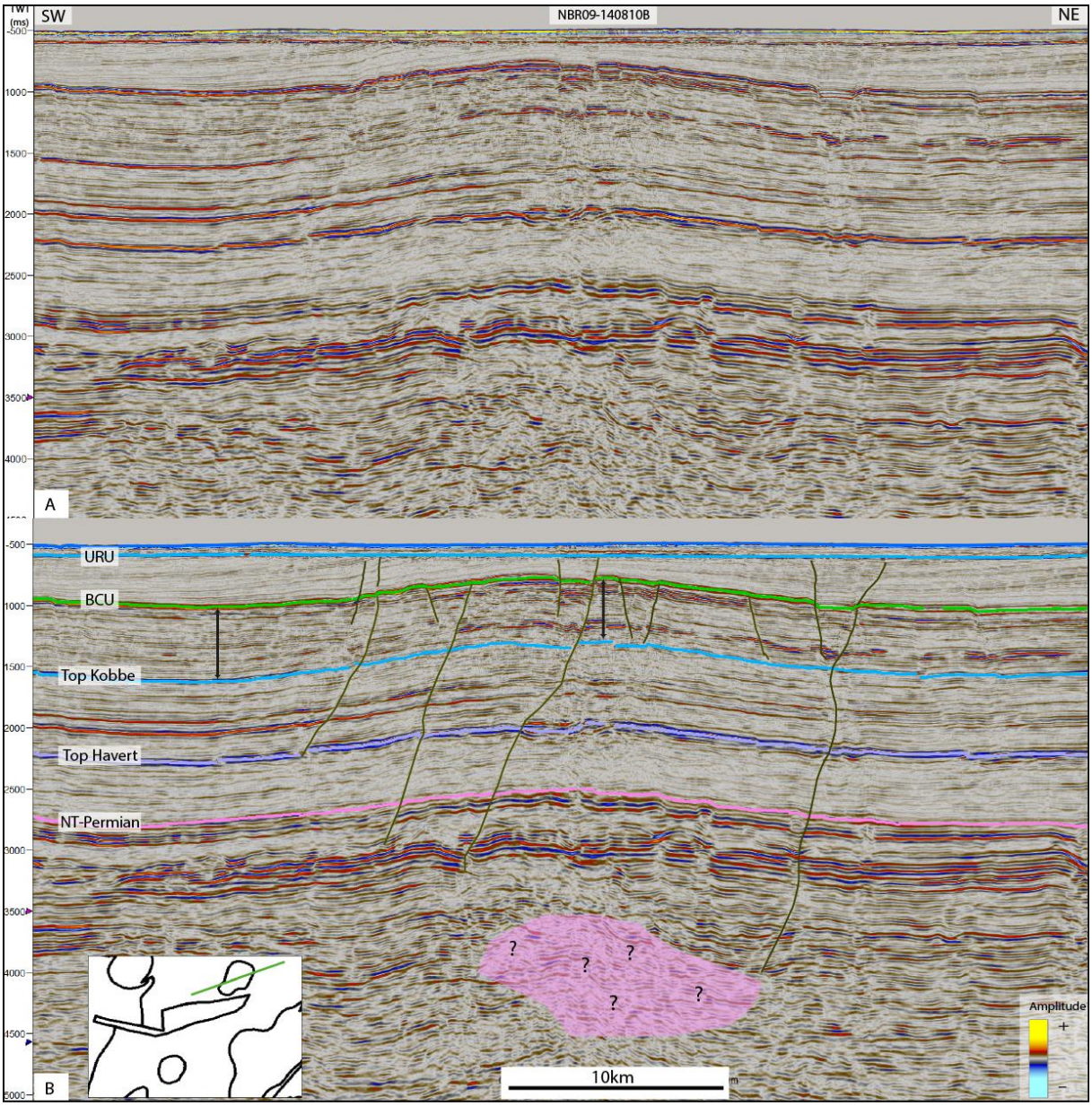

Figure 4.24: Seismic profile across the Norvarg Dome, where units appear uniform in thickness apart from a discrete thickness increase to the southwest (indicated by black arrows). The interpreted salt pillow is indicated in transparent pink. A) Uninterpreted, B) interpreted. Line orientation shown on inset map.

4.4.4 Samson Dome

At the Samson Dome (Figure 4.25), sub-URU strata appear with an asymmetrical doming over a salt-core with maximum vertical extent of more than 1000 ms. Here too, there is a depression located adjacent to the salt body. The Lower to Middle Triassic- and Middle Triassic-Jurassic units appear thicker in this depression than over the crest of the structure; the Lower to Middle Triassic unit decreases from 700 ms to 550 ms towards the crest, while the Middle Triassic-Jurassic decreases from 750ms to 500ms.

Low seismic resolution in the area above the salt body makes tracking of internal reflections challenging. Nevertheless, for the Middle Triassic-Jurassic unit it is possible to observe some convergence of internal reflections towards the dome, especially in the upper half of the unit, as indicated in Figure 4.25.

Directly over and northwest of the crest, the URU displays a zone of very high amplitudes. Between the BCU and URU, a sediment unit follows the same morphology as the sub-BCU units. However, below the high amplitudes observed for the URU there is a zone of high transparency, where reflections appear flat and discordant to the overall domed morphology.

Faults are present at the crest of the dome, most obvious when observing the BCU. Due to the seismic resolution in this area, it is difficult to determine their full stratigraphic extent. They can however generally be traced from the Top Havert horizon, up to the supra-BCU sediments below the zone of highest transparency. Some of the faults also appear to trace into the salt itself.

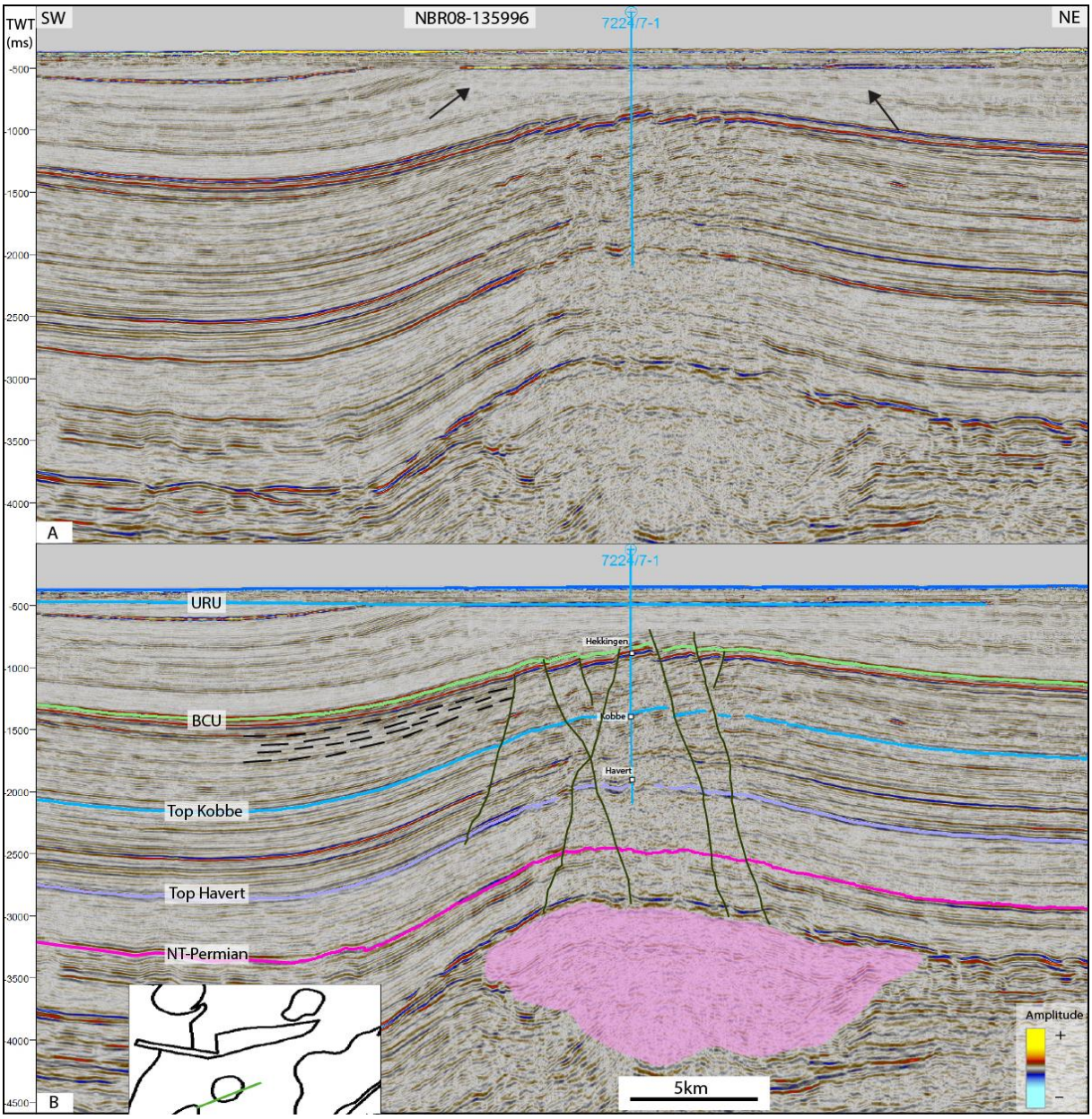

Figure 4.25: SW-NE orientated seismic profile across the Samson Dome. Sub-URU Strata appear domed over a core of salt. A zone of low amplitudes and horizontal reflections appear directly below high amplitudes of the URU (black arrows) A) Uninterpreted, B) Interpreted. Line orientation shown in inset map.

4.4.5 Svalis Dome

The Svalis Dome (Figure 4.26) differs from the previously described domes both in terms of the depth down to top of salt (0-500 ms, approximately 3000 ms for the Samson- and Norvarg domes), the fact that it pierces the overburden in places, as well as in being the only one that has a pronounced rim syncline related to it. The interpreted salt-pillow appears directly below the seafloor, with some uncertainties regarding upper lateral extent. It appears to have its crest situated below the URU in most places, except for an area along the eastern margin, where a smaller diapir pierces the URU to reach the seafloor (Figure 4.26D). A noisy seismic signature occurs below the salt pillow, resulting in uncertainties regarding the vertical extent of the salt body.

In the adjacent Maud Basin, convergence of reflections in the Lower to Middle Triassic and Middle Triassic-Jurassic unit occurs, together with an overall thinning of these two units towards the salt structure. This thinning is evident by a decrease from the previously described thicknesses of 600 ms (Lower to Middle Triassic) and 1000 ms (Middle Triassic-Jurassic), down to 250 ms and 500 ms respectively (Figure 4.26). An apparent erosional unconformity is present in the upper part of the preserved Cretaceous unit at approximately 750 ms, below the URU.

The interpreted URU is highly irregular in the area when compared to the study area as a whole, and becomes almost 200 ms deeper in a narrow area on the western side of the interpreted salt body.

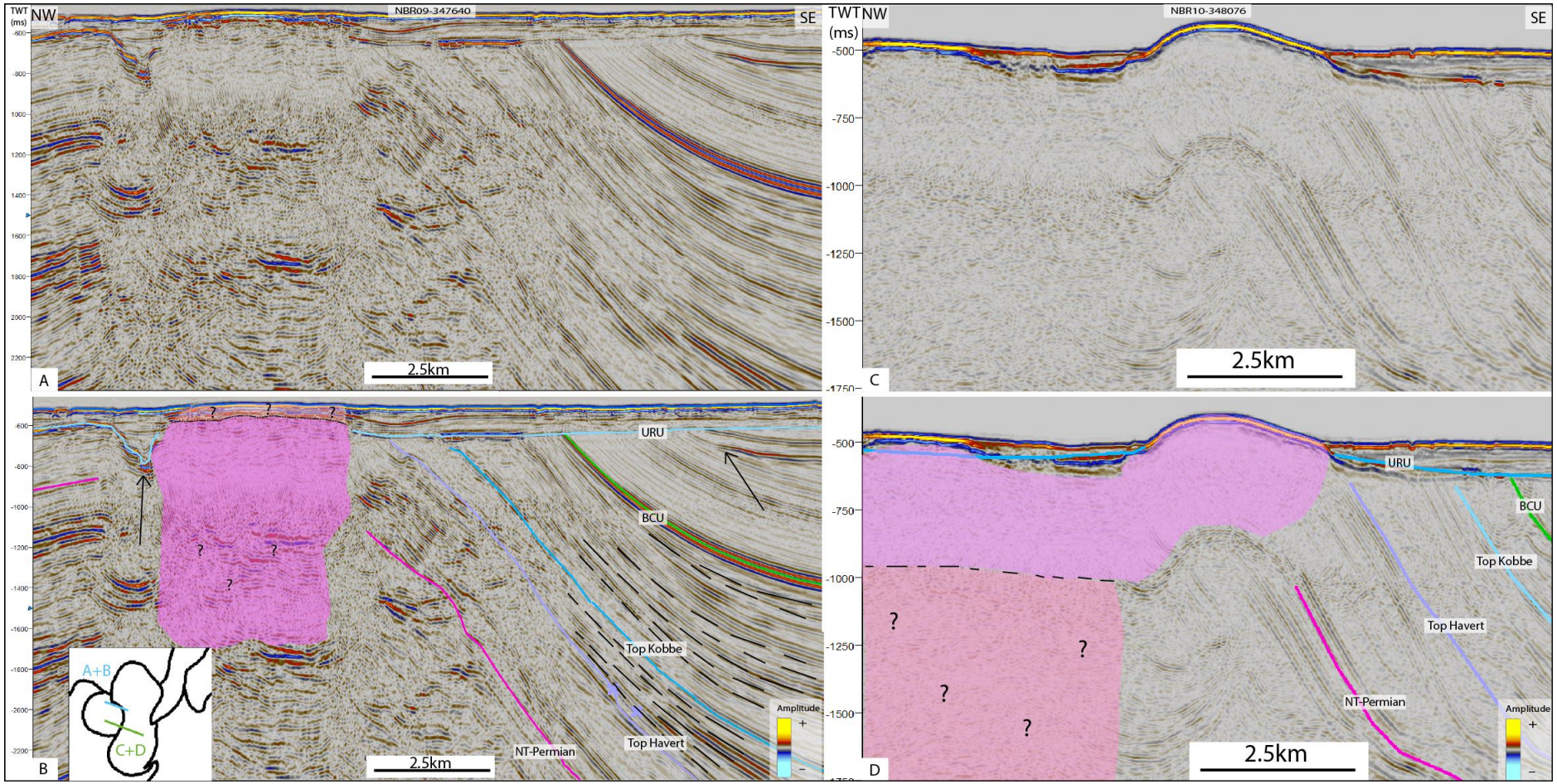

Figure 4.26: Seismic profiles extending from the Svalis Dome (NW) into the Maud Basin (SE). A salt pillow (bright transparent pink) rises towards the top of the dome, while converging reflectors are present in the Maud Basin (Black stippled lines). A) Uninterpreted line extending into the Maud Basin, B) Interpreted line showing the salt pillow and convergence of reflectors in the Maud Basin. A major unconformity occurs in the Upper part of the Cretaceous-recent unit (black arrow). C) Uninterpreted line where the seafloor is dome shaped, D) Interpreted line showing the diapir reaching the seafloor. The question marks indicate uncertainties regarding the extent of the salt body. Line orientations shown in inset map.

4.5 Summary of salt related stratigraphic variations

The main patterns of growth and thinning of strata towards salt structures are summarized in Table 4.1. Note that there are exceptions to this trend, such as thinning of the Lower Triassic unit towards some salt structures in the Nordkapp Basin. Instances where strata exhibit no thickness variations, but are clearly affected by later diapirism, will be addressed along with the exceptions to the trends in the following discussion. Diapirism is noted for the Quaternary at the Svalis Dome due to the present day positive relief of the seafloor.

Table 4.1: The main salt related stratigraphic trends found in the results.

Structural element / Timing	Northern Nordkapp Basin	Southern Nordkapp Basin	Svalis Dome	Samson Dome	Norvarg Dome
Quaternary	X	X	Diapirism	X	X
Cretaceous to pre-Quaternary	X	X	X	X	X
Middle Triassic-Jurassic	Some growth	Large growth	Thinning	Thinning	Uniform
Early to Middle Triassic	Large growth	Some growth	Thinning	Uniform	Uniform
Early Triassic	No clear trend	No clear trend	Uniform	Uniform	Uniform

5 Discussion

The Nordkapp Basin and Svalis-, Samson- and Norvarg domes show both differences and similarities in the character of the salt itself and in thickness variations in the bounding stratigraphy. The salt is assumed to be of Carboniferous age, deposited in three different provinces: the Nordkapp Basin, the Maud Basin (Svalis Dome) and the Ottar Basin (Samson- and Norvarg domes). In the following, a discussion related to the timing of salt growth in the different areas is presented. The relation of salt growth to the structural evolution will also be discussed.

5.1 Salt movements in the Nordkapp Basin

In the Nordkapp Basin, 32 salt structures were identified and mapped, based on where they sub-crop the BCU horizon. Thickness patterns of rim synclines show large variations between individual diapirs, with some regional trends for the entire basin, and some differing trends between the two subbasins. A late Permian-earliest Triassic (corresponding to the Bjarmeland- and Tempelfjorden groups) initial phase of salt growth has been found by Rojo & Escalona (2017). This phase will, however, not be addressed in the following. The stratigraphic framework herein differs somewhat from the seismic sequences and megasequences defined in previous works (Figure 5.1). The units discussed are defined by bounding key horizons, representing depositional breaks within the established chronostratigraphic framework. Figure 5.2 shows the main growth phases and -mechanisms of the Nordkapp Basin diapirs during the Triassic.

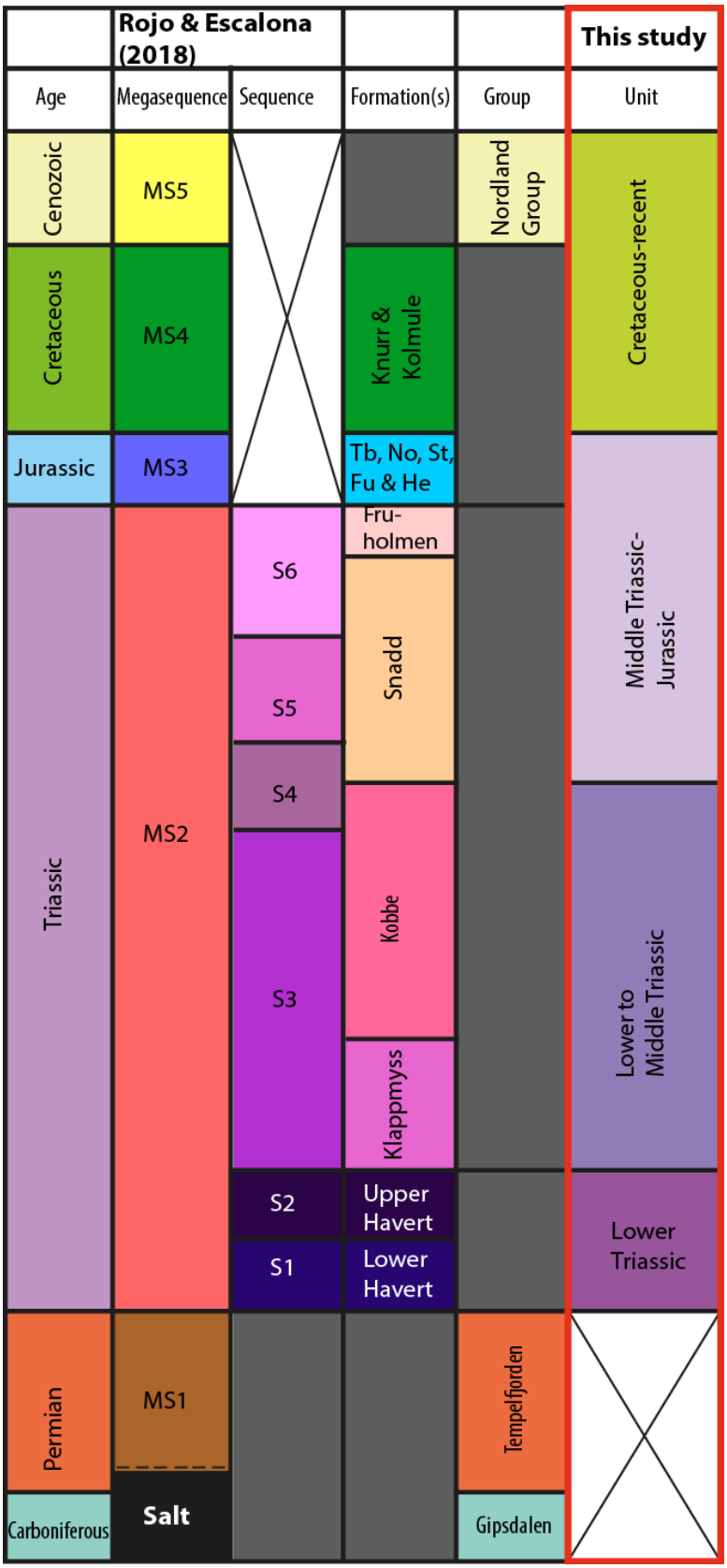

Figure 5.1: Table showing relationship between the seismic units defined herein and sequence stratigraphic framework used in previous work.. Tb=Tubåen, No=Nordmela, St=Stø, Fu=Fuglen, He=Hekkingen. Modified from Rojo & Escalona (2018)

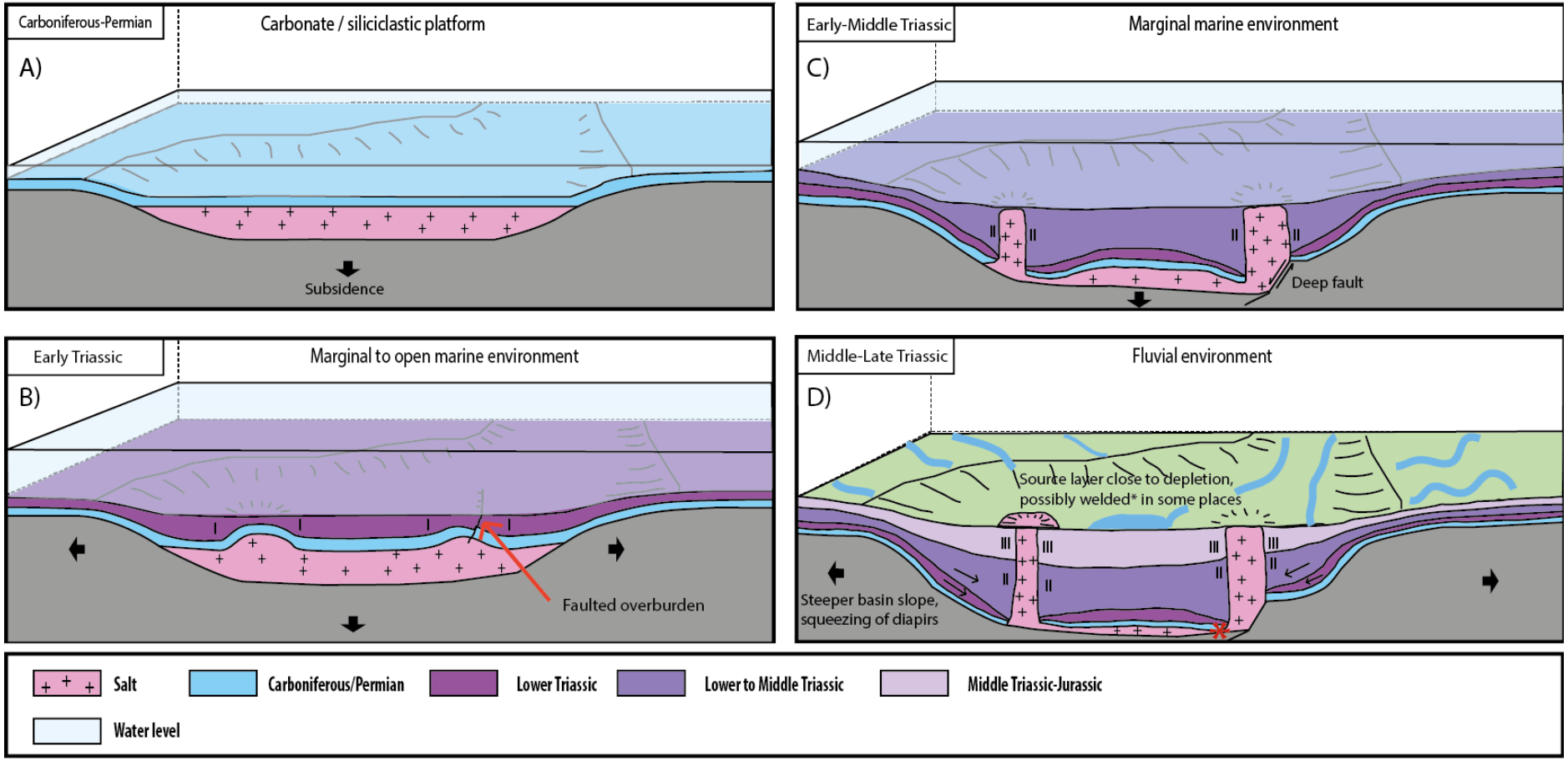

Figure 5.2: Schematic figure of the main phases of salt growth during the Triassic. A) Carboniferous-Permian carbonates deposited over the salt. B) Primary rim synclines (I) were generated in Early Triassic. Faulted overburden due to extension could have facilitated growth. C) The transition to diapiric rise created secondary rim synclines (II). Basin deepens along pre-existing fault. D) Continued growth facilitated by steepening slopes along the basin margin, leading to gravity gliding and squeezing of diapirs. Possible welding marked by red asterisk. The black arrows indicate subsidence and extension.

5.1.1 Early Triassic (Induan)

The Lower Triassic Havert Formation was deposited during the Induan and is characterized by small thickness variations across the entire study area. The formation consists of pro-delta facies probably derived from the Fennoscandian shield to the south during early parts of deposition, later shifting to a main input from the Uralian mountain chain to the southeast (Glørstad-Clark et al., 2010). No clear large-scale thickness variation trend was observed within the study area. In both subbasins however, some salt structures show examples of both thinning (D21, D22, D31 and salt pillow adjacent to D5) and thickening (D17b) of the unit towards diapirs. These observations are suggestive of early pillow stages and diapirism respectively (Figure 5.2). Furthermore, the thickest accumulations of this unit appear to be located towards the center of the two subbasins.

Early Triassic salt mobilization is documented in several previous works (Koyi et al., 1992, 1993; Nilsen et al., 1995; Rojo and Escalona, 2018), but with different triggering mechanisms suggested. Nilsen et al. (1995) and Rojo and Escalona (2018) argue that regional extension is the most likely triggering mechanism for the salt movements. This is opposed to a model where differential loading caused by a prograding sedimentary system triggered the movements (e.g. Faleide et al., 2015), and observations supporting the former is found within the data here too. Salt structure D31 (Figure 4.19) is located above a normal fault with displacement visible down into Permian strata, and possibly deeper. Weakening of the overburden related to extension thus could have facilitated diapirism here (Figure 5.2b).

Faults were observed adjacent to salt pillows, with offsets down to the NT-Permian horizon. Near diapir D5, the unit thins over a salt pillow, in both the hanging- and footwall block of the associated fault. It does however exhibit a larger overall thickness in the hanging wall than in the footwall (Figure 4.21). This could be interpreted as an example of extensional forces controlling salt flow towards the basin margin (Gabrielsen et al., 1992; Rojo and Escalona, 2018). It is worth noting that the faults here have a visible offset in younger stratigraphy as well, including the shallower Lower to Middle Triassic unit. This means that if the faults are associated with salt pillow growth as suggested, a reactivation of these preexisting Early

Triassic faults must likely have happened later in the Triassic. Such a development is supported by the observed thinning of the Lower to Middle Triassic unit in the footwall block. Loading due to normal faulting is the suggested mechanism here, resulting in a relatively larger thickness in the hanging wall, and pushing salt into the existing pillow along the basin margin (Figure 5.3).

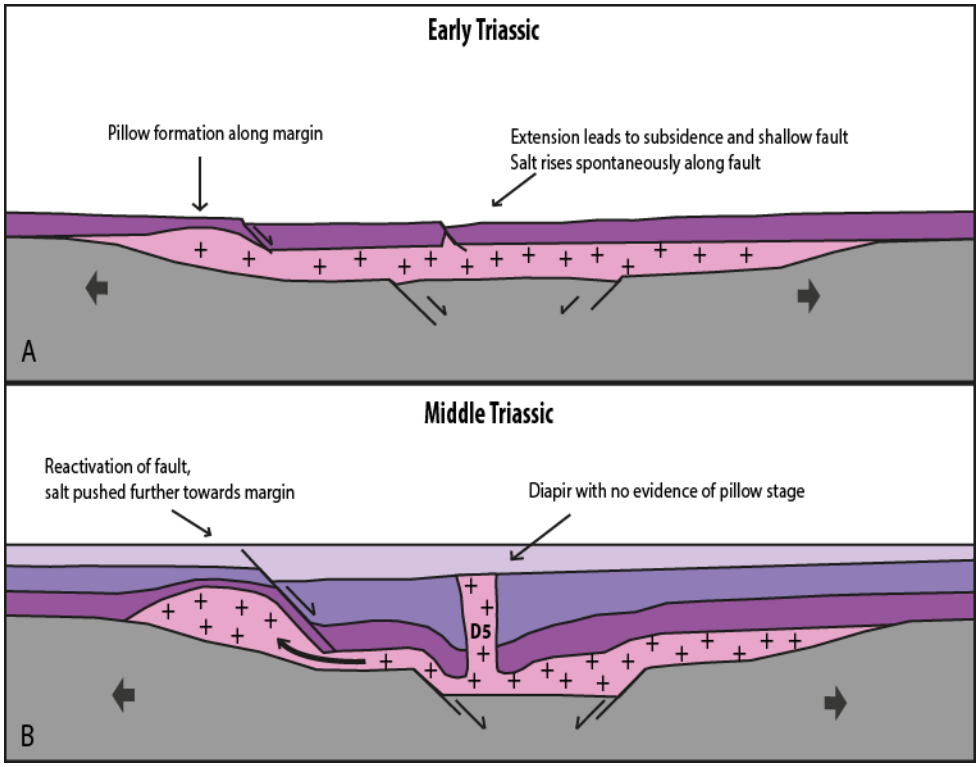

Figure 5.3: Concept illustration of the salt growth mechanisms around diapir D5 in the southern sub-basin. A): Normal faulting along the margin controls pillow growth, and possibly spontaneous diapiric rise further into the basin (D5). B): Reactivation of fault along the margin pushed more salt into the pillow. No thinning towards diapir D5 suggests that it initiated without a pillow stage.

A model where differential loading was caused by a prograding system cannot be ruled out as a trigger based on this study. However, the unit shows relatively uniform thicknesses and no clinoforms in the Nordkapp basin. Low internal amplitudes suggest little facies variations, reflecting a stable depositional environment such as marginal to open marine. Relict salt pillows along the margins and thinning of the unit towards diapirs suggests that some of the structures probably were initiated as salt pillows as suggested by Koyi et al. (1993). An opposing model has also been proposed, where the initial movements were of piercing nature (Nilsen et al., 1995). Observations that could support the latter model were also made; no

thinning towards diapir D5 suggests that it might have initiated as a piercing structure (Figures 4.21 and 5.3).

Thus, it is suggested that the Early Triassic salt movements were initiated locally in both subbasins due to extensional forces, causing the basin to subside. Whereas many salt structures initiated as pillows, faulting of the overburden allowed for direct piercement in other instances.

5.1.2 Early to Middle Triassic (Olenekian-lower Ladinian)

The Early to Middle Triassic period is in the study area represented by the deposition of the Klappmyss- and Kobbe formations, and even though the boundary between them was not established through well correlation, it is likely that the upper part, where diverging reflections are predominant, corresponds to the Kobbe Formation. The interpreted unit, which corresponds to the S3 unit in Rojo & Escalona (2018) (Figure 5.1) displays a substantial thickening in the northern subbasin, as observed towards diapirs D31 and D21 (Figure 4.19 and 4.20). The thickness variations are less prominent adjacent to diapirs in the southern sub-basin. The unit also thins over some salt pillows along the basin margin, (e.g. Figure 4.21). Several authors have suggested that salt diapirs were piercing in the late Early to Middle Triassic (e.g. Koyi et al., 1993; Nilsen et al., 1995; Rojo and Escalona, 2018).

In the northwestern rim syncline of D22 in the northern sub-basin, the Lower to Middle Triassic unit thickens significantly, suggesting that this was a depocenter where salt movements provided the accommodation space (Figure 4.18). The largest thickness increase is observed in the upper part of the unit, where reflections diverge significantly, suggesting that this was a time of relatively high subsidence in the rim syncline. Below the diverging reflections, the salt appears to be rising vertically, while the structure is widening in the upper part of the unit. The widening indicates that salt supply increased relative to sediment supply between deposition of the lower and upper part of the unit (Fossen, 2016).

Rapid passive and reactive growth, with substantial salt flow, has been described for the Middle Triassic, with salt withdrawal from a source layer (Koyi et al., 1993; Rojo and Escalona, 2018) and gravity gliding (Nilsen et al., 1995) as suggested mechanisms.

Despite the fact that both the SW and NE subbasins of Nordkapp Basin display rim-synclinal growth during the interval, substantially larger increase of thicknesses is observed in the northern subbasin, suggesting that larger salt evacuations here created more accommodation space. According to Nilsen et al. (1995), depletion of the source layer occurred in the Middle Triassic, sometime during the Anisian. However, gravity gliding enabled continued growth of the salt structures after welding; basement-involved normal faulting resulted in a deeper basin with steeper slopes, which in turn caused gravity-driven gliding of sediments towards the diapirs. This gravity gliding resulted in squeezing of the diapirs, laterally shortening them and pushing salt upwards (Nilsen et al., 1995) (Figure 5.2D).

Nilsen et al. (1995) showed that welding and related deformation styles are useful models when investigating triggers and timing of salt growth, these topics are however beyond the scope of this study. Thus, it is difficult to make conclusions around whether the source layer was depleted at the time. A greater early subsidence in the northern subbasin has been documented, which resulted in the deposition of a substantially thicker (4.0-5.0 km) initial salt layer than in the southern subbasin (2.0-2.5 km) (Jensen and Sørensen, 1992; Nilsen et al., 1995). It seems likely that the larger supply of salt in the northern subbasin has been crucial to the increased thicknesses observed there, as salt evacuations into the rising diapirs could create more accommodations space, regardless of the timing of welding.

5.1.3 Middle Triassic-Jurassic (Ladinian-Oxfordian)

This interval is within the study area represented by the Ladinian to early Norian Snadd Formation, the Norian Fruholmen Formation, and a condensed Jurassic section consisting of mainly the Oxfordian Hekkingen Formation (Dalland et al., 1988). The Middle Triassic-Jurassic unit corresponds to sequences S4-S6 and megasequence MS3 in Rojo & Escalona (2018) (Figure 5.1). The unit shows a thickness trend in the two subbasins opposite of that observed in the Early to Middle Triassic: thicknesses are relatively uniform towards the salt

diapirs of the northern subbasin, while increasing thicknesses occur towards the salt in the southern subbasin.

According to Nilsen et al. (1995), squeezing of diapirs and growth due to gravity gliding ended by the Late Triassic, which is coeval to deposition of the upper Snadd Formation and Fruholmen Formation. Rojo & Escalona (2018) on the other hand, found that despite some minibasin welding (Figure 5.2), salt evacuations continued and diapirs were rising passively through the Late Triassic and Jurassic.

While the southern subbasin displays growth strata around several diapirs, the relatively uniform thicknesses observed in rim synclines of the northern subbasin could indicate depletion of the source layer sometime in the Middle Triassic-Jurassic period. However, an increase of thickness is evident along the Nysleppen Fault Complex, between the Bjarmeland Platform and the outermost rim synclines of the northern subbasin (Figure 4.20). The thicker, but uniform, accumulations in the hanging wall indicates that deposition happened at the same time as downwards movement along the fault. The lack of further thickness variations towards the salt however, suggests that there was no salt evacuation from an underlying salt layer. Thus, any salt movements in the northern subbasin during the period are likely to have been facilitated by thin-skinned extension and gravity gliding at the time (Nilsen et al., 1995). Documentation for these movements are however lacking.

Contrarily, the increasing thicknesses that occur across the fault complex in the southern subbasin continue to increase gradually towards the salt (e.g. diapirs D12 and D17a, Figures 4.22 and 4.23). This suggests that fault movement was not in itself the controlling factor for the thickness variations, but that salt evacuated from a non-depleted salt layer resulted in a classical secondary rim syncline configuration (Trusheim, 1960). At the D5 diapir (Figure 4.21), the unit is unaffected by faulting, and thicknesses remain uniform towards the salt. The implied lack of diapiric rise could be due to either a locally depleted source layer (welding), or alternatively, due to a lack of fault activity along the basin margin. The latter would indicate that extensional forces were a controlling factor for the Middle Triassic-Jurassic salt movements seen elsewhere in the southern subbasin (e.g. D12 and D17a), aiding the

movements by steepening the basin slope and causing gravity gliding (Nilsen et al., 1995) (Figure 5.2).

5.1.4 Cretaceous-recent

The rifting event that initiated in late Middle Jurassic continued into the Early Cretaceous, leading to large-scale subsidence in newly formed basins along the southwestern Barents Sea margin, i.e. Harstad-, Tromsø-, Sørvestnaget- and Bjørnøya basins (Faleide et al., 1993; Gernigon et al., 2014). In the Nordkapp Basin, passive subsidence has been described during this period (Rojo and Escalona, 2018). Furthermore, uplift in the north related to the opening of the Amerasian Basin resulted in a depositional system prograding towards the south of the Barents shelf (Henriksen et al., 2011). Based on clinoform geometries, the main source area for the Lower Cretaceous succession in the Nordkapp Basin is assumed to have been located to the east/northeast (Marin et al., 2017).

Timing of the last phases of salt growth is challenging to decide, due to erosion of the Upper Cretaceous strata by the URU. Along some diapirs the Upper Jurassic strata appear to onlap the salt structures (e.g. D5 and D17b, Figures 4.21 and 4.23), supporting a Late Jurassic growth phase. The Cretaceous strata are steeply upturned towards the flanks of the diapirs, making potential evidence of onlaps or thickness variations generally difficult to observe (Figures 4.20 and 4.22). Evidence of the salt growth related to Early Cretaceous gravity gliding is thus largely missing. On the other hand, normal faults along the Nysleppen- and Måsøy fault complexes show displacement of the entire sub-URU succession (e.g. D12, D17, D21), supporting a later, i.e. Late Cretaceous, growth phase related to gravity gliding. Above diapir D17b (Figure 4.23), the entire preserved Cretaceous succession appears uplifted and concordant to the salt morphology, and with faulted parallel reflections. This further supports the theory of a later stage of salt growth.

Some diapirs (e.g. D22 and D5, Figures 4.18 and 4.21) are located away from the Nysleppen- and Måsøy fault complexes (Figure 4.17), and in these areas, the BCU is continuous and seemingly unaffected by the extensional forces that affected it along the fault complexes. Furthermore, faults in the Cretaceous overburden are generally less pronounced in these

areas. A steeply upturned Cretaceous succession following the morphology of the diapirs still indicates that major salt movements happened here as well, sometime after deposition of the preserved Cretaceous strata.

Assuming the salt layer was depleted at the time, it appears likely that Cenozoic compression triggered these movements. Continued diapiric rise after welding can only be facilitated by shortening (Nilsen et al., 1995). Unless Late Cretaceous gravity gliding along the fault complexes influenced the entire basin, regional compression was probably the mechanism that facilitated the shortening required to squeeze diapirs. The lack of evidence for compression elsewhere in the study area could be explained by the large amounts of salt structures deforming, thereby "absorbing" most of the strain (Nilsen et al., 1995).

There are different opinions regarding the final stages of diapirism in the Nordkapp Basin. The Nysleppen-, Måsøy- and Thor Iversen fault complexes were reactivated during Late Cretaceous, and this extensional episode has been linked to rejuvenation of the Nordkapp Basin diapirs, with gravity gliding and consequent squeezing of diapirs as the suggested mechanism (Nilsen et al., 1995). Due to previously mentioned issues with erosion and steeply upturned Cretaceous strata, the growth is difficult to confirm or disprove. Activity along the fault complexes does however support the suggested gravity gliding. Rojo and Escalona (2018) describe an earlier growth phase related to the same mechanisms during Late Jurassic to Early Cretaceous. Jurassic strata onlapping the salt structures support this phase. Furthermore, a final stage of salt movements has been attributed to Cenozoic regional compression (Nilsen et al., 1995; Rojo and Escalona, 2018), which is supported by the late growth of diapirs in areas where the Cretaceous strata are unaffected by faulting (e.g. D22, Figure 4.18).

5.2 Salt movements at the Svalis Dome

With its location on the northeastern margin of Loppa High, the Svalis Dome represents a salt structure that differs significantly from the salt in the Nordkapp Basin and in the Samson- and Norvarg domes. The structure is considered a salt pillow, albeit with a possible diapir at its crest (Gabrielsen et al., 1990). Unlike the Samson- and Norvarg domes, it has a primary rim syncline (the Maud Basin) associated with the initial doming. The salt was deposited during late Carboniferous, in a time where the area of the present-day Svalis Dome was probably part of a larger, fault-bounded basin that also included the present day Maud Basin (Gabrielsen et al., 1990). During Early to Middle Triassic, growth faulting along the Hoop Complex coincided with salt movements from the Maud Basin towards the Svalis Dome (Gabrielsen et al., 1990). Repeated cycles of uplift and subsidence have defined the Loppa High, since at least Carboniferous times (Wood et al., 1989). Figure 5.4 shows a simplified conceptual model of some key elements of the salt growth history of the Svalis Dome from Triassic to the present.

5.2.1 Early Triassic (Induan)

The Lower Triassic unit displays no change in thickness between the Bjarmeland Platform and Loppa High (Figure 4.13). Furthermore, thickness of the unit remains uniform in the Maud Basin towards the Svalis Dome (Figure 4.26). This indicates that deposition happened without any subsidence in the Maud Basin, and before the salt was mobilized. This is indicated by the uniform thickness of the first suprasalt unit in Figure 5.4b. According to Gabrielsen et al. (1990), salt movements initiated in Early Triassic, while the observations herein support Henriksen et al. (2011) in a later initiation.

5.2.2 Early to Middle Triassic (Olenekian-lower Ladinian)

The Lower to Middle Triassic unit displays a pronounced westward thinning in the Maud Basin towards the dome, suggesting that salt movements initiated in the Early to Middle Triassic (Figure 4.26 and 5.4b). Furthermore, a slight thickness increase from the Bjarmeland Platform into the Maud Basin suggests that accommodation space was increasing (Figure 4.14). According to Henriksen et al. (2011), the salt movements initiated during the Anisian. Convergence of reflections towards the Svalis Dome in the Lower to Middle Triassic unit

supports an early pillow stage sometime between the Olenekian and the Ladinian (Figure 4.26).

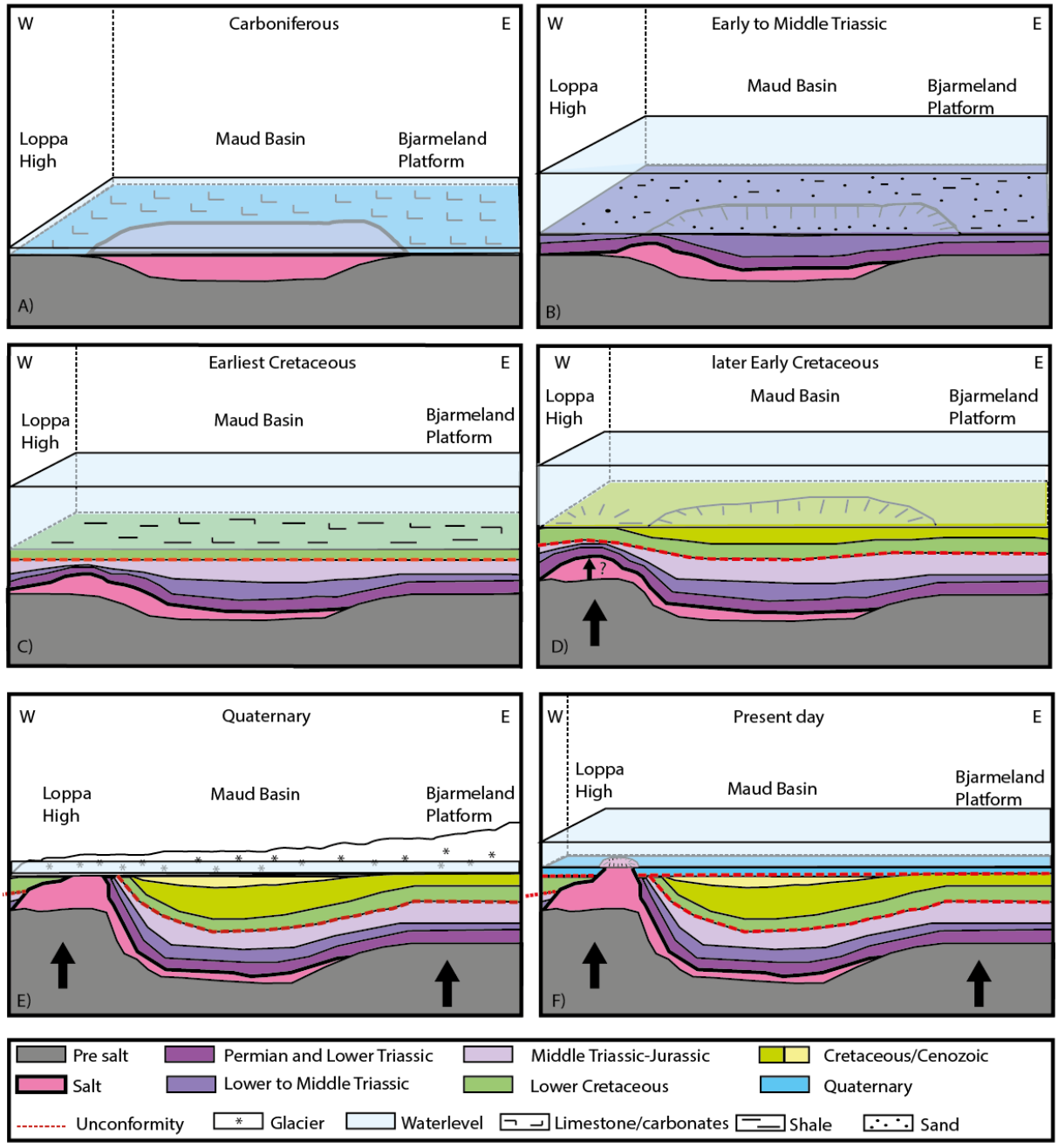

Figure 5.4: Simplified conceptual model showing the Svalis Dome salt growth history. A) Deposition of salt in the Maud Basin, carbonate development in the surrounding areas. B) Lower to Middle Triassic initial movements, marine setting. Lower to Middle Triassic unit thins towards the salt. C) Lower Cretaceous interbedded shales are deposited over the Middle Triassic-Jurassic unit. Transgression during Late Jurassic filled in previous relief. D) Renewed salt growth at the Svalis Dome later in Cretaceous, Maud basin is subsiding. Cretaceous strata thin towards the salt. E) Quaternary glacial erosion of the entire SW Barents Sea. Salt growth has resulted in steeply dipping strata sub-cropping towards the erosive boundary. F) Present day configuration after glacial erosion and isostatic rebound, diapirism leading to salt evacuation on the seafloor.

5.2.3 Middle Triassic-Jurassic (Ladinian-Oxfordian)

Thinning of the Middle Triassic-Jurassic unit suggests that salt flow continued (or rejuvenated) in this period. At this time, the Loppa High probably expressed no structural relief to surrounding areas (Wood et al., 1989). Convergence of reflections towards the Svalis Dome in large parts of the unit indicates that salt movements may have occurred through long periods within the Middle Triassic-Jurassic period. Gabrielsen et al. (1990) state that the main movements at the Svalis Dome occurred in Late Jurassic-Early Cretaceous and Late Cretaceous-early Cenozoic. It is challenging to establish accurate timings for the growth within the Middle Triassic-Jurassic unit, but from the distribution of converging reflections within the unit, it seems likely that there were significant movements already from late Middle Triassic and Late Triassic. It remains unclear whether the movements continued into (or rejuvenated in) the Jurassic, due to a lack of interpreted horizons between the Top Kobbe- and BCU horizons.

In the period between Late Jurassic and Early Cretaceous, the Loppa High was an elevated landmass, where canyons eroded all the way down to Triassic strata (Wood et al., 1989). Evidence of the deep erosion is however not present herein. This period is coeval with rift-related faulting in the Tromsø-, Bjørnøya-, and Hammerfest basins (Sund et al., 1984; Wood et al., 1989; Gernigon et al., 2014), and the Middle Triassic-Jurassic salt growth at the Svalis Dome thus could have been related to the uplift of the Loppa High.

5.2.4 Cretaceous- recent

The lowermost Cretaceous strata appear to have parallel reflections and uniform thicknesses in the Maud Basin, with no onlap towards the Svalis Dome. This indicates that the northeastern margin of Loppa High was a site of deposition during the earliest Cretaceous, and that the salt body was dormant at the time (Figure 5.4c). A mapped unconformity with thinning and onlap geometries further up in the Lower Cretaceous however, suggest that the Svalis Dome again was uplifted in the later Early Cretaceous (Figure 4.26b and 5.4d). Gabrielsen et al. (1990) state that the first of two main growth phases continued from Late Jurassic into Early Cretaceous, which is not supported from the parallel reflections observed in

the lowermost Cretaceous. It is thus suggested that there was a period of quiescence in the earliest Cretaceous, before the salt became active again in the later Early Cretaceous. Following the uplift of Loppa High that ended in Early Cretaceous, the landmass started subsiding again, but parts remained emergent until early Cenozoic (Sund et al., 1984; Wood et al., 1989). The observed onlap geometries in the later Early Cretaceous sediments thus occur at a time where the Loppa High generally was subsiding. This implies that the local uplift of the Svalis Dome could have been caused by renewed salt growth.

Cenozoic sediments are not preserved in the area, but evidence of the latest stage(s) of salt movements are found in and around the top of the salt structure itself. On the northwestern flank (Figure 4.26b), the otherwise flat URU suddenly becomes much deeper, and highly irregular compared to surrounding stratigraphy. This could imply that the salt was present near the seafloor by Pliocene/Pleistocene times, and that it affected local erosional patterns. An alternative interpretation is that the URU did not erode deeper adjacent to the salt structure, but that the present vertical displacement of the URU is rather due to subsequent collapse-graben formation. The second scenario implies that significant salt movements took place in recent times, which is supported by the presence of positive relief of the Svalis Dome on today's seafloor

According to Wood et al. (1989), Loppa High was onlapped by early Cenozoic sediments. Thermal uplift related to opening of the Norwegian-Greenland Sea followed, with large-scale erosion. Between 500 and 1000 m of early Cenozoic sediments were eroded at the high, due to a combination of fall in sea level and thermal uplift. This erosional unconformity was later enhanced by glacial erosion, i.e. the URU (Wood et al., 1989) (Figure 5.4e).

Even though regional extension usually is a crucial factor for salt to pierce its overburden, it can also happen in the absence of it, as long as the overburden is thin and the salt is enclosed in denser sediments (Vendeville and Jackson, 1992). At the Svalis Dome, the salt body appears juxtaposed to upturned Permian, and possibly older, strata. In the light of this, it is suggested that the last stage(s) of salt movements at the Svalis Dome were facilitated by the repeated uplift of Loppa High (i.e. regional tectonics). The uplift caused overburden thinning due to

erosion, which could enable continued salt growth in the absence of other mechanisms such as extension, compression, gravity gliding and sediment loading, and has contributed to the present configuration with a diapir that reaches the seafloor (Figure 5.4f).

5.3 Salt movements at the Samson Dome

No or very little thickness variations of the Mesozoic strata are observed at the Samson Dome. The part of the stratigraphy showing some variations is the Middle Triassic-Jurassic unit (Figure 4.25). Some convergence of internal reflections towards the salt indicates that there might have been initial doming during the interval. It does however seem unlikely that all of the salt movements can be attributed to this stage; the Upper Triassic-Jurassic unit thins by only approximately 250 ms and the salt body appears to have a maximum vertical extent of more than 1000 ms (Figure 4.25). In a classical primary rim syncline, the excess rock volume should correspond to the salt volume that has migrated into the growing salt pillow (Trusheim, 1960). Despite lacking volume calculations, it seems clear that this is not the case at the Samson Dome. Additionally, reflections in the Cretaceous unit appears to have a morphology very similar to those from Permian-Jurassic. This implies that they were deformed by the same forces, and it is thus suggested that most of the salt movements happened later in the Cretaceous or Cenozoic.

Flat reflections, discordant to the overall domed morphology, was found in a zone of low amplitudes directly below the URU. Previous authors have suggested erosional truncations towards this zone (Mattos et al., 2016, their Figure 5a). The lateral extent of the flat reflections however, seems to be restricted to an area directly below where the URU exhibits very high amplitudes. Coupled with the low amplitudes in this zone, it seems more likely that the flat reflections are simply seismic “noise”, and that the true configuration of the Cretaceous strata is masked by a strong seismic event at the URU.

The suggested salt growth timings are partly in agreement with previous works. Gabrielsen et al. (1990) state that salt movements took place before the Cretaceous, but with a late reactivation of the structure during Late Cretaceous, or even more recently. Mattos et al. (2016) claim that the Cretaceous unit is the only one thinning towards the dome, and

attributes this to erosional truncation of the upturned Cretaceous strata. However, their fault analysis does support the Triassic initial doming found herein. They further argue that the main phase of salt growth took place in late Mesozoic-early Cenozoic, evident by the formation of a broad anticline that affects the Late Cretaceous strata, along with reactivated faults that affect strata of Middle Triassic-Cretaceous age. This study also found an abundance of Cretaceous faults concentrated around the dome. However, their upper extent remains unclear due to the transparency of the seismic data in the upper half of the Cretaceous-recent unit.

5.4 Salt movements at the Norvarg Dome

At the Norvarg Dome, little or no changes in thickness of the mapped units are observed (Figure 4.24). Small variations in thicknesses, and no observable seismic stratigraphic characteristics suggestive of changes in environment or accommodation space, makes it difficult to assess the initial stage of salt mobilization. According to Gabrielsen et al. (1990), a thinning of Triassic and Jurassic strata over the dome indicate that doming took place before the Cretaceous. Evidence of this appears to be lacking in the seismic data interpreted in this thesis, however.

It is possible to see a discrete thinning of the Middle Triassic-Jurassic unit, but this thickness change is only evident when approaching the dome from the western side (Figures 4.15 and 4.24). In other words, any potential salt growth during Triassic-Jurassic probably would have to involve some asymmetry, leading to salt evacuation and amplified accommodation space at one side of the structure only. Furthermore, thinning of the Middle Triassic-Jurassic unit would in this case not be enough to argue for salt growth during the period. The unit is bounded by the BCU at its top, so thinning of the unit could be due to erosion at the top. Thereby it would be necessary to look for convergence of internal reflections to indicate salt growth-related thinning of the sequence. No such convergence was found. It is worth noting that fault patterns and low continuity of reflections makes it challenging to track individual reflections in the area. So even though no convergence was found, it should not be completely disregarded.

The Lower Cretaceous strata located between the BCU and URU show parallel reflections that are dome-shaped over the crest. The flat URU cutting into the domed Cretaceous strata leaves only an approximately 200 ms thick package of Cretaceous sediments over the crest. These strata appear to be part of a southwest prograding sedimentary system, which has been described by Marin et al. (2018). It does not seem like the salt movements affected the prograding system, since the clinoforms do not onlap the salt. Based on the observations above, salt growth must have happened sometime later in the Cretaceous-Cenozoic, with evidence in the sense of thinning layers, later removed by the URU. From this, it appears likely that the first stage of salt growth coincides with the reactivation of Late Cretaceous-Cenozoic age described by Gabrielsen et al. (1990), and that no, or very limited, salt growth took place during Triassic-Jurassic times. The URU and overlying sediments are all flat in the area, so there is no evidence suggesting reactivation since Quaternary times.

5.5 Structural differences

The Nordkapp Basin has already been established as a site of major salt deposition during the Carboniferous, with salt thicknesses up to 2 and 4-5 km in the southern and northern subbasins respectively (Jensen and Sørensen, 1992; Nilsen et al., 1995) (section 2.3.1). Salt deposition also occurred in the Carboniferous Maud- and Ottar basins. While there is very little information to be found regarding the amounts of salt deposited in the Maud Basin, salt thickness reached up to 2.4 km in the Ottar Basin (Breivik et al., 1995). From the interpreted seismic data, it seems clear that there are differences in the further structural evolution of the three provinces. While the Maud- and Nordkapp basins stand out as structural depressions at all stratigraphic levels from Permian to Cretaceous, the Ottar Basin does not stand out significantly at the relatively flat Bjarmeland Platform (Figures 4.3-4.8). Very little thickness variations were observed in Mesozoic strata near the Samson- and Norvarg domes (apart from those induced by late erosional truncations), and no major fault zones were identified apart from the Swaen Graben. This implies that regional tectonics have had a very limited effect on this part of the Bjarmeland Platform. A further implication is that the lack of early salt

movements, and stable tectonic setting, provided a thick and rigid overburden, which prohibited the salt structures from evolving further than the pillow stage (Breivik et al., 1995).

5.5.1 Carboniferous

While there has been very little focus on the Carboniferous in the seismic data, one element seems to be of importance in the Nordkapp Basin. The 2-3 km difference in salt thickness between the northern and southern subbasins implies that there was more faulting and/or subsidence in the northern subbasin during Carboniferous. The main consequence implied from the results and previous discussion is that this enabled larger scale salt movements recorded in the Early to Middle Triassic unit.

5.5.2 Early Triassic

During Early Triassic, uncertainties are related to the role of extension in the early salt mobilizations in the Nordkapp Basin. Permian-Early Triassic rift-related faulting has been described (Section 2.1.1), and it is possible that this tectonic event had an influence on the Nordkapp Basin margin. It is unclear however, why this phase presumably did not affect the salt in the Maud Basin/Svalis Dome, where the Early Triassic unit appears with uniform thicknesses. This becomes particularly intriguing when combined with the mentioned uplift and normal faulting that occurred at Loppa High at the same time.

5.5.3 Early to Middle Triassic

During this period, salt structures were growing in both the Nordkapp Basin, and on the Svalis Dome. It is difficult to draw conclusions around the triggers of salt movements at the Svalis Dome; very few faults are present in the preserved strata. In the Nordkapp Basin there is more evidence thin-skinned extension; the lack of initial thinning towards some diapirs suggest that the structures went through no pillow stage, but rather were initially piercing due to overburden faulting (Nilsen et al., 1995). There were no movements on the Samson- and Norvarg domes.

5.5.4 Middle Triassic-Jurassic

Observations indicate that extension during the Middle Triassic-Jurassic interval played a role in diapiric rise in the Nordkapp Basin, the Middle Triassic-Jurassic unit generally appears

uniform towards the salt in areas where it is not faulted along the margin. In areas where the unit is faulted however, there is evidence of syn-tectonic sedimentation and salt growth (section 5.1.3). The role of extension in pillow growth at the Svalis Dome remains uncertain due to the lack of documented faults. The regional tectonic setting during the interval was dominated by rifting in the Atlantic (Smelror et al., 2009; Gernigon et al., 2014). According to Gernigon et al. (2014), faulting of Loppa High mainly occurred from Jurassic-Cretaceous. Based on the salt growth timings that have been presented however, it appears that extensional forces might have been active from the Late Triassic, or even latest Middle Triassic. This episode seems to have had very little effect on the Bjarmeland Platform, apart from possibly enabling the earliest salt growth at the Samson Dome.

5.5.5 Cretaceous-recent

During this interval, there are clear indications of regional tectonics affecting the Maud Basin, the Bjarmeland Platform and the Nordkapp Basin. The tectonic setting in Cretaceous was dominated by extensional forces related to the opening of the Atlantic, which resulted in the formation of Cretaceous basins such as the Sørvestnaget- and Hammerfest basins (Brekke and Olaussen, 2013). A relative uplift of the Svalis Dome was found in the upper part of the preserved succession. While it is uncertain whether the salt was growing at this time, it does seem clear that the Maud Basin was subsiding relative to the Loppa High, leading to the previously mentioned onlap geometries (Figure 5.4D). Evidence of extension was also found from normal faults along the margin of Nordkapp Basin, and while a direct correlation to salt growth was not obtained herein, previous authors have described salt growth during the Early Cretaceous (Koyi et al., 1992; Nilsen et al., 1995; Rojo and Escalona, 2018).

In section 5.1.4, an example was highlighted where the entire preserved Cretaceous succession was uplifted over the underlying salt, in an area seemingly unaffected by regional extension. This could be an example of Late Cretaceous/early Cenozoic compression affecting the southwestern Barents Sea, as described by previous authors (Brekke and Riis, 1987; Nilsen et al., 1995; Faleide et al., 2008). Near the Samson- and Norvarg domes on the Bjarmeland Platform, there are no signs of extension. The only significant faulting observed seems directly

related to the salt bodies. It is therefore suggested that the regional compression that presumably affected the Nordkapp Basin, also had an influence on the Bjarmeland Platform, doming the salt and folding the overburden at the Samson- and Norvarg domes.

It is unclear how the Late Cretaceous/early Cenozoic compression might have affected the Svalis Dome. The present configuration however, shows the salt pillow and Lower Triassic strata in close vicinity to the seafloor, which indicates that the area has been subject to a larger uplift than the rest of the study area. It seems that the salt at some point in the early history of the Maud Basin moved into an area that would later be more controlled by the structural evolution of the Loppa High than the Maud Basin.

5.5.6 Influence of structural setting on salt growth

From the presented data, salt growth in the southwestern Barents Sea appears to be controlled by the structural evolution of the area. The Svalis Dome and Nordkapp Basin have been tectonically active through several phases of extension from Triassic-Cretaceous, which seems to have driven the salt growth. A later compressive event also appears to have reactivated the salt structures. At the Svalis Dome, uplift appears to have played an important role in the salt growth, whereas fracturing of overburden, steepening of basin slope and gravity gliding of sediments were important factors in the Nordkapp Basin. It also appears that salt growth in platform areas (Samson- and Norvarg domes) has been less extensive due to the stable tectonic setting there. Compressive forces however, seem to influence salt growth even on a relatively stable platform, evident by the late salt growth at the Samson- and Norvarg domes.

6 Conclusions

- Different tectonic events during the Triassic to recent have controlled salt growth in the Nordkapp Basin and on the Svalis-, Samson- and Norvarg domes.
- Salt growth in Nordkapp Basin was initiated during Early Triassic. Thinning of the Lower Triassic unit indicates that some diapirs initiated as salt pillows, possibly due to, or influenced by, thin-skinned extension.
- Some diapirs in the basin appear to have initiated without a prior pillow stage, indicating that they grew as diapirs after overburden faulting.
- Despite a possibly exhausted salt layer, diapirs continued to grow during the Middle Triassic-Jurassic. Basement related normal faults indicate that gravity-driven gliding of sediments on a steepening slope facilitated the growth by squeezing the diapirs.
- Normal faults affecting the entire preserved Cretaceous succession indicate that Late Cretaceous extension resulted in renewed growth.
- Cenozoic compression resulted in a final rejuvenation of the diapirs.
- Salt in the Svalis Dome/Maud Basin appears to have been evolving as a pillow from Early to Middle Triassic, and possibly into the Jurassic. The processes behind these movements remain unknown.
- Onlap of Cretaceous (or possibly Cenozoic) strata indicate that the Svalis Dome again was subject to uplift during the Cretaceous.
- Today there is a diapir at the crest of the Svalis Dome; this indicates that uplift and erosion at the Loppa High has led to recent salt growth.
- The main salt movements at the Samson- and Norvarg domes occurred during Cenozoic compression.
- From this, it is evident that the salt growth relates to different structural evolutions of the provinces. Extension controlled the growth in the Nordkapp Basin, uplift controlled salt growth at the Svalis Dome, and compression controlled salt growth at the Samson- and Norvarg domes.

7 Future studies

This thesis has provided information about salt growth on a regional scale in the southwestern Barents Sea. The dense coverage of 2D- and 3D seismic datasets have been useful to build upon several of the previous suggested theories for the Nordkapp Basin (Gabrielsen et al., 1992; Koyi et al., 1993; Nilsen et al., 1995; Grimstad, 2016; Rojo and Escalona, 2018).

The 2D dataset used in this study offered insight into the growth history of a large number of salt structures within the Nordkapp Basin. The Svalis-, Samson- and Norvarg domes are all single salt structures, and could be studied in more detail. The Svalis Dome in particular appears to have a complex structural evolution influenced by both salt movements and uplift. It could be beneficial with 3D seismic data to resolve their growth history.

Issues that could be worked further are:

- Try to delineate the salt bodies at the Svalis-, Samson- and Norvarg Domes with larger certainty, to relate their size and geometry to deformation of adjacent strata.
- Identify and analyze possible thickness variations and onlap geometries within Mesozoic strata at the Samson- and Norvarg domes, to determine if there was any salt growth in this period.
- Investigate the connection between the uplifted Svalis Dome and its rim-syncline (Maud Basin), to see if the same salt growth processes apply to both Maud- and Nordkapp Basin by;
- Mapping faults around the Svalis Dome and Maud Basin to reveal the uplift history of the Svalis Dome, and relate fault processes to salt growth, and;
- Analyzing well data from the Maud Basin. This could to provide a more detailed stratigraphic framework for studying thickness variations towards the Svalis Dome, particularly for the Cretaceous/Cenozoic succession.

References

Badley, M., 1985. Practical Seismic Interpretation, Badley, Ashton, and Associates Ltd. https://doi.org/10.1029/EO067i047p01342-06

Breivik, A.J., Gudlaugsson, S.T., Faleide, J.I., 1995. Ottar Basin, SW Barents Sea: a major Upper Palaeozoic rift basin containing large volumes of deeply buried salt. Basin Research 7, 299–312.

Brekke, H., Olaussen, S., 2013. "Høyt hav og lave horisonter," in: Ramberg, I.B., Bryhni, I., Nøttvedt, A. & Rangnes, K. (Red) The Making of a Land- Geology of Norway. Norsk Geologisk Forening, pp. 422–448.

Brekke, H., Riis, F., 1987. Tectonics and basin evolution of the Norwegian shelf between 62N and 72N. Norsk Geologisk Tidsskrift 67, 295–322.

Brown, A.R., 2011. Interpretation of Three-Dimensional Seismic Data, 5th ed, AAPG Memoir series. Society of Exploration Geophysicists and American Association of Petroleum Geologists, Tulsa, Oklahoma. https://doi.org/10.1190/1.9781560802884

Bugge, T.O.M., Mangerud, G., Elvebakk, G., Mørk, A., Nilsson, I., Fanavoll, S., Vigran, J.O.S., 1995. The Upper Palaeozoic successton on the Finnmark Platform , Barents Sea. Norsk Geologisk Tidsskrift 75, 3–30.

Dalland, A., Worsley, D., Ofstad, K., 1988. A lithostratigraphic scheme for the Mesozoic and Cenozoic succession offshore mid- and northern Norway. NPD Bulletin no 4 65.

Dorè, A.G., 1995. Barents Sea Geology , Petroleum Resources and Commercial Potential. Arctic 48, 207–221.

Dorè, A.G., 1991. Structural foundation and evolution of Mesozoic Seaways between Europe and the Arctic. Palaeogeography, Palaeoclimatology, Palaeoecology 87, 441–492.

Faleide, J.I., Bjørlykke, K., Gabrielsen, R.H., 2015. Geology of the Norwegian Continental Shelf, in: Petroleum Geoscience: From Sedimentary Environments to Rock Physics, Second Edition. pp. 603–637. https://doi.org/10.1007/978-3-642-34132-8

Faleide, J.I., Tsikalas, F., Breivik, A.J., Mjelde, R., Ritzman, O., Engen, Ø., Wilson, J., Eldholm, O., 2008. Structure and evolution of the continental margin off Norway and the Barents Sea. Episodes 82–91.

Faleide, J.I., Vågnes, E., Gudlaugsson, S.T., 1993. Late Mesozoic-Cenozoic evolution of the south-western Barents Sea in a regional rift-shear tectonic setting. Marine and Petroleum Geology 10, 186–214. https://doi.org/10.1016/0264-8172(93)90104-Z

Fossen, H., 2016. Structural Geology, 2nd ed. Cambridge University Press, Cambridge.

Gabrielsen, R.H., Færseth, R.B., Jensen, L.N., Kalheim, J.E., Riis, F., 1990. Structural elements of the Norwegian continental shelf. Part I: The Barents Sea Region. NPD Bulletin no 6.

Gabrielsen, R.H., Kløvjan, O.S., Rasmussen, A., Stølan, T., 1992. Interaction between halokinesis and faulting: structuring of the margins of the Nordkapp Basin, Barents Sea region, in: Structural and Tectonic Modelling and Its Application to Petroleum Geology - NPF Special Publication. pp. 121–131.

Gernigon, L., Brönner, M., Roberts, D., Olesen, O., Nasuti, A., Yamasaki, T., 2014. Crustal and basin evolution of the southwestern Barents Sea: From Caledonian orogeny to continental breakup. Tectonics 33, 347–373. https://doi.org/10.1002/2013TC003439

Glørstad-Clark, E., Birkeland, E.P., Nystuen, J.P., Faleide, J.I., Midtkandal, I., 2011. Triassic platform-margin deltas in the western Barents Sea. Marine and Petroleum Geology 28, 1294–1314. https://doi.org/10.1016/j.marpetgeo.2011.03.006

Glørstad-Clark, E., Faleide, J.I., Lundschien, B.A., Nystuen, J.P., 2010. Triassic seismic sequence stratigraphy and paleogeography of the western Barents Sea area. Marine and Petroleum Geology 27, 1448–1475. https://doi.org/10.1016/j.marpetgeo.2010.02.008

Golonka, J., Bocharova, N.Y., Ford, D., Edrich, M.E., Bednarczyk, J., Wildharber, J., 2003. Paleogeographic reconstructions and basins development of the Arctic. Marine and Petroleum Geology 20, 211–248. https://doi.org/10.1016/S0264-8172(03)00043-6

Grimstad, S., 2016. Master Thesis in Geoscience: Salt tectonics in the central and northeastern Nordkapp Basin , Barents Sea.

Halbouty, M.T., 1967. Salt Domes: Gulf Region, United States, & Mexico, 2nd ed. Gulf Publishing Company, Houston, Texas.

Henriksen, E., Ryseth, A.E., Larssen, G.B., Heide, T., Rønning, K., Sollid, K., Stoupakova, A. V., 2011. Tectonostratigraphy of the greater Barents Sea: implications for petroleum systems. Geological Society, London, Memoirs 35, 163–195. https://doi.org/10.1144/m35.10

Jackson, M.P.A., Hudec, M., 2017. Salt Tectonics: Principles and Practice. Cambridge University Press, Cambridge. https://doi.org/doi:10.1017/9781139003988

Jackson, M.P.A., Talbot, C.J., 1986. External shapes , strain rates , and dynamics of salt structures. Geological Society of America Bulletin 97, 305–323. https://doi.org/10.1130/0016-7606(1986)97<305

Jensen, L.N., Sørensen, K., 1992. Tectonic framework and halokinesis of the Nordkapp Basin, Barents Sea. Structural and Tectonic Modelling and its Application to Petroleum Geology - NPF Special Publication 109–120. https://doi.org/https://doi.org/10.1016/B978-0-444-88607-1.50012-7

Klausen, T.G., Ryseth, A.E., Helland-Hansen, W., Gawthorpe, R., Laursen, I., 2015. Regional development and sequence stratigraphy of the Middle to Late Triassic Snadd Formation, Norwegian Barents Sea. Marine and Petroleum Geology 62, 102–122. https://doi.org/10.1016/j.marpetgeo.2015.02.004

Koyi, H., Talbot, C.J., Tørudbakken, B.O., 1993. Salt diapirs of the southwest Nordkapp Basin: analogue modelling. Tectonophysics 228, 167–187. https://doi.org/10.1016/0040-1951(93)90339-L

Koyi, H., Tørudbakken, B.O., Talbot, C.J., 1992. Salt Tectonics in the Northeastern Nordkapp Basin , Southwestern Barents Sea. Aapg Memoir 65, 437–447.

Laberg, J.S., Andreassen, K., Vorren, T.O., 2012. Late Cenozoic erosion of the high-latitude southwestern Barents Sea shelf revisited. GSA Bulletin 124, 77–88. https://doi.org/10.1130/B30340.1

Larssen, G.B., Elvebakk, G., Henriksen, L.B., Nilsson, I., Samuelsberg, T.J., Stemmerik, L., Worsley, D., 2002. Upper Palaeozoic lithostratigraphy of the Southern Norwegian Barents Sea. NPD Bulletin 9.

Lundschien, B.A., Høy, T., Mørk, A., 2014. Triassic hydrocarbon potential in the Northern Barents Sea; integrating Svalbard and stratigraphic core data. NPD Bulletin 11 3–20.

Maher, H.D., 2001. Manifestations of the Cretaceous High Arctic Large Igneous Province in Svalbard. The Jounal of Geology 109, 91–104.

Marin, D., Escalona, A., Sliwihska, K.K., Nøhr-Hansen, H., Mordasova, A., 2017. Sequence stratigraphy and lateral variability of Lower Cretaceous clinoforms in the southwestern Barents Sea. AAPG Bulletin 101, 1487–1517. https://doi.org/10.1306/10241616010

Mattos, N.H., Alves, T.M., Omosanya, K.O., 2016. Crestal fault geometries reveal late halokinesis and collapse of the Samson Dome , Northern Norway : Implications for petroleum systems in the Barents Sea. Tectonophysics 690, 76–96. https://doi.org/10.1016/j.tecto.2016.04.043

Nilsen, K.T., Vendeville, B.C., Johansen, J.-T., 1995. Influence of Regional Tectonics an Halokinesis in the Nordkapp Basin, Barents Sea. Salt tectonics: a global prespective: AAPG Memoir 65 413–436.

NPD (2014) Litostratigrafisk diagram Norsk del av Barentshavet. Available from: https://www.npd.no/globalassets/1-npd/fakta/geologi-norsk/bh-od1409003-2014norsk.pdf. (Accessed 01.05.2019)

NPD (2019) NPD factpages: Exploration wells. Available from: http://factpages.npd.no/factpages/default.aspx?culture=nb-no&nav1=wellbore&nav2=TableView|Exploration|All. (Accessed 01.05.2019)

NPD (2019) NPD factpages: Seismic surveys. Available from: http://factpages.npd.no/FactPages/default.aspx?nav1=survey&nav2=PageView%7cFinished%7c2006&nav3=4397&culture=en. (Accessed 01.05.2019)

Peel, F.J., 2014. How do salt withdrawal minibasins form? Insights from forward modelling, and implications for hydrocarbon migration. Tectonophysics 630, 222–235. https://doi.org/10.1016/j.tecto.2014.05.027

Rojo, L.A., Escalona, A., 2018. Controls on minibasin infill in the Nordkapp Basin: Evidence of complex Triassic synsedimentary deposition influenced by salt tectonics. AAPG Bulletin 102, 1239–1272. https://doi.org/10.1306/0926171524316523

Smelror, M., Petrov, O.V., Larsen, G.B., Werner, S., 2009. Geological History of the Barents Sea. Geological Survey of Norway, Trondheim.

Sund, T., Skarpnes, O., Nørgård Jensen, L., Larsen, R.., 1984. Tectonic development and hydrocarbon potential offshore Troms, northern Norway. AAPG Special Volumes. 40, 615–627.

Trusheim, F., 1960. Mechanism of salt migrration in northern Germany. Bulletin of The American Association of Petroleum Geologists 44, 1519–1540.

Vendeville, B.C., 2002. A New Interpretation of Trusheim ' s Classic Model of Salt-Diapir Growth. Gulf Coast Association of Geological Societies Transactions 52, 943–952. https://doi.org/10.1016/j.diabres.2015.09.006

Vendeville, B.C., Jackson, M.P.A., 1992. The rise of diapirs during thin-skinned extension. Marine and Petroleum Geology 9, 331–353.

Vigran, J.O., Mangerud, G., Mørk, A., Worsley, D., Hochuli, P.A., 2014. Palynology and geology of the Triassic succession of Svalbard and the Barents Sea. Geological Survey of Norway Special Publication 14.

Vorren, T.O., Richardsen, G., Knutsen, S.M., Henriksen, E., 1991. Cenozoic erosion and sedimentation in the western Barents Sea. Marine and Petroleum Geology 8, 317–340. https://doi.org/10.1016/0264-8172(91)90086-G

Wood, R.J., Edrich, S.P., Hutchison, I., 1989. Influence of North Atlantic Tectonics on the Large-Scale Uplift of the Stappen High and Loppa High, Western Barents Shelf: Chapter 36: North Sea and Barents Shelf. AAPG Special Volumes. M 46, 556–559.

Worsley, D., 2008. The post-Caledonian development of Svalbard and the western Barents Sea. Polar Research 27, 298–317. https://doi.org/10.1111/j.1751-8369.2008.00085.x